CHAPTER 6

TEMPORAL SENSITIVITY

ANDREW B. WATSON

NASA Ames Research Center, Moffett Field, California

CONTENTS

The stimulus for vision is light distributed over space, time, and wavelength. The distribution in each of these dimensions influences our visual experience. This chapter focuses upon the temporal dimension. The time course of the stimulus affects our experience in two ways: it affects our sensitivity to the stimulus, for example, whether we see it or not, and it affects the appearance of the stimuli that are seen, for example, by controlling the apparent time course of the sensation. Both are important, but this chapter deals primarily with the first sort of effect, which is called *temporal sensitivity*.

This chapter begins with a brief description of the stimuli that are used to measure temporal sensitivity. A set of terms is introduced that serves to describe in a consistent way a wide variety of possible configurations. Some mathematical notation is specified for luminous stimuli distributed over space and time.

The study of temporal sensitivity has always made extensive use of mathematics, primarily Linear Systems Theory. Models of sensitivity and of the underlying mechanisms are frequently couched in these terms. To provide a point of reference, a brief survey of Linear Systems Theory is provided.

Because so many of the phenomena of temporal sensitivity can be explained by a simple generic model, and because this model has appeared piecemeal in the work of a number of authors, a "working model" is given concrete form in Section 4. A working model is one that provides a reasonable quantitative account of the available data, but whose mathematical structure is somewhat arbitrary and whose details are subject to change in the light of new evidence. Wherever possible in the remainder of the chapter, empirical results are compared to the predictions of the working model.

Sections 5–8 review empirical and theoretical analyses of the visibility of a number of particular temporal wave forms: sinusoids, pulses, and pairs of pulses. These wave forms are selected because they have received the bulk of experimental attention, and because they reveal important aspects of temporal sensitivity.

As will be evident, the temporal dimension of a stimulus cannot be studied entirely in isolation from the other dimensions. For example, statements regarding temporal sensitivity can rarely be made independently of the spatial distribution of the stimulus. This interdependence is acknowledged throughout the chapter, and is addressed directly in Section 10.

In natural imagery, as distinct from the artificial stimulus creations of the laboratory, temporal variation arises primarily through image motion, whether through motion of the observer, of the eyes, or of the objects viewed. Image motion is a special sort of temporal variation in which the time wave form is a function of spatial position. In Section 11, the temporal variations induced by image motion are considered, and some basic results on sensitivity to moving patterns are reviewed. The relation of temporal sensitivity to motion sensitivity is also discussed.

As the ambient level of illumination is raised, the eye exchanges sensitivity for temporal resolution. Overall sensitivity is reduced, but the ability to see rapid fluctuations is relatively enhanced. Section 12 reviews the empirical effects of light adaptation upon temporal sensitivity, and considers some theoretical models for these effects.

1. THE TEMPORAL STIMULUS

At its most general, the stimulus for vision includes anything that influences our visual sensations and reactions. This might include our state of light adaptation, our distance from a viewed object, what we had for lunch, and to whom we last spoke. In order to draw the line at a point that will best serve the purpose of this chapter, the stimulus is considered to be a distribution

of light lying in a plane orthogonal to the line of sight and in front of the observer. This *image* covers some portion of the visual field and endures for some finite amount of time.

1.1. Intensity

Because we are only rarely concerned with variations in the wavelength of light, it is sufficient to specify the *intensity* of the light at each point in the image. This intensity distribution can be written $I(x, y, t)$, where x and y are horizontal and vertical coordinates of the image measured in degrees of visual angle (degrees), and t is time. Three measures of intensity are used here. The first is *luminance*, expressed in units of candelas per square meter. The precise definition of luminance is quite complicated (Wyszecki & Stiles, 1967). But given our earlier definition of an image, luminance is then the amount of light emitted or reflected toward the eye per unit area of the source, weighted by the photopic luminous efficiency function. The optics of the eye transform the image luminance distribution into a distribution of light upon the retina. This transformation involves many factors, including spatial blurring, chromatic aberration, and attenuation by the pupil. The last effect is taken into account by a second measure, the so-called *retinal illuminance*. It is defined as the luminance ($cd \cdot m^{-2}$) multiplied by the area of the pupil (mm^2), and is given in units of *trolands* (td). This measure is used when the precise level of illumination on the retina is important, as in investigations of light adaptation. A third measure, most commonly used in studies of color vision, specifies image intensity in quanta per square degree per second at some particular wavelength or at each wavelength in a spectrally extended source. The troland value can be determined from this measure by way of formulas given by Wyszecki and Stiles (1967) (see also Chapter 5 by Hood & Finkelstein and Chapter 8 by Pokorny & Smith).

1.2. Spatial Configuration and Contrast

The spatial configuration of the stimulus has important effects upon temporal sensitivity. As noted above, our general description of an image is its complete three-dimensional intensity distribution, $I(x, y, t)$. However, the stimuli used in the majority of laboratory experiments can be described in less general but simpler form. Figure 6.1 illustrates this discussion.

An area of intensity I_B is designated as the *background*. A larger area, extending outward from the limit of the background and with intensity I_S, is called the *surround*. Surround intensity is most often set equal to background intensity, or is absent altogether. Authors rarely specify lighting conditions beyond the borders of the surround.

Superposed on and coextensive with the background is the *target* with an intensity given by the function $I_T(x, y, t)$. We allow the target intensity to have negative values, as when light is subtracted from the background, but of course the sum of target and background must be positive. *Contrast* is defined as the ratio of target intensity to background intensity,

$$C(x,y,t) = \frac{I_T(x,y,t)}{I_B} . \quad (1)$$

Note that contrast may have negative as well as positive values, though it may never be less than -1. Combining background and target, the intensity within the target area is given by

$$I(x,y,t) = I_B + I_T(x,y,t) = I_B[1 + C(x,y,t)] . \quad (2)$$

The segregation of the stimulus into contrast and background terms is a tradition that arose from the observation that sensitivity is more nearly invariant with respect to contrast than with respect to intensity. The background intensity must be specified, however, for it controls the state of adaptation which in turn governs sensitivity. Various definitions of background intensity are used, among them the unvarying level upon which the target is superposed, the space-average intensity of the image, the space-time average, or the average of the maximum and minimum intensities in the image. Each of these may be appropriate in some circumstance, but it is important that the expression for contrast be correct relative to the definition of background used.

1.3. Separability

In many experimental situations, the spatial contrast distribution does not vary over time, and likewise the temporal distribution is the same at all points in the image. In this case the spatial and temporal dimensions of the stimulus are said to be *separable* and the overall distribution can be written as a product:

$$C(x,y,t) = C_{x,y}(x,y)C_t(t) . \quad (3)$$

This condition holds, for example, for a disk target that is flashed on briefly, or for a spatial grating that is counterphase modulated

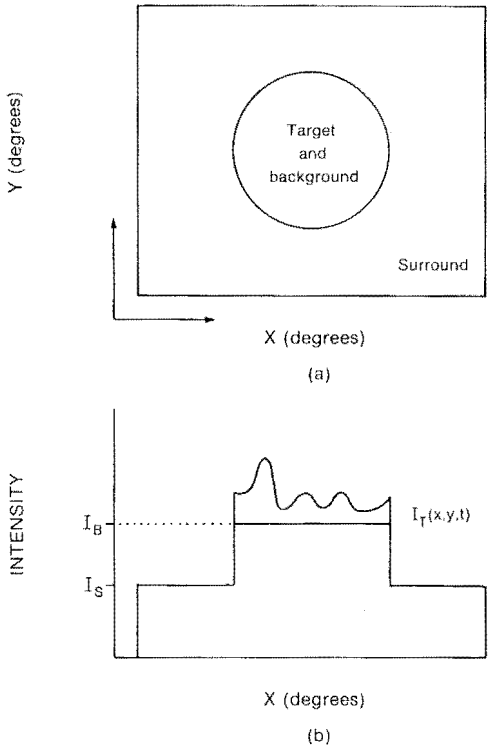

Figure 6.1. Some terms used to describe visual stimuli. (a) The spatial configuration of the image. The target and background are superposed on some specified area, shown here as a disk. The surround lies outside the target and background. (b) A horizontal cross-section through the intensity distribution $I(x,y,t)$ of the image. The surround has intensity I_S, the background I_B, and the target $I_T(x,y,t)$. Target contrast is the ratio I_T/I_B.

in time. It does not hold for one important class of stimuli, namely, patterns in motion. In spite of this exception, most work on temporal sensitivity has been confined to separable stimuli, and for this reason we focus upon the time wave form $C_t(t)$, abbreviated $C(t)$. If $C(t)$ is to continue to express contrast as defined above, then $C_{x,y}(x, y)$ must be normalized so as to have an overall contrast of 1. This convention has been adopted throughout this chapter. Where intensity rather than contrast is considered, we will specify the intensity wave form $I(t)$.

In reducing the description of the stimulus to the temporal wave form $C(t)$, it must be borne in mind that both background intensity and spatial distribution (which are no longer reflected in the wave form) can have important effects upon temporal sensitivity. These effects are discussed in Sections 9 and 11.

1.4. Temporal Wave Forms

A wide range of temporal wave forms has been studied for their effects upon visual sensitivity. For various reasons, not all entirely sensible, certain wave forms have received most of the attention. These are rectangular incremental pulses, decremental pulses, pulse pairs, square waves, and sinusoids. Sensitivity to each of these wave forms is considered, and they are sketched in Figure 6.2. A useful distinction among these wave forms is that the sinusoid and the square wave are *periodic*, whereas the others are *aperiodic*. A periodic wave form is one that repeats itself forever. Formally, it is a wave form $I(t)$ such that

$$I(t) = I(t - T) \qquad \text{for all } t \ , \tag{4}$$

where T is the *period* of the wave form. No visual stimulus goes on forever, but if the number of cycles in the wave form is large enough so that adding more does not alter sensitivity, then it is reasonable to treat the wave form as periodic.

2. LINEAR SYSTEMS THEORY IN THE TIME DOMAIN

Linear Systems Theory (LST) is an important mathematical tool in the analysis of human temporal sensitivity. Bracewell (1978) provides an excellent introduction to this branch of mathematics. The purpose of this section is to provide a brief, intuitive overview of LST and to note a number of the important results so that they may be referred to in the text.

The experimental analysis of a physical system often consists of applying various inputs and measuring the resulting outputs. The inputs we consider here are real-valued functions of time, $f(t)$. This function typically describes the luminance or contrast of a visual stimulus over time (see Section 1). The output, or response, is also some real-valued function of time, $r(t)$. This function might represent some internal state of excitation, for example, the momentary discharge frequency of a visual neuron. More often it is a purely hypothetical quantity, whose value can be deduced from psychophysical responses only with the aid of additional assumptions. These assumptions are considered here. The *system* is that collection of physical processes that intervenes between the input and the response. In the example above, the system would include all those events between stimulus and neural response, including optical imaging, transduction, and transmission from neuron to neuron.

A complete empirical characterization of the system would consist of a description of the output resulting from any input. When the number of possible inputs is infinite, as is true in the case of temporal wave forms, a purely experimental approach would require an infinite number of measurements. If the system is *linear*, however, LST provides a way of characterizing the system by measuring the response to a single input. LST also supplies a set of mathematical tools for predicting, from this characterization, the response to an arbitrary input.

2.1. Superposition

It is useful to denote the action of the system mathematically by an operator, L. Just as a function $f(t)$ maps values of t to values of $f(t)$, so the operator maps the input *function* $f(t)$ into the output function $r(t)$. We write this mapping in the form

$$L[f(t)] = r(t) \ . \tag{5}$$

Where it is possible to do so without confusion, we omit the function arguments and write f for $f(t)$.

A system is linear if it obeys the principle of superposition. This principle states that for any two inputs f_1 and f_2, and any constant a,

$$L[af_1] = aL[f_1] \tag{6}$$

$$L[f_1 + f_2] = L[f_1] + L[f_2] \ . \tag{7}$$

Thus superposition entails two properties, homogeneity and additivity. The system is homogeneous when multiplying an input multiplies the output by the same amount. The system is additive when the response to the sum of two inputs is the sum of the responses to the individual inputs.

2.2. Time Invariance

Let $r(t) = L[f(t)]$. The system is *time invariant* if

$$L[f(t - \tau)] = r(t - \tau) \ . \tag{8}$$

Note that $f(t - \tau)$ is the input $f(t)$ delayed by τ; likewise $r(t - \tau)$ is the response $r(t)$ delayed by τ. Equation (8) states that delaying the input by τ delays the output by τ but leaves it otherwise unaltered. This means that the properties of the system do not change over time.

2.3. Orthogonal Basis Functions

Two functions $b_1(t)$ and $b_2(t)$ are *orthogonal* if their *inner product* is zero:

$$b_1(t) \cdot b_2(t) = \int_{-\infty}^{\infty} b_1(t) b_2(t) dt = 0 \ . \tag{9}$$

A *basis* is a set of functions that *spans* some set of functions; that is, any member of the latter set can be constructed from a linear combination of the basis functions. If we have a set of orthogonal basis functions $\{b_j(t)\}$ which span the set of real-valued functions $\{f(t)\}$, then for any function f,

$$f(t) = \sum_{j=-\infty}^{j=\infty} a_j b_j(t) \ , \tag{10}$$

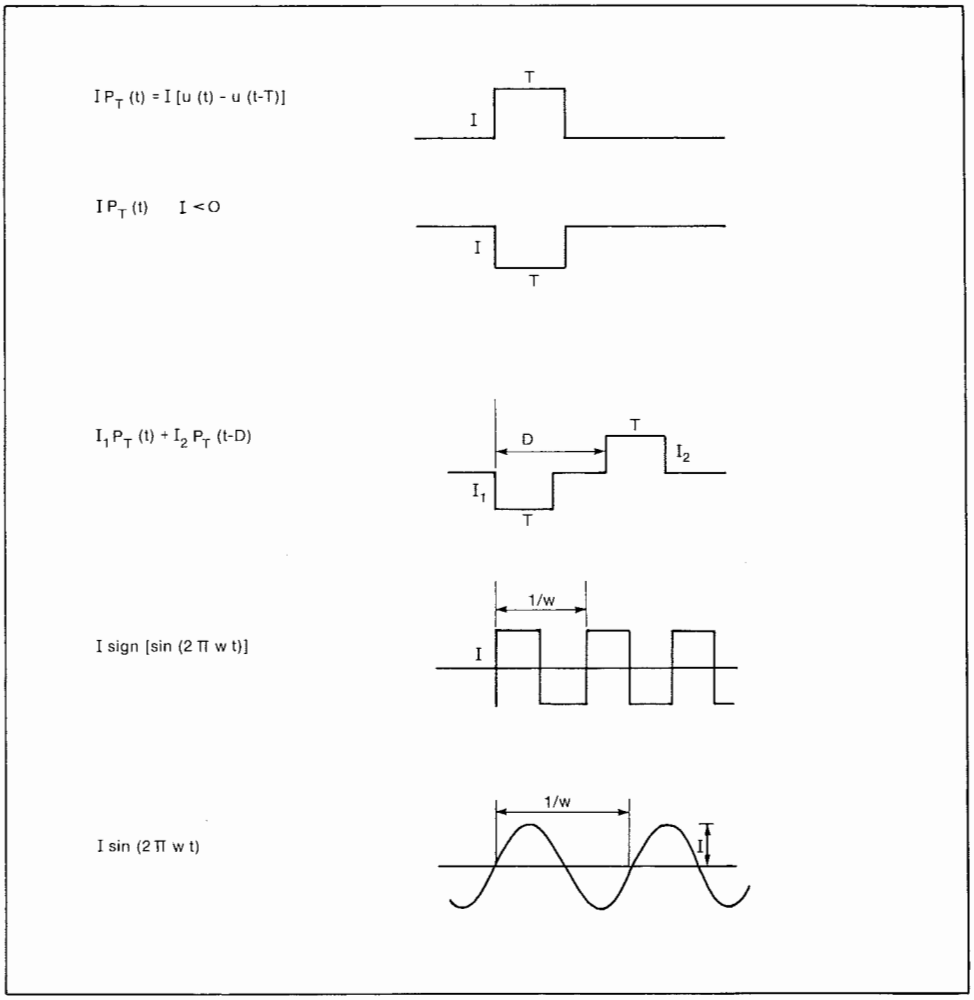

Figure 6.2. Some wave forms used to study visual temporal sensitivity. Each wave form specifies the target intensity as a function of time. An equation defining each wave form is given on the left. From top to bottom the wave forms are a rectangular pulse increment of intensity I and duration T; a pulse decrement of intensity I and duration T; a pulse pair with durations T, intensities I_1 and I_2, and delay between pulses of D; a square wave of intensity I and frequency w; and a sinusoid of intensity I and frequency w. Intensity may be a quantity such as luminance, retinal illuminance, or quanta·degree^{-2}·sec^{-1} at some wavelength. Because light cannot have negative intensity, each wave form must be added to a background more intense than the largest negative excursion in the wave form.

where the a_j are the coefficients of the linear combination, and where both a and b may be complex. Because the basis is orthogonal, the set of coefficients a_j that go to make up a particular f are unique and easily determined.

Now we let f be the input to a linear system. Applying the principle of superposition to Eq. (10), we see that the response to f will be

$$L[f] = \sum_{j=-\infty}^{j=\infty} a_j L[b_j] \ . \tag{11}$$

Thus if we knew the response to each basis function ($L[b_j]$), we could calculate the response to any arbitrary input. The procedure would be as follows: (1) evaluate the coefficients a_j required to represent the input f, (2) multiply each basis response $L[b_j]$ by the coefficient a_j, and (3) add them up to produce the response $L[f]$.

2.4. Impulse and Impulse Response

One natural set of orthogonal basis functions is the set of *impulses* located at different points in time. An impulse $\delta(t)$ is a pulse with infinite height, infinitesimal width, and unit area, located at $t = 0$. The input is easily represented in terms of shifted and scaled impulses,

$$f(t) = \int_{-\infty}^{\infty} f(\tau)\delta(t - \tau)\, d\tau = f(t) * \delta(t) \tag{12}$$

where $*$ indicates convolution. Note that this equation is the continuous version of Eq. (10), with $f(\tau)$ playing the role of the coefficients a_j. Let the response of the system to an impulse be $h(t)$, the *impulse response*. We write

$$h(t) = L[\delta(t)] \ . \tag{13}$$

We can now follow the procedure above to determine the response to $f(t)$. Combining the preceding three equations, and applying the principles of superposition and time invariance, we get

$$r(t) = \int_{-\infty}^{\infty} f(\tau)h(t - \tau)\, d\tau = f(t) * h(t) . \quad (14)$$

Thus the response is equal to the convolution of the input and the impulse response. If the impulse response is known, the response to an arbitrary input can be calculated. Thus the impulse response completely characterizes the system.

2.5. Eigenfunctions

An alternative derivation of $r(t)$ is possible if each basis function is an *eigenfunction*, satisfying the condition

$$L[b_j(t)] = c_j b_j(t) . \quad (15)$$

The response to an eigenfunction is the function itself, multiplied by some complex constant c_j, known as the *eigenvalue*. Fortunately, for a linear, time-invariant system there exists a set of eigenfunctions that are also orthogonal basis functions for the set of real-valued functions $\{f(t)\}$. They are the *complex exponentials*, $e^{i2\pi wt}$ with frequency w. The function f is synthesized from these exponentials in the manner described in Section 2.3, as a linear combination with complex coefficients $F(w)$,

$$f(t) = \int_{-\infty}^{\infty} F(w)e^{i2\pi wt}\, dw . \quad (16)$$

Because the complex exponentials are eigenfunctions, the response of the linear system to f is easily determined:

$$r(t) = \int_{-\infty}^{\infty} H(w)F(w)e^{i2\pi wt}\, dw . \quad (17)$$

The *system function* $H(w)$ (also called the *transfer function*) specifies the complex constant (eigenvalue) by which the complex exponential of frequency w is multiplied as it passes through the system. Note that $H(w)$, like the impulse response, completely specifies the behavior of the system. All we need now are methods for evaluating $F(w)$ and $H(w)$.

2.6. Fourier Transforms

The coefficients $F(w)$ that are required to construct $f(t)$ from complex exponentials are obtained by the *Fourier transform*

$$F(w) = FT[f(t)] = \int_{-\infty}^{\infty} f(t)e^{-i2\pi wt}\, dt . \quad (18)$$

There is also an inverse transform, by which the original wave form is reconstituted from component exponentials with coefficients $F(w)$,

$$f(t) = FT^{-}[F(w)] = \int_{-\infty}^{\infty} F(w)e^{i2\pi wt}\, dw . \quad (19)$$

Fourier transforms are treated extensively by Bracewell (1978).

2.7. The Convolution Theorem

A particularly valuable property of the Fourier transform is that if $f_1(t)$ and $f_2(t)$ are two functions, and $F_1(w)$ and $F_2(w)$ are their transforms, then

$$f_1(t) * f_2(t) = FT^{-}[F_1(w)F_2(w)] . \quad (20)$$

Thus the complicated convolution operation is converted to the simple multiplication operation in the frequency domain. As an example, Eq. (14) shows that the response of a linear system is the convolution of the input and the impulse response. Applying the convolution theorem,

$$r(t) = FT^{-}[F(w)FT[h(t)]] \quad (21)$$

$$= \int_{-\infty}^{\infty} F(w)FT[h(t)]e^{i2\pi wt}\, dw . \quad (22)$$

Comparison of this result with Eq. (17) shows that the transform of the impulse response is the system function,

$$FT[h(t)] = H(w) . \quad (23)$$

A linear, time-invariant system can therefore be completely described by either its impulse response or its system function, which are Fourier transforms of each other.

2.8. Amplitude and Phase

The complex system function $H(w)$ may be represented as the sum of real and imaginary parts

$$H = R + iI \quad (24)$$

where $i = (-1)^{1/2}$. Each value of this function is a point in the complex plane at a distance $|H|$ from the origin and at an angle $< H$ from the positive real axis, where

$$|H| = (R^2 + I^2)^{1/2} \quad (25)$$

$$< H = \tan^{-1}\frac{I}{R} . \quad (26)$$

Application of Euler's theorem shows that

$$H = |H|\, e^{i<H} . \quad (27)$$

The advantage of this last expression is that the response to an eigenfunction $e^{i2\pi wt}$ is now simply

$$L[e^{i2\pi wt}] = |H(w)| \exp\{i[2\pi wt + <H(w)]\} . \quad (28)$$

With a more familiar real input of $\cos 2\pi wt$, we see that the output of the system is

$$L[\cos 2\pi wt] = |H(w)| \cos [2\pi wt + <H(w)] . \quad (29)$$

In other words, the response is also a cosine of the same frequency but altered in amplitude by the factor $|H|$ and in phase by an

amount $<H$. Thus $|H|$, the *amplitude response* of the system, describes the gain with which each frequency passes through the system, and $<H$, the *phase response*, describes how much each frequency is advanced or delayed.

2.9. Causality

In a passive physical system operating in the time domain, the response never precedes the input, and the system is said to be *causal*. Formally,

$$H(t) = 0 \qquad \text{for } t < 0 \ . \tag{30}$$

This has various consequences. Most important here is that amplitude and phase responses are even and odd functions, respectively. Accordingly, these functions need only be determined or specified for positive frequencies.

2.10. Some Simple System Functions

The system function of a linear combination of independent systems is the linear combination of their separate system functions. The cascade of two systems yields a system function equal to the product of their individual system functions. By means of these two rules, rather complicated systems can be assembled from simple components. In the following sections some simple systems are considered. For each, impulse response, system function, amplitude response, and phase response are noted in Table 6.1.

2.10.1. Multiplication by a Constant. If a signal is multiplied by a constant k, but not otherwise altered, the transfer function is a constant k. In electrical terms, this would be the action of an ideal amplifier with a gain of k.

2.10.2. Delay. If the signal is delayed by a time τ, but not otherwise altered, the amplitude response is equal to 1, and the phase response to $2\pi w\tau$.

2.10.3. Differentiator. Differentiation of a signal with respect to time is a linear operation, and may be represented by an impulse response that is the derivative of the impulse function, $\delta'(t)$. More generally, the nth time derivative may be represented by an impulse response that is the nth derivative of the impulse. The transfer function is $(i2\pi w)^n$.

2.10.4. Integrator. Integration over the interval $[-\infty, t]$ is equivalent to convolution with the unit step function, $u(t)$. Its system function is therefore the Fourier transform of the step function, $[\delta(w) - i/(\pi w)]/2$. Note that, except at 0, its action is precisely the inverse of that of the differentiator. This is logical, because except for their action on constants, differentiation and integration are inverse operations.

2.10.5. Leaky Integrator. Rather than performing a perfect integration, like that described in Section 2.10.4, many physical devices integrate the input but leak at a rate proportional to the amount accumulated. If the constant of proportionality is $1/\tau$, then the impulse response is

$$h(t) = u(t)e^{-t/\tau} \tag{31}$$

where $u(t)$ is the unit step function. If n identical leaky integrators are cascaded, then

$$h(t) = u(t)\frac{\tau^{n-1}}{(n-1)!}(t/\tau)^{n-1}e^{-t/\tau} \tag{32}$$

and

$$H(w) = \tau^n(i2\pi w\tau + 1)^{-n} \ . \tag{33}$$

Amplitude and phase responses are

$$|H(w)| = \tau^n[(2\pi w\tau)^2 + 1)^{-n/2} \tag{34}$$

$$<H(w) = -n\tan^{-1}(2\pi w\tau) \ . \tag{35}$$

These functions are drawn in Figure 6.3. Note that the system acts as a low-pass filter. Beyond a frequency of $(2\pi\tau)^{-1}$, the amplitude approaches an asymptote of $(2\pi w)^{-n}$, whereas below $(2\pi\tau)^{-1}$ it asymptotes at τ^n. In log-log coordinates, the lower limb is flat whereas the upper limb falls with an asymptotic slope of $-n$. This is sometimes called a resistance-capacitance filter, by analogy to an electrical circuit composed of a resistor and a capacitor.

Table 6.1. Some Simple Linear Systems

System	Impulse Response, $h(t)$	System Function, $H(w)$	Amplitude Response, $\|H(w)\|$	Phase Response, $<H(w)$
Cascade	$h_1 * h_2$	H_1H_2	$\|H_1\|\,\|H_2\|$	$<H_1 + <H_2$
Sum	$h_1 + h_2$	$H_1 + H_2$	$\|H_1 + H_2\|$	$<[H_1 + H_2]$
Constant	$k\,\delta(t)$	k	$\|k\|$	0
Delay	$\delta(t-\tau)$	$e^{-i2\pi w\pi}$	1	$-2\pi w\tau$
nth derivative	$\delta^{(n)}(t)$	$(i2\pi w)^n$	$(2\pi\|w\|)^n$	$n\,\mathrm{sgn}(w)\pi/2$
$\int_{-\infty}^{t}$	$u(t)$	$[\delta(w) - i/(\pi w)]$	$[\delta(w) + 1/(\pi\|w\|)]$	$-\mathrm{sgn}(w)\pi/2$
Low-pass filter	$\dfrac{u(t)t^{n-1}e^{-t/\tau}}{(n-1)!}$	$\dfrac{\tau^n}{(i2\pi w\tau + 1)^n}$	$\dfrac{\tau^n}{[(2\pi w\tau)^2 + 1]^{n/2}}$	$-n\tan^{-1}(2\pi w\tau)$

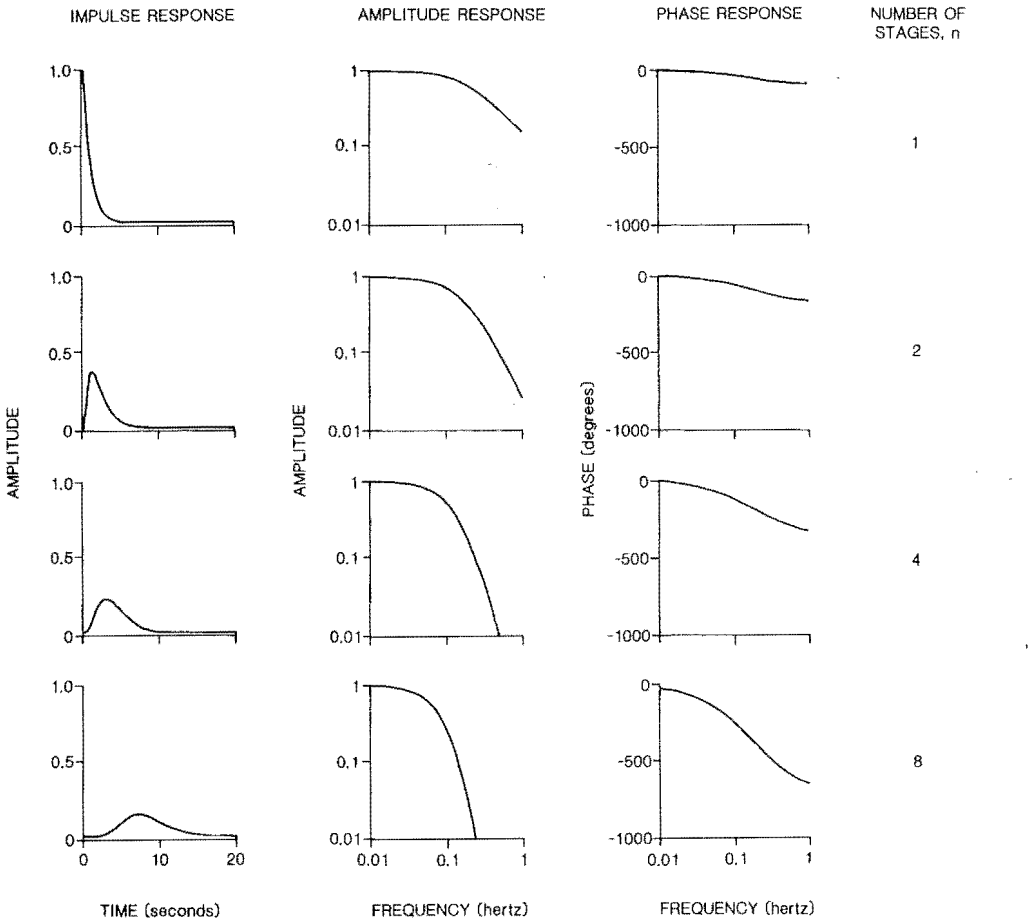

Figure 6.3. Responses of an n-stage low-pass filter with time constant $\tau = 1$. The columns show respectively the impulse response, the amplitude response, and the phase response. Different rows are for different numbers of stages (n), as indicated. With increasing stages, the impulse response becomes longer, lower, more symmetrical, and its peak occurs later in time. All the impulse responses have the same integral (area) of 1. The falling limb of the amplitude response has an asymptotic log-log slope of $-n$. At a given frequency, the phase response is proportional to n.

3. BASIC THEORETICAL CONCEPTS

This section introduces a number of concepts that are used frequently in discussions of temporal sensitivity.

3.1. Time-Invariant Linear Filter

Definitions of linear filters and time invariance are given in Section 2. A time-invariant linear filter often plays the role of the first element in models of the pathway between visual stimulus and psychophysical response. The filter input is the temporal wave form of intensity or contrast, and the output is some hypothetical internal response. Because the observer's psychophysical response is usually discrete rather than time varying (for example, the press of a button), it is necessary to assume some additional, usually nonlinear process between filter output and psychophysical response. Several examples are given here. The properties of the linear filter inferred from psychophysical data depend upon the the final response rule assumed.

Temporal models are often expressed in terms of integration or differentiation with respect to time. These operations may also be represented as linear filters, as described in Section 2. Occasionally integration over some epoch τ is considered. This is equivalent to a filter whose impulse response is a rectangle of height $1/\tau$ between times 0 and τ.

3.2. Threshold Mechanisms

The simplest link between filter output and observer response is some sort of threshold mechanism. Commonly it is assumed that an excursion of the response that exceeds some threshold value leads to a "correct" or "yes, I see it" response from the observer. Depending on the model in question, the threshold may be either a fixed property of the detection apparatus or a statistical criterion, which may be adjusted by the observer to satisfy certain objectives. Because decrements as well as increments can be detected, a threshold for negative excursions of the filter output must also be assumed.

3.3. Probability Summation Over Time

Both the visual stimulus and the physical mechanisms that mediate detection are subject to random perturbations. If the internal response is subject to noise, one cannot be certain which point in the response, if any, will exceed threshold. Accordingly, the probability that each point exceeds threshold must be considered.

A simple treatment of this situation is as follows. Suppose that a response of some duration may be broken into a sequence of n brief intervals, and that within each interval the response is essentially a constant r_i. Assume the probability that the response exceeds threshold in interval i, written p_i, is independent of all other intervals. Assume the signal is detected whenever the response in at least one interval exceeds threshold. The probability of detection will then be

$$p = 1 - \prod_{i=1}^{n} (1 - p_i) . \quad (36)$$

Quantitative predictions of sensitivity from this relation depend upon the assumed relationship between p_i and the value of the response r_i. One convenient and plausible assumption is that

$$p_i = 1 - e^{-|r_i|^\beta} \quad (37)$$

where r_i is the value of the internal response within interval i. If this response is linear, r_i is proportional to stimulus strength. The probability of detection is then

$$p = 1 - e^{-\Sigma|r_i|^\beta} . \quad (38)$$

Thus for all stimuli at threshold (defined as some fixed value of p)

$$1 = \sum_{i=1}^{n} |r_i|^\beta . \quad (39)$$

Note that this expression defines the amplitude scale of the internal response. If the relationship between the stimulus and the internal response sequence r_i is known (for example, if we know the transfer function of an internal linear filter), then this expression provides a method of calculating the effects of probability summation over time.

A successful experimental test of predictions from this analysis was provided by Watson (1979). Additional information on this subject is contained in Sections 4.2, 5.6, and 6.5.2. Other theoretical treatments of probability summation are possible. Nachmias (1981) has shown that details of this analysis (in particular the threshold assumption) are probably incorrect. But this treatment has the virtue of simplicity and is undoubtedly more correct than neglecting probabilistic effects altogether.

3.4. Nonlinear Mechanisms

The threshold mechanism and probability summation are examples of nonlinear operations in the chain of events between stimulus and psychophysical response. Many other nonlinear elements figure in models of temporal sensitivity. These may be loosely divided into three types. The first, such as thresholds and probability summation, are *output* nonlinearities, lying between some internal response and the psychophysical response. Rashbass's early model provides another example. There the linear response is squared, integrated over some epoch, and thresholded (Rashbass, 1970).

The second sort of nonlinearities are adaptive processes. Adaptation is inherently nonlinear, because by definition it violates the principle of superposition. Thus a linear model may be adequate for small signals in a fixed state of adaptation, but a nonlinear mechanism is required to alter the system properties with changes in adaptive state. These frequently appear as feedforward or feedback mechanisms that control the parameters of a linear filter (Fourtes & Hodgkin, 1964).

A third, less frequently considered nonlinearity occurs when signals may pass through any of several independent detection pathways. Examples are so-called *sustained* and *transient* pathways. Even if each pathway is linear, the system is nonlinear, because signals that travel through different pathways violate superposition. This notion is considered further in Section 9.4.

3.5. Detectors and Channels

It is sometimes useful to consider the collection of elements up to and including a threshold device as a single unit, which we call a *detector*. A single stimulus may excite many detectors, and each detector is subject to noise, so a stimulus may from trial to trial be detected by any one of a set of detectors. We call this set of detectors a *channel*.

When a "high threshold" interpretation of the detection process is employed, the channel is that set of detectors in which the response has a nonzero probability of exceeding threshold. If the observer is viewed as applying a more sophisticated computation to the detector outputs, the channel is those detectors entering into the computation.

3.6. Labeled Detectors

If an observer is asked to make some judgment about the appearance of stimuli, then the model must contain some mechanism for the coding of sensory quality. A simple assumption is that the response of each detector can be distinguished from that of all other detectors. This is called a *labeled detector*. Application of this concept is discussed in Section 9.4.1.3.

3.7. Fast, Slow, Transient, and Sustained

In the literature on temporal aspects of vision a number of terms are used whose meanings are not well defined. To avoid confusion, the following clarifications are proposed.

3.7.1. Fast and Slow. The term "fast" has been used to describe either a rapidly developing response, as might lead to a brief reaction time, for example, or the system's ability to follow rapid variation, as reflected in a high fusion frequency. In a linear system, these two properties may be governed by two quite different aspects of the system function. For example, it is quite possible for a high fusion frequency to be associated with a long reaction time, because the latter could be accomplished by an arbitrary delay that does not alter the amplitude response. Unless some other meaning is made explicit, it seems wise to reserve the terms "fast" and "slow" to describe changes in the time scale of the response. In this sense, a faster response shows both of the effects noted.

3.7.2. Transient and Sustained. These terms were used originally by Cleland, Dubin, and Levick (1971) to describe two classes of visual neurons in the cat. The feature of the sustained cell's response that presumably evoked this label was its sustained response to a steady stimulus, whereas a transient cell responded only at onset and offset. Subsequently, the terms have been applied to a wide range of phenomena and hypothetical

mechanisms, many of which have little to do with the form of the temporal response. Thus transient mechanisms are frequently presumed to be nonlinear and relatively more sensitive at low spatial frequencies. It seems important, therefore, to distinguish between the use of these terms as adjectives to describe a characteristic property of the temporal response, and their use as names of hypothetical mechanisms.

We consider below the evidence for distinct mechanisms called by these names. Outside of that context, we reserve the terms to describe a property of the temporal response of a linear filter. A *transient* system is one in which the response to a step input vanishes beyond some time T. Because the response to a step is the convolution of step and impulse response, which is in turn the integral of the impulse response from 0 to t, it is evident that a transient impulse response has an integral of 0 and is briefer than T. It is simple to show that the amplitude response of a transient system vanishes at 0 frequency; thus transience implies attenuation of low frequencies.

The *sustained* system response to a step grows monotonically, eventually reaching an asymptote. Thus the integral of the impulse response is also monotonic, from which we see that the impulse response is always of the same sign. The amplitude response of a sustained system is easily shown to have a maximum at 0 frequency.

Many systems are neither entirely transient nor sustained, in which case the terms may be used in a relative sense. Thus of two systems, that with the greater attenuation at low frequencies would be described as more transient.

Occasionally the term "transient" is taken to imply a higher fusion frequency, or higher sensitivity at high temporal frequencies. The definition given here does not include this implication, which does not in any case agree with the common sense meaning of the word.

4. A WORKING MODEL OF TEMPORAL SENSITIVITY

Many aspects of temporal sensitivity can be understood in the context of a working model, which we introduce here. The model has three important features: (1) a linear filter, (2) probability summation over time, and (3) asymmetric thresholds for increments and decrements.

Aspects of the working model have been suggested by numerous authors. The notion of the eye as a linear temporal filter was first developed by Ives (1922) and later in more detail by de Lange (1952). It has been pursued with great energy by Kelly (1961b) and Roufs (1972b). The idea of probability summation over time has appeared in the work of Blackwell (1963), Ikeda (1965), Roufs (1974b), and many others. The specific computational form used here is given in part by Watson and Nachmias (1977), Rashbass (1976), and Watson (1979) and is introduced in Section 3.3.

4.1. The Linear Filter

The first component in the model is a causal, time-invariant linear filter with impulse response

$$h_1(t) = u(t)[\tau(n_1 - 1)!]^{-1}(t/\tau)^{n_1-1}e^{-t/\tau} , \qquad (40)$$

where $u(t)$ is the unit step function. (The impulse response, system function, and amplitude response are defined in Section 2.) This is the impulse response of a cascade of n_1 identical low-pass stages, each with time constant τ (the low-pass filter is described in Section 2.10.5). It has been normalized so that it has unit area. The maximum occurs at $\tau(n_1 - 1)$ and is equal to $[(n_1 - 1)e^{-1}]^{n_1-1}/\tau(n_1 - 1)!$.

The next component is a second filter identical to the first except that it has time constant $\kappa\tau$, n_2 stages, and is multiplied by a factor ζ. The linear filter of the working model is the difference of these two filters, multiplied by a factor ξ. The impulse response of the working model is then

$$h(t) = \xi[h_1(t) - \zeta h_2(t)] . \qquad (41)$$

The parameter ξ is a sensitivity factor or gain that scales the impulse response and amplitude response up or down in amplitude. The parameter ζ is the "transience factor." When ζ is 0, only the first positive component (h_1) remains, and the impulse response is "sustained" in the sense that the response to a step input rises to a maximum and stays there indefinitely. When ζ is 1, the response is "transient" in the sense that the step response rises to a peak and then declines and vanishes. Examples of the impulse response with various transience factors are shown in Figure 6.4. The system response of the working model is easily derived by noting that

$$H_1(w) = (i2\pi w\tau + 1)^{-n_1} \qquad (42)$$

where w is temporal frequency in hertz and $i = \sqrt{-1}$. This system response can be decomposed into the amplitude response

$$|H_1(w)| = [(2\pi w\tau)^2 + 1]^{-n_1/2} \qquad (43)$$

and the phase response

$$<H_1(w) = -n_1 \tan^{-1}(2\pi w\tau) . \qquad (44)$$

From the linearity of the Fourier transform,

$$H(w) = \xi[H_1(w) + \zeta H_2(w)] . \qquad (45)$$

It is then simple to show that the amplitude response of the linear filter of the working model is

$$|H| = \xi[|H_1|^2 + \zeta^2|H_2|^2 - 2\zeta|H_1||H_2|\cos(<H_1 - <H_2)]^{1/2} \qquad (46)$$

and the phase,

$$<H = \tan^{-1}\left\{\frac{|H_1|\sin<H_1 - \zeta|H_2|\sin<H_2}{|H_1|\cos<H_1 - \zeta|H_2|\cos<H_2}\right\} . \qquad (47)$$

Examples of the impulse, amplitude, and phase responses of the working model are shown in Figure 6.4, along with the corresponding impulse responses. Note that when the transience index is 0, the amplitude response reaches a maximum of unity at 0 Hz, whereas when the index is 1, the amplitude response goes to 0 at 0 Hz.

This particular formulation of the impulse response has been chosen because it is a good approximation to empirical results and for mathematical convenience. For example, the degree of low-frequency attenuation is easily varied by means

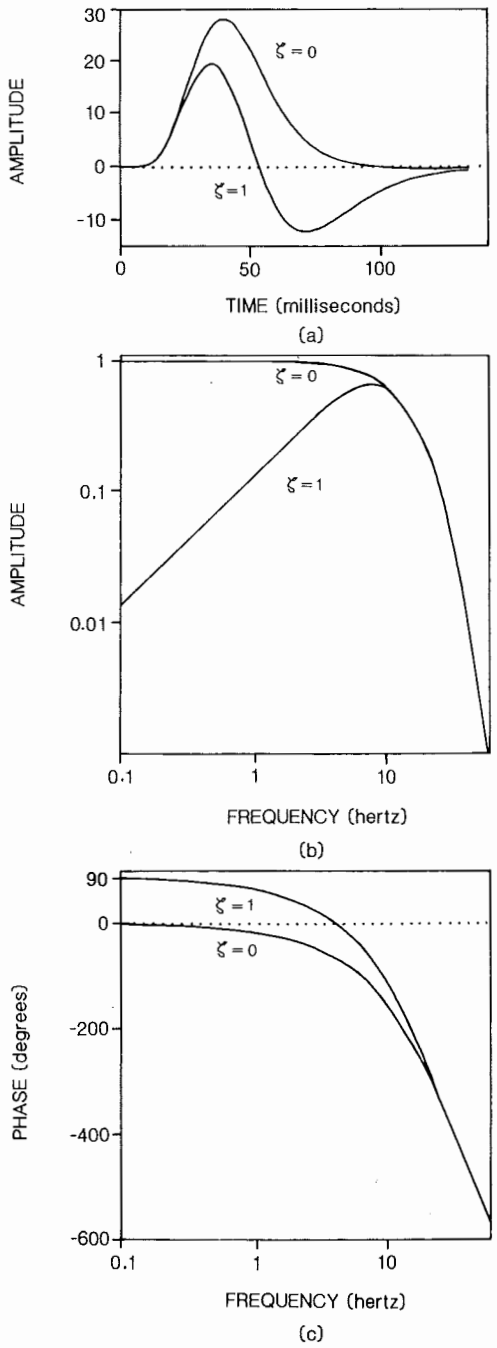

Figure 6.4. The linear filter of a working model of human temporal sensitivity. (a) Impulse responses. (b) Amplitude responses. (c) Phase responses. Responses are shown for the two extreme values of the transience parameter, $\zeta = 0$ and $\zeta = 1$. The other parameters of the filter are time constant $\tau = 4.94$ msec, time constant ratio $\kappa = 1.33$, number of stages in excitatory mechanism $n_1 = 9$ and in inhibitory mechanism $n_2 = 10$, and sensitivity $\xi = 1$. The time constants and number of stages are roughly appropriate for a human observer at high background luminance.

of the transience parameter, the horizontal scale is easily controlled by the time constant τ, and the slope of the high-frequency limb can be controlled by means of κ, n_1, and n_2. By suitable choice of these five parameters, a version of this filter can be found that agrees reasonably well with empirical results. This agreement is illustrated in Figure 6.5. Other models might fit these data equally well. The purpose here is to find a realistic and mathematically convenient form that we can use to illustrate the general properties of temporal sensitivity.

The response to an arbitrary input is the convolution of the input and the impulse response. It is convenient to express the input contrast wave form $C(t)$ as the product of a normalized wave form with unit amplitude, $f(t)$, and a positive constant C equal to the peak contrast of the wave form. The response is then

$$r(t) = Cf(t) * h(t) \tag{48}$$

where $*$ indicates convolution. To compute values of the response it is often necessary to approximate the convolution by a finite sum,

$$r_i = C\Delta t \sum_j f_j h_{i-j} \tag{49}$$

where Δt is the time interval between samples and i and j run over the support of each function. The interval Δt must be made sufficiently small that it can capture the most rapid fluctuations in the response; calculations in this chapter use a value of 5 msec.

4.2. Probability Summation Over Time

The concept of probability summation over time was introduced in Section 3. It is described by the following equation, which states a condition met by all stimuli at threshold:

$$1 = \sum_i |r_i|^\beta \tag{50}$$

where r_i is the value of the response in time interval i and β is the slope of the psychometric function. Combining Eqs. (49) and (50), and rearranging terms so as to leave us with an expression for the contrast at threshold, we get

$$C = \Delta t^{-1}\left[\sum_i \left|\sum_j f_j h_{i-j}\right|^\beta\right]^{-1/\beta}. \tag{51}$$

This equation predicts threshold for an arbitrary temporal wave form, given the parameters of the model. Note that the comparisons between model and data shown in Figure 6.5 do not take probability summation into account. In the experiments involved, the duration of the stimulus was not controlled so that a calculation of Eq. (51) cannot be performed. Had probability summation been included, the sensitivity factor ξ would be reduced by a small amount.

4.3. Asymmetric Thresholds

It has been assumed thus far that the model is equally sensitive to positive and negative excursions of the response; the absolute value operation in Eq. (51) ensures that positive and negative response values contribute equally to the probability of detection. Under many circumstances, this is an accurate assumption. In other cases, the system is more sensitive to decrements than to increments (see Section 8). This situation is incorporated into the working model by assuming a higher threshold for increments than for decrements. Computationally, it is done by weighting positive increments by a parameter ρ. Then we can replace Eq. (50) by

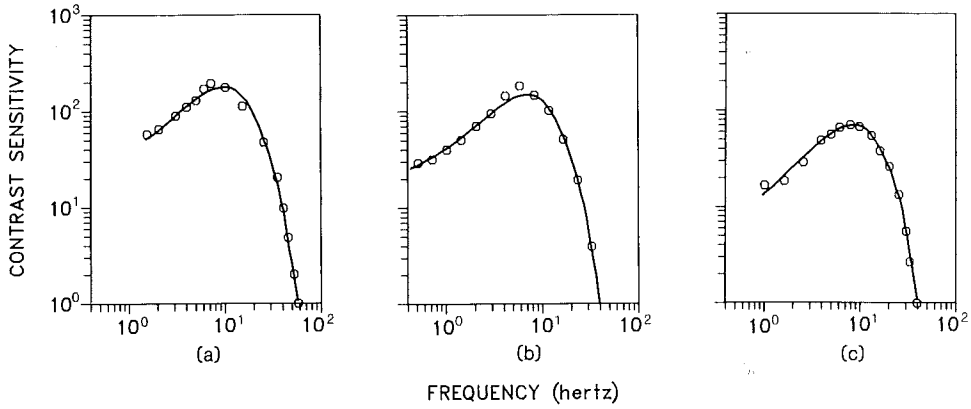

Figure 6.5. Temporal contrast sensitivity functions of the working model (curves) and of human observers (points). All thresholds collected by method of adjustment. Standard deviations probably about 0.05 log unit. Curves are the amplitude response of the linear filter of the working model, with parameters adjusted to approximately match the data. Model parameters common to all curves: $\kappa = 1.33$, $n_1 = 9$, $n_2 = 10$. (a) Data from de Lange (1958), observer V, 2° disk, background and surround 1000 td. Model parameters: $\tau = 4.3$ msec, $\zeta = 0.9$, $\xi = 269$. (b) Data from Robson (1966), 0.5 cycles·degree^{-1} grating, background and surround 20 cd·m^{-2} (≈200 td). Model parameters: $\tau = 6.22$ msec, $\zeta = 0.9$, $\xi = 214$. (c) Data from Roufs and Blommaert (1981), observer JAJR, 1° disk, background 1200 td, no surround. Model parameters: $\tau = 4.94$ msec, $\zeta = 1$, $\xi = 200$.

$$1 = \sum_i \begin{cases} (\rho r_i)^\beta & r_i \geq 0 \\ (-r_i)^\beta & r_i < 0 \end{cases} . \qquad (52)$$

When $\rho = 0$, only negative excursions are effective; when $\rho = 1$, positive and negative excursions are equally effective; and when $\rho > 1$, positive excursions are more effective than negative.

4.4. Summary of Parameters of the Working Model

The eight parameters of the working model are the time constant τ, the ratio of time constants κ, the stage numbers n_1 and n_2, the sensitivity factor ξ, the transience factor ζ, the exponent β, and the asymmetry factor ρ.

5. SENSITIVITY TO SINUSOIDS

5.1. Background

Although they appear to give off a steady, constant illumination, many light sources in our world (fluorescent lamps, television, and movies are commonplace examples) in fact produce an amount of light that varies rapidly in time. The effort to understand this insensitivity of the eye to rapid fluctuations has generated a prodigious amount of research, a great deal of it concerned with the *critical flicker frequency* (CFF) for periodic wave forms. A periodic wave form, of which the examples given are instances, repeats itself once each period of T sec. Limited means of controlling light intensity confined early studies to wave forms alternating between "on" and "off." By increasing the frequency of alternation, a light could be made to pass from "flicker" (perceptible variation in intensity) to "fusion" (steady appearance of a fluctuating light). The CFF marked the border between flicker and fusion. These early experiments were concerned primarily with the effects of wave form (the particular shape of the function during one period), with the wave form amplitude, and with the brightness of a periodic stimulus beyond the fusion limit. Some progress was made on the latter two issues: CFF was found to rise linearly with the log of time-average background intensity (the *Ferry-Porter law*: Ferry, 1892; Porter, 1902), and a fused stimulus was found to be as bright as a steady stimulus of the same time-average intensity (the *Talbolt-Plateau law*). The first law is only approximate (as can be seen in Figure 6.28 in Section 11), and has been amended by Kelly (1964).

In the early 1950s, and culminating in his papers of 1954 and 1958, de Lange developed a novel approach that so altered the experimental and theoretical perspective on this problem that much of the earlier work was rendered obsolete (de Lange 1954, 1958). Three aspects of de Lange's work were remarkable. First, he provided independent control of background and target luminance. In previous experiments in which the light alternated only between on and off, a change in the amplitude of the wave form inevitably resulted in a change in the time-average background intensity, and consequently in the adaptive state of the eye. De Lange adopted a procedure whereby wave form amplitude might be changed without alteration of the time-average background. This in turn allowed production of wave forms with equal time-average background, but differing contrast.

This technical innovation paved the way for de Lange's second advance. By generating a wave form of unit contrast and adjusting frequency until flicker gave way to fusion, he could measure the conventional CFF. But by setting contrast to values less than unity and repeating the procedure, he could also measure the more complete function relating fusion frequency to contrast. Several examples of this function, obtained with various wave forms on various backgrounds, are shown in Figure 6.6.

De Lange's third and most important innovation was his use of linear systems theory to provide a coherent interpretation of data like those in Figure 6.6. To illustrate his approach, consider the uppermost wave form in the inset to Figure 6.6. It is reproduced in Figure 6.7, along with its *amplitude spectrum*, the function specifying the amplitudes of sinusoids into which the wave form may be decomposed. In the case of the 10-Hz square wave illustrated here, the spectrum contains odd *harmonics* of frequencies 10, 30, and 50 Hz, and so on, with amplitudes of $I(4/\pi)$, $I(4/3\pi)$, $I(4/5\pi)$, and so on.

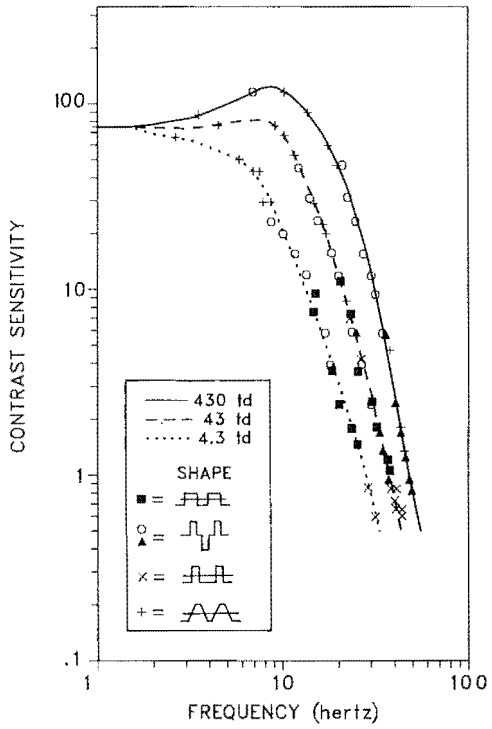

Figure 6.6. Contrast sensitivity for several periodic wave forms as a function of temporal frequency. The wave forms are shown in the inset. Sensitivity is plotted as the inverse of the contrast of the fundamental sinusoidal component in each wave form. Thresholds are the same for all wave forms above 10 Hz, as predicted by a linear model. Target was a 2° foveal disk with a large surround. Data for three background luminances are shown. (From H. de Lange, Relationship between critical flicker frequency and a set of low-frequency characteristics of the eye, *Journal of the Optical Society of America*, 1954, *44*. Reprinted with permission.)

If the visual system responds linearly to perturbations near the threshold of visibility, then its behavior can be characterized by a *transfer function*, specifying the amplitude and phase with which various frequencies are passed through the system (see Section 2). Suppose that the amplitude component of this function is given by the curves in Figure 6.6, at least above 10 Hz. To determine the amplitude spectrum of the response to a square wave of 10 Hz, we simply multiply the input spectrum by the function describing de Lange's data. The result, shown in Figure 6.7, is very nearly a pure sinusoid of 10 Hz. The higher harmonics have been almost entirely filtered out. This suggests that at 10 Hz the contrast threshold for a square wave should be the same as that for a sinusoid of equal fundamental amplitude. This rule should hold even more precisely for frequencies above 10 Hz, because the higher harmonics will be still more severely attenuated.

This rule also applies to any periodic wave form in which the higher harmonics, after multiplication by the amplitude response function, are much smaller than the fundamental. This includes most simple periodic wave forms with fundamentals above 10 Hz. The various symbols in Figure 6.6 show the success of this analysis. Thresholds for all four wave forms used by de Lange fall upon a common curve above 10 Hz, as the linear hypothesis predicts.

The first consequence of this observation was to bring to an end more than a century of investigation of wave form *per se* as a determinant of sensitivity. Beyond those experiments required to document the premise of linearity, empirical measurements of sensitivity to various wave forms were no longer required. The second consequence was to initiate a quarter century of vigorous pursuit of the many ramifications of the linear theory. A third consequence was to confer special status (perhaps too special) upon the sinusoid as a temporal stimulus. The following section reviews some of the fundamental aspects of thresholds for sinusoidal modulation. Table 6.2 notes some of the more important contributions in this area. An interesting view of the subject of "flicker" at an early and active stage in its development is given by the symposium papers in Henkes and van der Tweel (1964). The classic review is by Kelly (1972b).

5.2. The Temporal Contrast Sensitivity Function

When the contrast of a target is varied sinusoidally at some frequency, sufficiently small amplitudes are invisible; that is, they are not distinguishable from a target with zero contrast. The oscillation is said to have "fused." As the amplitude is raised, the target may become visible. The transition to visibility is called the *contrast threshold*, and its inverse, *contrast sensitivity*. A plot of contrast sensitivity versus temporal frequency is called a *temporal contrast sensitivity function* (TCSF).

In the experiments shown in Figure 6.6, de Lange was unable to generate true sinusoids, although his trapezoidal wave form was quite close. In 1958, however, he published extensive measurements of the TCSF for two observers at a number of background intensities. Some of these classic results are reproduced in Figure 6.8. They illustrate several general features of the TCSF. At the higher luminances, a peak in sensitivity of about 200 (a threshold contrast of about 0.005) occurs at about 8 Hz. Above this frequency, sensitivity falls precipitously. In log-log coordinates, the curve appears to accelerate downward. For a sinusoid, the CFF is the highest frequency at which contrast sensitivity is equal to 1. Following the curve downward, the CFF is reached at a frequency of between 50 and 70 Hz. Sensitivity also declines at low frequencies, but the drop is less rapid and stops at a sensitivity of about 50.

It should be emphasized that the TCSF is not a single invariant function. Rather, the form of the TCSF is subject to large alterations, depending primarily upon the background intensity, the spatial configuration of target and surround, the observer, and the method by which the thresholds are obtained. Several authors have noted that the TCSF may be viewed as a slice through a many-dimensioned surface (Kelly, 1972a; Koenderink & van Doorn, 1979). This perspective is often useful in appreciating the interaction between temporal frequency and some other variable, but is obviously limited to two variables at a time.

Before considering the many variations to which the TCSF is subject, it may be worth noting certain general properties of these effects. First, many experimental manipulations appear to have different consequences for those frequencies above the right-hand shoulder of the curve and for those below it. In the traditional log-log coordinates that we use, the high-frequency limb tends only to translate horizontally or vertically. These motions correspond to scaling operations on frequency or sensitivity (equivalent to changes in the time scale τ and sensitivity parameter ξ of the working model). Effects on the low-frequency limb of the curve are more complex, but generally consist of changes in the degree to which the curve drops at low frequencies (equivalent to changes in the transience parameter ζ of the working model). These are simplifications, and should not blind the reader to more subtle features of the TCSF. They are meant

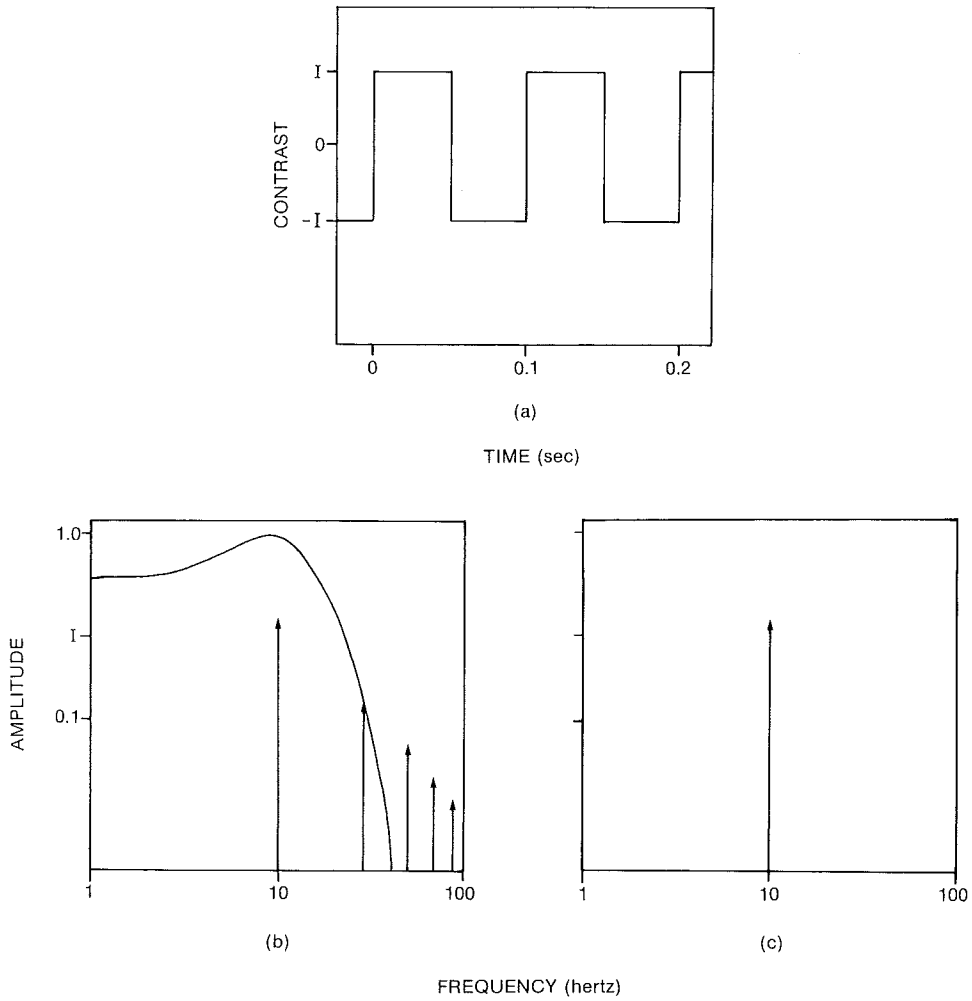

Figure 6.7. An explanation of why thresholds for a square wave and a sine wave are equal at high temporal frequencies. (a) The square wave of frequency 10 Hz and intensity I. (b) The amplitude spectrum of the square wave. The height of each impulse indicates the intensity of the component at the corresponding temporal frequency. The impulse at 10 Hz is the fundamental. Also shown is the amplitude response of a hypothetical linear filter, adapted from de Lange's data in Figure 6.6. (c) The result of multiplying the amplitude spectrum of the square wave by the amplitude response of the filter. Only the fundamental remains, hence thresholds for the square wave and its fundamental are the same.

only to help guide the eye over the results in the following sections.

5.3. The Working Model

To predict empirical thresholds for sinusoidal wave forms from the working model we must know the duration of each stimulus, because probability summation over time causes threshold to decline for as long as the stimulus is exposed. However, when thresholds are collected by method of adjustment (as has most often been the case for sinusoidal wave forms), the duration is unspecified. But if we assume that probability summation over time affects all frequencies equally, then we can compare the amplitude response of the linear filter of the model directly to the empirical TCSF. This is done for three selected data sets in Figure 6.5 in Section 4. The figure illustrates that the model gives a good account of the TCSF under these conditions. The changes in model parameters in the three cases are small and confined to the overall sensitivity ξ, the time constant τ, and the transience ζ. These changes are due to differences in background intensity and spatial configuration. Larger changes in spatial configuration often produce more substantial changes in model parameters.

5.4. Effects of Spatial Configuration

The effects of spatial configuration upon temporal sensitivity are dealt with in Section 9. A summary of those effects is that the form of the high-frequency limb of the TCSF is largely unaffected by spatial configuration, but that the low-frequency limb is raised by the presence of edges, high spatial frequencies, or a surround. Taken together, these results are consistent with the idea that effective high spatial frequencies in the stimulus result in a more "sustained" TCSF. This effect is lessened at low background intensities, all spatial targets then giving a more or less "sustained" result.

5.5. Effects of Background Intensity

This subject is examined in detail in Section 11. In general, as background intensity is raised, luminance thresholds increase. However, the increase is less rapid at high temporal frequencies

Table 6.2. Selected Studies of Sinusoidal Flicker

Reference	Spatial Stimulus	Variables
de Lange, 1954	2° disk with surround	Wave form, background intensity
de Lange, 1958	2° disk with surround	Background intensity
Kelly, 1959	2, 4, 60° disks with & w/o surround	Target size, surround
Kelly, 1961a	60° disk, blurred edges	Background intensity
Robson, 1966	Sinusoidal grating	Spatial frequency
van Nes, Koenderink, Nas, & Bouman, 1967	Drifting grating surround	Background intensity, threshold criteria
Keesey, 1972	1° × 4 min bar, surround	Threshold criteria
Kelly, 1972a	Sinusoidal gratings	Spatial frequency, background intensity
Roufs, 1972a	1° disk with & w/o surround	Background intensity
Kulikowski & Tolhurst, 1973	Sinusoidal gratings	Threshold criteria, spatial frequency
Roufs, 1974b	1° disk w/o surround	Duration
Koenderink, Bouman, Bueno de Mesquita, & Slappendel, 1978	Sinusoidal grating no surround	Eccentricity, background intensity
Koenderink & van Doorn, 1979	Sinusoidal gratings	Spatial frequency
Watson, 1979	Sinusoidal gratings	Duration
Virsu, Rovamo, Laurinen, & Nasanen, 1982	Patch of grating	Eccentricity, spatial frequency

than at low. Expressed in contrast terms, sensitivity increases more rapidly at high temporal frequencies than at low as the background is raised. As a consequence, the low-frequency limb of the TCSF drops as background intensity is increased, as shown by de Lange's data in Figure 6.5. This figure also shows that raising background intensity also shifts the TCSF to higher frequencies. In terms of the working model, these two effects can be accommodated by lowering the time constant τ and increasing the transience ζ as background intensity is raised.

5.6. Effects of Duration

If the duration of a sinusoidal wave form is brief, its spectrum extends above and below its nominal frequency, and sensitivity depends in a complex way upon frequency, duration, and the TCSF. Similarly, if the onset and offset of the sinusoid are abrupt, higher frequencies are introduced that may influence sensitivity. If the duration is substantial (greater than 100 msec) and if the onset and offset are gradual, these problems are largely eliminated, yet duration still has a small but significant effect upon sensitivity. When a gradual onset and offset are accomplished by means of a Gaussian gating function, sensitivity increases approximately as the ¼ power of duration (Watson, 1979). Roufs (1974b), using a slightly different gating function, has obtained comparable results.

Roufs (1974b) and Watson (1979), using somewhat different assumptions, have shown that this is predicted by probability summation over time (see Sections 3.3 and 4.2). In essence, each moment of the presentation provides an independent opportunity to detect the stimulus; as the duration is extended, the number of opportunities grows, and the overall probability of detection is increased. In Watson's formulation, sensitivity should increase with duration at a log-log slope of $1/\beta$, where β is the slope of the psychometric function. The observed slope of ¼ corresponds well to observed psychometric function slopes of about 4 for these conditions (Watson, 1979).

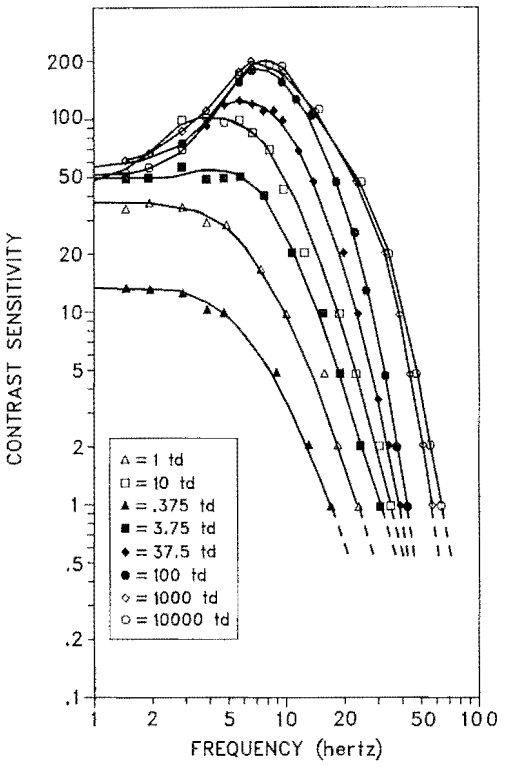

Figure 6.8. The temporal contrast sensitivity function at several background intensities. The temporal wave form was sinusoidal; target was a 2° disk with a large surround. Curves are drawn by eye. On a bright background, sensitivity increases with temporal frequency from about 50 to a peak of about 200 at around 8 Hz, then falls to a CFF of about 60 Hz. The ordinate is extended to sensitivities of 0.5 (contrast = 2.0) because although sinusoids with contrast of 2.0 cannot be constructed, wave forms with a fundamental this large can be produced (data from observer V of de Lange, 1958).

5.7. Effect of Eccentricity

Rather little is known about how the TCSF depends upon the location of the target within the visual field. Sharpe (1974) measured temporal contrast sensitivity for gratings of 0.8, 1.5, 3.5, and 5.5 cycles·degree^{-1}, centered 10° into the left temporal visual field, drifting at various velocities. His results resemble those of Robson (1966) (Figure 6.20 in Section 9) in showing more transience at low spatial frequencies. Apart from the expected decline in spatial resolution, there is little systematic change from the foveal results.

Koenderink, Bouman, Bueno de Mesquita, and Slappendel (1978) have published results that show little variation in the shape of the TCSF when measured with a 0.5 × 0.5°, 4 cycles·degree^{-1} grating target with dark surround at locations of 1, 2, 4, 6, and 8°. With a 4 × 4 °, 0.5 cycles·degree^{-1} target, slightly more relative attenuation is evident at the fovea than at locations of 6, 12, 21, 32, and 50°. The lack of surround and small target size (2 cycles of the grating) make these results somewhat difficult to compare to other data.

One recent result suggests that the temporal properties of the retina are homogeneous, and that all variations with eccentricity are due to spatial inhomogeneity. Virsu, Rovamo, Laurinen, and Nasanen (1982) found that sensitivity to foveal targets was approximately the same as that to peripheral targets that had been magnified so as to occupy an equal cortical projection area. This is consistent with the idea that spatial processing is homogeneous across the retina except for a change in spatial scale. They also found that this result held equally well at temporal frequencies of 0, 1, 4, and 18 Hz. This strongly suggests that the temporal processing is also homogeneous across the retina. In this view, the variations in temporal behavior with eccentricity reported elsewhere are consequences of the change of spatial scale, rather than of temporal processing.

5.8. Effect of Threshold Criteria

In his 1958 report, de Lange noted a difference in the nature of the flicker perception depending on "frequency." This observation has been echoed by many subsequent authors: at high temporal frequencies, stimuli near threshold appear to "flicker," whereas at low temporal frequencies the percept is of a more gradual variation (aptly termed "swell" by Roufs, 1972a). When an adjustment method is used, it may be difficult to equate criteria in the two frequency ranges.

Van Nes, Koenderink, Nas, and Bouman (1967) made a further distinction. With drifting gratings as targets, they reported that as contrast was reduced, the spatial variations in brightness disappeared before temporal variations, so that separate "flicker" and "pattern" thresholds could be observed. Similar suggestions were made by Rashbass (1968), Watanabe, Mori, Nagata, and Hiwatashi (1968), Pantle (1970), and Richards (1971).

Keesey (1972), noting a similar distinction among judgments for a narrow bar whose contrast was modulated sinusoidally in time, measured each of the two thresholds separately at temporal frequencies between 0.4 and 30 Hz. The two temporal sensitivity functions did not differ by a constant factor, and the flicker threshold was not invariably below the pattern threshold.

With grating targets of various spatial frequencies, Kulikowski and Tolhurst (1973) obtained temporal sensitivity functions using both flicker and pattern criteria (see Fig. 6.24 in Section 9). In agreement with Keesey's data, flicker sensitivity declines at low temporal frequencies, but pattern sensitivity does not. The two curves intersect at an intermediate temporal frequency, so that at high temporal frequencies, flicker sensitivity is greater than pattern, whereas at low temporal frequencies the reverse is true. Their interpretation was essentially that of Keesey: each criterion was attributed to a different mechanism, as though the two curves described the temporal contrast sensitivities of distinct flicker and pattern detectors. As further evidence for this idea, they noted that the two curves moved independently with changes in spatial frequency. An increase in spatial frequency lowered the sensitivity curve of the flicker mechanism much more than it lowered the curve of the pattern mechanism.

By analogy to retinal cells of the same name (Cleland et al., 1971), and because the flicker curve showed low-frequency attenuation whereas the pattern curve did not, these two sorts of detectors were called *transient* and *sustained* mechanisms, respectively. Section 9.4 contains a review of the theory of sustained and transient detectors.

5.9. Effect of Eye Movements

When a stimulus contains both temporal and spatial variations, movements of the eye influence the temporal distribution of the stimulus. The TCSF is ordinarily measured with the eye fixating a mark, but it is well known that various eye movements occur during fixation (Riggs, Armington, & Ratliff, 1954).

Therefore the effect of these fixational eye movements upon the TCSF must be considered.

One method of assessing the effects of eye movements is to remove them by stabilizing the image upon the retina. Kelly (1979) and Tulunay-Keesey and Jones (1980) have shown that prolonged viewing of high-contrast, stationary, stabilized gratings leads to very large reductions in sensitivity. This reduction may be 1 log unit or more at the lower spatial frequencies. It appears that these conditions give rise to a strong afterimage, which profoundly alters the properties of the contrast-detecting mechanisms (Burbeck & Kelly, 1982; Kelly, 1982).

However, when brief (7-sec) presentations at contrasts near to threshold are used, the difference between stabilized and unstabilized thresholds is always less than 0.3 log units (Tulunay-Keesey & Jones, 1980; Tulunay-Keesey, 1982). These differences were obtained with a temporal presentation (Gaussian with duration of 7 sec) that is essentially a measure of sensitivity to 0 Hz. Because we would expect higher temporal frequencies to reduce the difference between stabilized and unstabilized thresholds, we may conjecture that the TCSF measured with brief, fixated, unstabilized presentations of near-threshold contrast would differ from the equivalent stabilized data by less than 0.3 log units. This would imply that the TCSF is adequately measured with unstabilized viewing. But, remarkably, no data have been published that directly compare stabilized and unstabilized TCSFs under these conditions. Kelly (1977) has published comparisons of stabilized and unstabilized TCSFs, but these thresholds were collected following prolonged viewing (and hence adaptation), and thus do not reflect purely the contribution of fixational eye movements to the TCSF. Nevertheless, they show that most of the effect of stabilization is absent when the temporal frequency is 0.1 Hz or above.

5.10. Combinations of Frequencies

Much of the theoretical value of the TCSF rests upon the assumption that thresholds are governed by a linear filtering process. One possible test of this assumption is to examine thresholds for combinations of several frequencies. A nonlinearity of particular interest is that introduced by multiple independent channels selective for temporal frequency. Summation between different frequencies is an appropriate test for the existence of such pathways. However, we shall see that the predictions of the linear model in this context depend rather strongly on the nature of the assumed output nonlinearity.

J. Z. Levinson (1960) measured thresholds for compound wave forms made by adding together sinusoids of 10 and 20, or 20 and 40 Hz. The two components had "equal sensation levels"; that is, each was added in proportion to its individual threshold. The wave forms controlled the contrast of a 1° disk target (background = 685 cd·m^{-2}, surround = 130 cd·m^{-2}). Levinson noted that threshold for the compound, expressed as fraction of threshold for either component alone, varied according to the relative phase of the two components, as shown in Figure 6.9. Levinson pointed out that the compound wave form inverts itself with every 180° change in relative phase, but the threshold minima occur only every 360°. He suggested that this might be explained by a detector with a higher threshold for excursions of one sign than of the other, and demonstrated the principle with an analog model (J. Z. Levinson & Harmon, 1961).

Asymmetric thresholds can be introduced into the working model by weighting positive excursions by a factor ρ, as noted in Section 4.3. When ρ = 1, positive and negative excursions

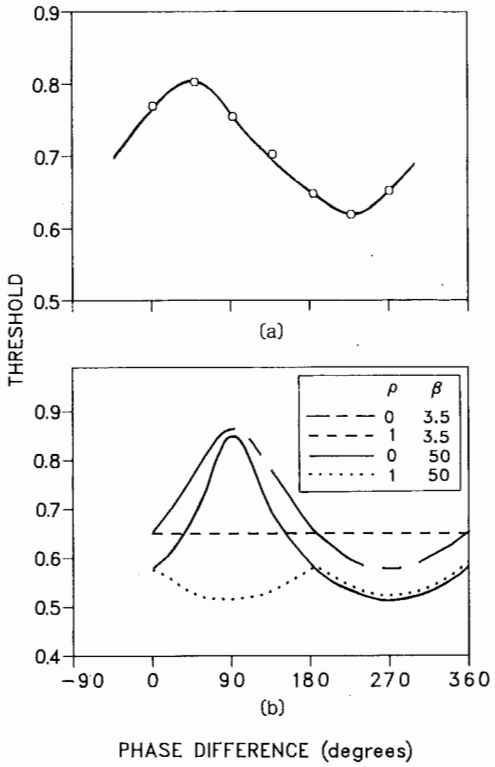

Figure 6.9. Threshold for the sum of two different temporal frequencies as a function of the phase difference between the two components. (a) Data from J. Z. Levinson (1960). The frequencies were 10 and 20 Hz, and the contrast of each component was an equal fraction of its threshold. The phase difference is the lag of the high-frequency component. Thresholds are plotted as fractions of the single-component thresholds (sensation magnitudes). The smooth curve is the fit of the working model with a threshold asymmetry factor (ρ) of 0.65, a β of 3.5, and a phase difference between component responses of about 45°. The curve has also been shifted upward by 0.05. (b) Predictions of the working model for various values of β and ρ. A β of 3.5 simulates probability summation; a value of 50 simulates no probability summation. A ρ value of 0 means that positive excursions of the filter output are invisible; a value of 1 means that positive and negative excursions are equally effective. The model fits best when the phase response at 10 Hz is about 45° greater than that at 20 Hz, when there is probability summation, and when decrements in the filter response are considerably more effective than increments.

are equally effective; when ρ = 0, only negative excursions are effective. Recall that probability summation may be modeled with β = 3.5, and the absence of probability summation with β = 50. Some predictions of this model are shown in Figure 6.9. The data seem to refute any version that lacks probability summation, both because they show too little summation (the prediction is generally below the data), and because the data show only a modest dependence on phase. Likewise the data reject a model with probability summation but with no asymmetry, because it predicts no dependence upon phase. The data seem reasonably well fitted by the probability summation model if ρ is set to 0.65 and a phase difference of about 45° is assumed between 20 and 10 Hz. The curve must also be displaced upward by about 1 standard deviation, as might occur if the normalizing threshold for the single component were overestimated by this much.

A threshold asymmetry might be encouraged by Levinson's adjustment method. For example, the observer might adjust until a certain criterion darkness was seen, and ignore the

bright phases. It would certainly be of interest to repeat these experiments with a forced-choice method, both to reexamine the evidence for threshold asymmetry, and because they may constitute the only known method of estimating the phase response of the linear model.

Using spatially sinusoidal grating targets, Watson (1977) examined thresholds for combinations of a wide range of temporal frequencies. The general finding was that for spatial frequencies of 2, 4, and 10 cycles·degree^{-1} and temporal frequencies of between 1 and 20 Hz, with pairs separated by as much as 8 Hz, only modest departures were observed from the predictions of a linear model with probability summation. The departures were never of the size predicted by narrow band (less than 8 Hz) temporal frequency tuned channels. The data, however, could not rule out the existence of two independent pathways, one moderately selective for high temporal frequencies, the other moderately selective for low.

5.11. Theory

Landis (1953) provides an annotated bibliography of the profusion of experimental work, and some theory, done on periodic wave forms of various kinds during the years 1740–1952. The earliest explicit model of flicker sensitivity was given by Ives (1922), who proposed a log transform followed by diffusion, leaky transmission, and peak detection. De Lange (1952, 1954, 1958) explicitly introduced the application of Linear Systems Theory to temporal sensitivity, and showed how treating the eye as a linear filter could rationalize the great mass of data on flickering periodic wave forms. He also argued that the Talbolt-Plateau law (brightness above fusion is equal to time-average brightness) implied that any nonlinear elements should follow rather than precede the linear filter. His model of the filter consisted of 10 resistance-capacitance filters in cascade (see Section 2.10.5), together with an induction element to attenuate at low frequencies. J. Z. Levinson (1966) has noted that the n low-pass stages in de Lange's model are mimicked by a one-stage statistical process, so the n-stage model need not imply n physical stages.

Kelly (1961b) proposed a two-stage model to account for the pronounced attenuation at low frequencies found with large targets, and the effects of light adaptation. The first stage is a linear filter with both differentiating and integrating components. The second stage is a "pulse encoder" that acts as a nonlinear low-pass filter whose bandwidth is controlled by the background luminance.

Fourtes and Hodgkin (1964) noted that changes in background intensity have a much greater effect on sensitivity than upon the CFF (see Fig. 6.30 in Section 11.4). They observed that this was consistent with an n-stage low-pass filter with time constant τ, because sensitivity is proportional to τ^{n-1}, whereas CFF varies in inverse proportion to τ. They extended de Lange's model to a range of background intensities by introducing feedback stages controlling the time constants in each stage. Sperling and Sondhi (1968) and Matin (1968) have proposed more elaborate but similar models.

Departing from the custom of following the linear filter with a simple threshold mechanism, Rashbass (1970) proposed that the filter output was squared and integrated over an epoch of about 200 msec, and that this signal was then thresholded. Subsequent work has shown that this model, though an elegant solution to the problem it addressed, is not consistent with other results (Watson, 1979), but is a special case of a more general model (essentially the working model of Section 4).

Kelly (1969a) has proposed a diffusion model that gives a good account of the high-frequency asymptote of the TCSF collected at various background intensities (see Fig. 6.29 in Section 11.4). More recently Kelly and Wilson (1978) have partitioned this diffusion process into two stages, which they attribute to first- and second-order neurons. The diffusion process describes only the high-frequency portion of the TCSF. To account for the low-frequency performance Kelly (1971a, 1971b) has appended an inhibitory feedback loop whose parameters are controlled by the background intensity and spatial configuration.

Noting that certain pulse and pulse-pair thresholds call for more low-frequency attenuation than is evident in the TCSF, Roufs (1974a) has proposed that the TCSF is the envelope of two underlying functions, one band pass and sensitive to middle and high frequencies, the other low pass and sensitive only at the lower frequencies. Though based on quite different evidence, this theory closely resembles Kulikowski and Tolhurst's (1973) conjecture of separate "transient" and "sustained" channels (see Section 9.4). The two sets of authors agree in attributing distinct threshold sensations ("agitation" and "swell" in Roufs' terms) to the two filters.

6. SENSITIVITY TO RECTANGULAR PULSES

6.1. Background

A rectangular pulse target with duration T may be written

$$I(t) = Ip_T(t) = I[u(t) - u(t - T)] \qquad (53)$$

where $p_T(t)$ is a pulse of unit height and duration T that starts at $t = 0$, I is the intensity of the pulse, and $u(t)$ is the unit step function. The pulse has a value of I within the interval $(0, T)$ and a value of 0 elsewhere (see Figs. 6.2 and 6.10). Dividing $I(t)$ by the background intensity I_B gives the target contrast wave form $C(t)$. Experimental studies of sensitivity to pulses typically consist of measuring threshold intensity at various durations. A plot of threshold as a function of duration, conventionally on log-log coordinates, is called a *threshold-duration function.*

There have been numerous studies of this function since Bloch (1885). In most of the classical work, targets were circular disks, and principal variables investigated were stimulus size and background intensity. More recently, motivated by evidence that contrast detectors are selective for spatial frequency (see Chapter 7 by Olzak and Thomas), spatial grating targets have also been used.

In early work the threshold-duration function was explained largely in terms of "temporal summation," or integration over some interval of time. More recent explanations appeal to the integrative properties of a more general class of linear filters. Recognition of the stochastic nature of the detection process has led to additional improvements in our understanding of the threshold-duration function, particularly for pulses of long duration. Table 6.3 summarizes some of the published studies, indicating the spatial configuration of the target and the principal variables investigated.

Table 6.3. Selected Studies of Sensitivity to Pulses

Reference	Spatial Target	Variables
Arend, 1976	Sine grating	
Barlow, 1958	Foveal disk	Size, background intensity
Baumgardt & Hillmann, 1961	Peripheral disk	Size
Bouman, 1950	Peripheral disk	Size, background intensity
Breitmeyer & Ganz, 1977	Sine grating	Spatial frequency
Brindley, 1952	Foveal disk	brief durations
C. H. Graham & Kemp, 1938	Foveal hemidisk	Background intensity
C. H. Graham & Margaria, 1935	Peripheral disk	Size
Herrick, 1956	Foveal disk	Background intensity
Keller, 1941	1° hemidisk	Background intensity
Krauskopf & Mollon, 1971	Foveal disk	Background intensity, background wavelength
Legge, 1978	Sine grating	Spatial frequency
Nachmias, 1967	Square grating	Spatial frequency
Owen, 1972	Peripheral disk	Size, background intensity
Rashbass, 1970	17° foveal disk	
Roufs, 1972a	Foveal disk	Size, background intensity
Schober & Hilz, 1965	Square grating	Spatial frequency
Tolhurst, 1975a	Sine grating	Spatial frequency
Tulunay-Keesey & Jones, 1976	Sine grating	Stabilization, spatial frequency

6.2. The Threshold-Duration Function

A classical formula relating sensitivity to duration is that, where conditions are otherwise fixed, a pulse briefer than some *critical duration* will be at threshold when the product of its duration and intensity (the product of contrast and background intensity) equals a constant. This is *Bloch's law* (Bloch, 1885). In units of intensity it may be written

$$IT = I_c T_c \quad \text{for } T \leq T_c \ , \tag{54}$$

where T_c is the critical duration and I_c is the *critical intensity* given by the threshold intensity at the critical duration. For pulses longer than the critical duration, the classical formula states that threshold amplitude is constant,

$$I = I_c \quad \text{for } T > T_c \ . \tag{55}$$

By dividing target intensity by background intensity, these rules can be restated in terms of contrast, $CT = C_c T_c$ below the critical duration, and $C = C_c$ above it.

These rules are sketched in Figure 6.10. In log-log coordinates, Bloch's law [Eq. (54)] describes a line with a slope of -1. The second formula [Eq. (55)] is described by a horizontal line. These are the "two limbs" of the threshold-duration function. Actual data rarely conform precisely to this template, but it nevertheless serves as a useful model from which departures are readily described.

There seems little doubt that whatever the other dimensions of the stimulus and whatever the background conditions, there exists a critical duration below which Bloch's law is upheld. Such a range has been demonstrated for foveal and peripheral viewing, for disk targets with radii from 0.0059 to 17°, for targets with and without a surrounding background, for sinusoidal gratings between 0.3 and 10 cycles·degree^{-1} and for background intensities ranging from 0 to 6500 td (Arend, 1976; Barlow, 1958; Herrick, 1956; Rashbass, 1970; Roufs, 1972a). Brindley (1952) has shown that the range extends down to at least 400 nsec. There are several reports of initial slopes more gradual than prescribed by Bloch's law, but it seems most likely that they arise from the ambiguities inherent in fitting straight lines to a function whose slope changes gradually (Legge, 1978; Nachmias, 1967; Owen, 1972). If the fitting is confined to durations less than 20 msec, then there are no published instances

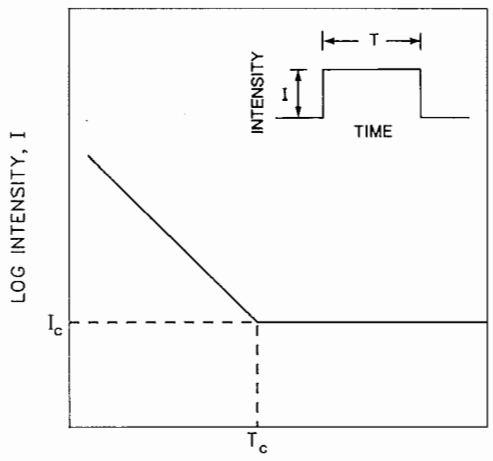

Figure 6.10. An idealized threshold-duration function. The function describes thresholds for rectangular pulses as a function of duration. In log-log coordinates, the left limb of the curve has a slope of -1 (Bloch's law); the right limb has a slope of 0. The transition between the two limbs occurs at the critical duration T_c and the critical intensity I_c. The inset shows the wave form of a rectangular pulse with duration T and intensity I.

of a significant violation of Bloch's law. As will be discussed, there are theoretical reasons for expecting reciprocity between amplitude and duration for some range of brief durations.

Outside of Bloch's regime, thresholds decline less rapidly with increasing duration. There is considerable variety in the actual pattern of decline, but two general trends are evident. For relatively large or low spatial frequency targets, there is a rapid transition to a slope of 0, consistent with Eq. (55), indicating a threshold that is independent of duration. This pattern is evident in Barlow's data shown in Figure 6.11, as well as in Herrick's (1956) and Roufs' (1972a) data for 1° foveal disks, in Nachmias's (1967) data for 0.7° square-wave gratings and in Legge's (1978) data for sine gratings of 0.75 cycles·degree^{-1} and below. For small or high spatial frequency targets, the departure from Bloch's law is more gradual, and does not necessarily resolve to a straight line in log-log coordinates. Barlow's data in Figure 6.11 for small peripheral targets provide good examples, as do Owen's data for small peripheral targets.

These two trends may be roughly characterized by the slope of the second limb of the threshold-duration function: for large targets the slope approaches 0, for small targets it is between 0 and -1. Legge (1978) estimated the slope of this second limb for targets of various spatial frequency. At 0.75 and 0.375 cycles·degree^{-1} the slope was about -0.02; for frequencies between 1.5 and 12 cycles·degree^{-1} it averaged about -0.29.

Higher background intensities also tend to reduce the slope of the second limb of the threshold-duration function, as may be seen in Barlow's data for small targets in Figure 6.11. The influence of both spatial configuration and background intensity upon this slope may be given a common theoretical interpretation, as discussed below.

6.3. Critical Duration

When data conform to the template in Figure 6.10, there is little ambiguity to the definition of critical duration. When, however, the departure from Bloch's law is gradual, and when the subsequent slope is not zero, critical duration is difficult both to define and to measure. Although a conservative definition, and that adopted here, is the duration at which the data first depart from Bloch's law, some authors have defined it as the point in the data at which the slope first changes (Breitmeyer & Ganz, 1977; Legge, 1978). Elsewhere, it has been operationally defined as the ratio of thresholds for short and long pulses, times the duration of the short pulse (Krauskopf & Mollon, 1971). These different methods can give quite different estimates of the critical duration.

In light of these difficulties, we may doubt whether the critical duration, however defined, is a useful or robust measure of the temporal properties of the visual system. For large or low spatial frequency targets on backgrounds of high intensity, T_c and I_c do adequately characterize threshold as a function of duration. For many other targets, they do not. Furthermore, as will be discussed in Section 6.5.5, threshold-duration functions are inherently incapable of providing a complete characterization of the temporal response.

6.4. Effects of Background Intensity

The effects of light adaptation upon temporal sensitivity are discussed in Section 11. Both critical duration and critical intensity vary systematically with background intensity. Critical duration declines monotonically with background illuminance,

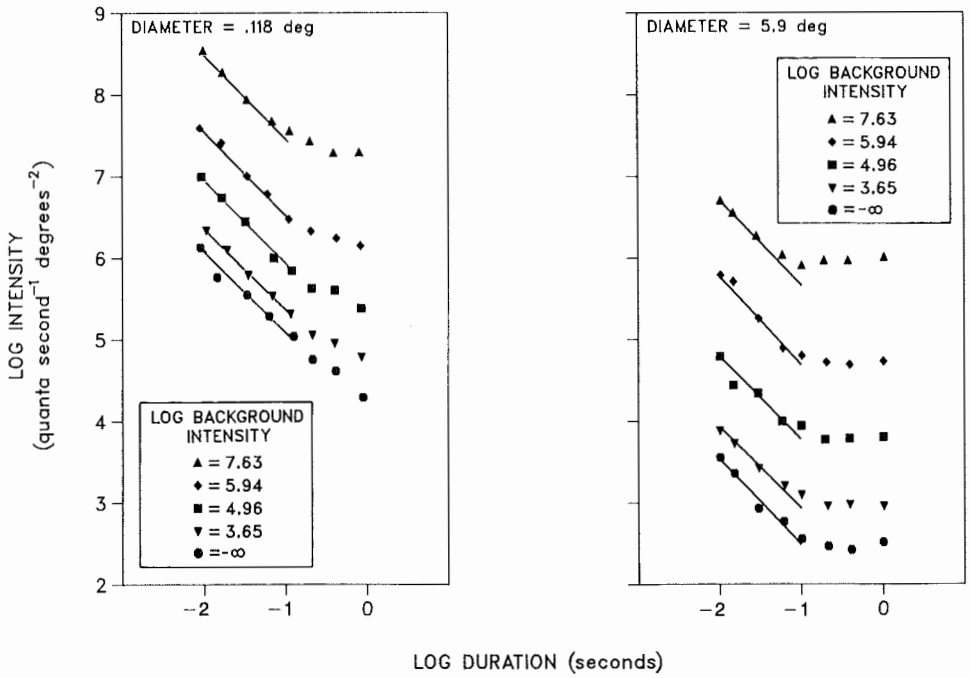

Figure 6.11. Threshold for a rectangular pulse as a function of duration. Target was a disk with diameter of 0.118° (7.1 min), in the left panel, or 5.9°, on the right. Different curves are for different background intensities. The straight lines have a slope of -1 (Bloch's law). Target was centered 6.5° from the fovea in the right eye upon a 13° surround. Intensities are expressed as the number of quanta at 507 nm that would yield an equivalent luminance. Method of adjustment and a 2-mm artificial pupil were used. (From H. B. Barlow, Temporal and spatial summation in human vision at different background intensities, *Journal of Physiology*, 1958, *141*. Reprinted with permission.)

from a value of about 100 msec at 0 log td to about 25 msec at 4 log td, as illustrated in Figure 6.31, Section 11.5.

Critical intensity increases monotonically with background intensity. Beyond about 10 td, the slope of the curve is about −0.91, close to the value of −1 prescribed by Weber's law (Roufs, 1972a). This scaling of sensitivity is comparable to that seen with thresholds for sinusoids and other wave forms. (See also the discussion of temporal summation in Chapter 5 by Hood & Finkelstein.)

6.5. Theory

6.5.1. Bloch's Law. The most widespread interpretation of Bloch's law is that the eye integrates perfectly over a time interval equal to the critical duration. According to this theory, it does not matter how the signal is distributed within the critical duration, provided that its integral equals a criterion value. That this interpretation is wrong may be clearly seen in an experiment of Rashbass (1970). He first measured the threshold-duration function for a 17° radius disk on a 700-td background. Critical duration was about 16 msec. He then measured threshold for a pair of 2-msec pulses, one positive and one negative, their onsets separated by 10 msec. The integral of this stimulus, all of which falls within the critical duration, is 0. If threshold is governed by this integral, the stimulus should be invisible. In fact, Rashbass found it required an amplitude only about 1.85 times that for a single pulse.

A determined advocate of the complete integration theory might counter that there are many possible intervals of 16 msec over which the integral might be taken, many of which would not give a 0 value. Presumably, then, the observer would use the interval with the largest integral, one containing just one of the pulses. But then why is the threshold 1.85 times that for a single pulse?

Rather than pursue the various theoretical dodges that might preserve some variant of the perfect integrator, we consider the more general class of causal, time-invariant linear filters, of which the perfect integrator is but one. First we consider the properties of the perfect integrator as a filter. Its impulse response is a pulse of duration τ, equal to the epoch of integration. This is rather implausible, if only because discontinuities are rarely found in biology. The amplitude response is proportional to $|\sin(\pi w\tau)/\pi w|$, which does not resemble very much the temporal amplitude sensitivity function of the human observer. In short, although the perfect integrator may predict Bloch's law, it is quite firmly refuted on other grounds.

In fact, Bloch's law is an inevitable consequence of any linear filter that passes only frequencies below some cutoff. This is most easily seen by considering the response in the frequency domain. The amplitude spectrum of a pulse of intensity I and duration T is given by

$$I\left|\frac{\sin(\pi Tw)}{\pi w}\right| . \tag{56}$$

The peak amplitude of this spectrum is IT and hence any two durations for which reciprocity holds (for which IT are equal) have amplitude spectra with equal peak values. Let us define the unit of intensity as the threshold for a 1-msec pulse. Then two pulses, of durations 10 and 20 msec and amplitudes 1/10 and 1/20, will each be at threshold. Their amplitude spectra are sketched in Figure 6.12.

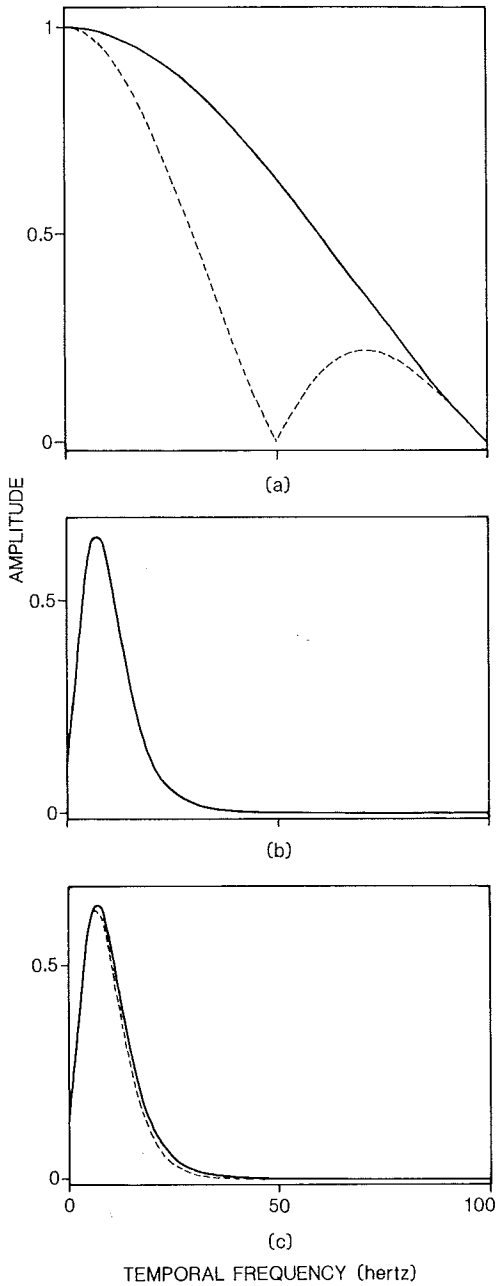

Figure 6.12. An explanation of the reciprocity between threshold duration and intensity (Bloch's law) by a linear filter. (a) Amplitude spectra for two pulses of threshold intensity with durations within the regime of Bloch's law. Let the unit of intensity be the threshold for a 1-msec pulse, so that at threshold $IT = 1$ when T is expressed in msec. Pulse durations are 10 (solid line) and 20 msec (dashed line), and intensities are 1/10 and 1/20. Both spectra are sinc functions. Because both durations are within the regime of Bloch's law, and because for both $IT = 1$, both pulses are at threshold. (b) Amplitude response of the linear filter of the working model, as taken from Figure 6.5(b). (c) Amplitude spectra of the responses of the filter to the 10-msec (solid line) and 20-msec (dashed line) pulses, obtained by multiplying the spectra in (a) by the amplitude response shown in (b). The resulting spectra are nearly identical; hence the stimuli should be equally visible.

If the visual response to these signals is linear, then the amplitude spectrum of the response is the product of amplitude spectra of signal and visual filter. The latter may be approximated for conditions like Rashbass's by the linear filter of the working model as fit to Robson's (1966) data [see Fig. 6.5(b)]. These are drawn in Figure 6.12. The resulting products, which

are the amplitude spectra of the responses to 10- and 20-msec pulses, are almost identical, as shown.

This argument is incomplete, because it says only that the amplitude spectra of pulses briefer than the critical duration are identical. The phase spectra of the two responses are in fact different, but as we shall show, they differ in a way not likely to affect threshold. The phase spectrum of a pulse centered at 0 is 0 at all frequencies. To begin the pulse at time 0, as our convention for inputs to a causal system requires, we delay the pulse by half its duration. Table 6.1 shows that a delay of $T/2$ results in a phase shift of $-\pi Tw$ at each frequency w. The phase spectrum of the response is obtained by simply adding, at each frequency, the phase response of the visual filter. This function is not easily estimated (see Section 5.10). But the *difference* in the phase of the response to two pulses of durations T_1 and T_2 is $\pi w(T_1 - T_2)$, regardless of the phase response of the visual filter. This difference is just that which would result from shifting the response by an amount $(T_1 - T_2)/2$. So we see that two pulses with durations less than the critical duration result in responses that are identical except for a shift in time equal to half the difference in their durations. Because absolute position in time does not usually influence sensitivity, we conclude that the two pulses are equally visible.

6.5.2. Sensitivity at Long Durations. With increasing duration beyond the critical duration, pulse thresholds either become independent of duration or decline at a more gradual rate than prescribed by Bloch's law. The second limb of the threshold-duration function is steeper at low background intensities and for small or high spatial frequency targets. The spatial effects are somewhat more potent, as may be seen in Barlow's data in Figure 6.11.

It is likely that these effects are due to variations in the degree of attenuation of low temporal frequencies, in combination with probability summation over time (Legge, 1978; Tolhurst, 1975a). All three manipulations—raising target spatial frequency, reducing target size, and lowering background intensity—elevate relative sensitivity to low temporal frequencies. In terms of the working model developed in Section 4, these manipulations reduce the *transience* of the underlying linear filter. In the case of background intensity, this change is probably due to parametric change in the filter. When the spatial stimulus is varied, it may occur because of a shift from one detector to another. This issue is discussed in Section 9.4.

In a purely transient filter, a response occurs only at the onset and offset of the pulse. In a purely sustained filter, the response persists for the duration of the pulse or longer. These properties of sustained and transient pulse responses are illustrated in Figure 6.13. As duration is increased, the sustained response provides a greater number of opportunities to detect the stimulus; hence threshold is reduced by probability summation. For the transient response, the number of opportunities remains constant, and threshold does not decline.

The two threshold-duration functions plotted in Figure 6.13 are predictions of the working model developed in Section 4. It consists of a linear filter whose output is perturbed by noise followed by a threshold mechanism. The two curves are for purely sustained (transience = 0) and purely transient (transience = 1) filters. The figure shows that a good qualitative account of the continuing improvement in sensitivity at long durations is provided by a sustained filter followed by probability summation.

The predictions of the working model depend somewhat upon the parameter β, which reflects the slope of the psychometric function. In particular, for the sustained detector the asymptotic slope of the threshold-duration function is $1/\beta$ in log-log coordinates. The predictions in Figure 6.13 employ a β of 3.5, typical of values found in many contrast detection experiments. The lowest reported values for β are around 1.5; hence the steepest asymptotic slope should be around -0.67, and should be encountered with small targets in dark-adapted conditions. This agrees with Barlow's data for a small target at absolute threshold (Fig. 6.11).

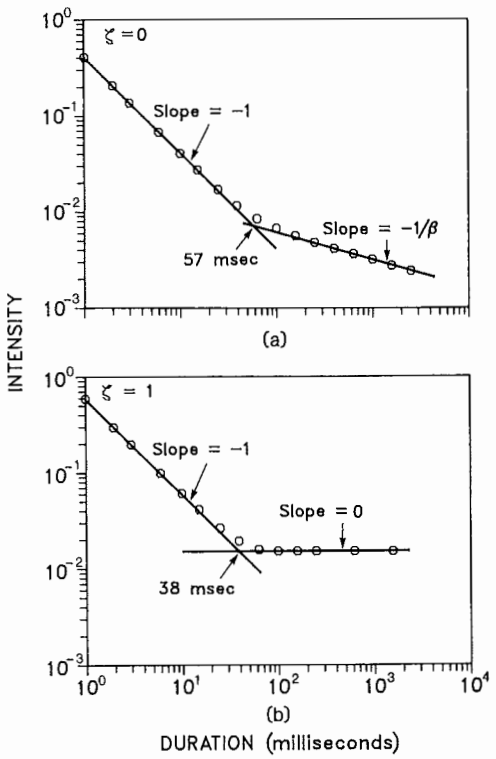

Figure 6.13. Threshold-duration functions predicted by the working model for two values of transience. Points are model predictions; curves are fitted by eye. Panel (a) shows that when the model behaves in a sustained fashion (transience parameter $\zeta = 0$), threshold continues to improve beyond the critical duration and the second limb of the function has a slope of $-1/\beta$ in log-log coordinates, where β governs the slope of the psychometric function of the model. When the model is transient ($\zeta = 1$) as shown in panel (b), the function is flat beyond the critical duration. Other parameters of the model used here are $\tau = 6.25$ msec, $\kappa = 1.33$, $n_1 = 9$, $n_2 = 10$, $\rho = 1.0$, $\beta = 3.5$.

6.5.3. Effects of Background Intensity on Critical Duration. As shown earlier, a threshold duration function may be easily calculated for any particular linear filter, once its transfer function is known. An estimate of the critical duration can then be taken from this curve. We have seen that as background intensity is raised, the amplitude response of the hypothetical filter, as reflected in flicker thresholds, is altered in characteristic ways. From these changes in the amplitude response (and provided some phase assumption is made) changes in critical duration with background intensity can be predicted. This direct prediction of T_c from flicker data has not yet been attempted, but the simpler qualitative prediction that follows suggests that it would succeed.

The explanation of Bloch's law (Fig. 6.12) shows the relationship between the critical duration and the high-frequency falloff of the amplitude sensitivity function. A pulse disobeys Bloch's law when its spectrum is narrow relative to this falloff.

The width of the spectrum of a pulse is inversely related to its duration, so the condition for reciprocity may be stated

$$\frac{K}{T} \leq F_c \ , \tag{57}$$

where F_c is some *critical frequency* and where K is some constant. The critical frequency specifies the location of the high-frequency falloff, and is defined as the frequency at which the amplitude response has fallen by some criterion amount from its maximum. The precise value of K depends on this criterion and the shape of the falloff, but so long as they are fixed, we may write

$$T_c F_c = K \ . \tag{58}$$

Any condition that alters F_c should therefore produce an inverse effect upon T_c.

Increases in background intensity increase the value of F_c without markedly changing the shape of the high-frequency falloff (see Section 11). These background increases should therefore result in decreases in T_c, of a size predicted by Eq. (58). Making a similar argument, Roufs (1972a, 1972b) has made extensive measurements of F_c-and T_c for backgrounds between $-\infty$ and 4.4 log td, and has found that Eq. (58) is obeyed reasonably well (compare Figs. 6.30 and 6.31 in Section 11). It seems then that the variation in critical duration with background intensity may be explained by the same processes required to account for the adaptive variations in the amplitude sensitivity function. These processes are considered in more detail in Section 11.

6.5.4. Relation Between Pulse and Flicker Data. A traditional test of any model of temporal sensitivity is its ability to account for sensitivity to both periodic and transient wave forms. Models embodying a linear filter and threshold device, however, invariably overestimate sensitivity to rectangular pulses relative to that for sinusoidal flicker (Roufs, 1972a, 1972b; Sperling & Sondhi, 1968). It seems quite likely that this discrepancy may be removed by introducing probability summation into the model. For example, in Roufs's experiments, observers were allowed unlimited time to judge the presence of sinusoidal signals, whereas the time available to detect a pulse is limited to its duration. This procedure enhances sensitivity to periodic stimuli relative to that for transients.

Predictions from the working model (which includes probability summation) can only be made for wave forms with finite duration. This is a problem for the traditional test noted earlier, because true sinusoids go on forever. Turning a sinusoid on and off abruptly gives it a finite duration, but also introduces a wide range of other frequencies. A practical solution is to use as flicker wave forms sinusoids windowed in time by a Gaussian function. These signals contain a narrow band of frequencies, and hence more or less directly define the amplitude response of the filter, yet they also have finite duration. Examples of the use of these signals to estimate the amplitude response of the filter of the working model may be found in Watson (1977, 1981).

6.5.5. Is the Threshold-Duration Function Informative? Despite their long history of use in visual theory, we may question whether the threshold-duration function and the critical duration are useful measures of temporal sensitivity. We have already noted the variety of forms that the curve may take, and the difficulty of estimating the critical duration. Even when it can be estimated with confidence, it does not give a generally useful description of the temporal response. For a linear system, this description would be provided by the impulse response or by the system function (see Section 3). Neither the critical duration nor the threshold-duration function is capable of defining these functions (Norman & Gallistel, 1978). It should be clear from the argument of Figure 6.12, for example, that the critical duration and critical intensity are insensitive to changes in the low-frequency end of the system function. Likewise they are insensitive to the phase response of the system (unfortunately, so are most other psychophysical measures). In certain simple cases, the critical duration may indicate some useful feature of the impulse response. For example, in the n-stage filter discussed earlier (Sections 3 and 4) the critical duration will be $\tau(n-1)![e/(n-1)]^{n-1}$ (Sperling, 1979). More generally, if the time scale of the impulse response is multiplied by some constant k, or equivalently the frequency scale of the system function is divided by k, then the critical duration is multiplied by k. This sensitivity of the critical duration to the time scale of the impulse response is what has recommended its use as a measure of the effects of light adaptation. But as we have seen, background intensity changes not only the time scale and sensitivity of the system, but also its degree of transience. These two effects cannot be separately assessed by a single measure of critical duration.

7. SENSITIVITY TO PULSE PAIRS

7.1. Background

A pulse pair is a wave form consisting of the sum of two pulses of equal duration T, intensities I_1 and I_2, separated by a delay D. The target intensity wave form can be written

$$I(t) = I_1 p_T(t) + I_2 p_T(t - D) \tag{59}$$

where $p_T(t)$ is a pulse of unit height and width T. The intensities I_1 and I_2 may be either positive (an intensity increment) or negative (a decrement). Dividing by the background intensity gives the contrast wave form $C(t)$. An example of a pulse pair is shown in Figure 6.14.

The pulse pair has most often been used to study the form of the temporal response. Intuitively, the first pulse evokes a response which may be probed by the second pulse. However, to draw strong influences from the data we must know (or assume) how the two overlapping responses are combined, and how the resulting quantity determines threshold.

A useful format in which to represent the results of a pulse-pair experiment is sketched in Figure 6.14 (Rashbass, 1970). Following Boynton, Ikeda, and Stiles (1964), we define S_1 as the intensity (or contrast) of the first pulse, divided by threshold for the first pulse, and S_2 as the intensity (or contrast) of the second pulse divided by its threshold. Quantities scaled by threshold in this way are sometimes called "sensation magnitudes." Now we construct a plot in which the abscissa expresses S_1 and the ordinate, S_2. Threshold for any particular pulse pair can be represented as a point in this space. Several examples are shown in Figure 6.14. A common experimental procedure is to fix the ratio S_2/S_1 and then to measure threshold for the pair. This consists of moving along a ray at an angle of $\tan^{-1}(S_2/S_1)$ in the summation diagram. For example, an experiment using only positive pulses of equal amplitude would be confined to a ray at 45°. When the experiment is repeated

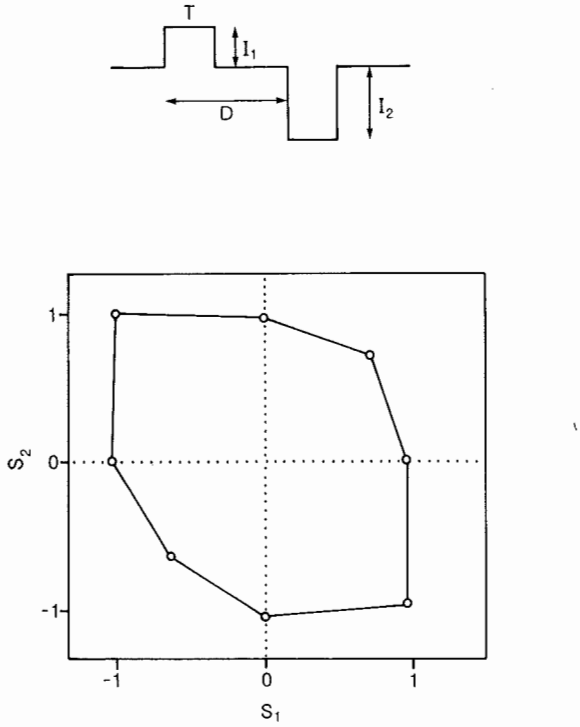

Figure 6.14. Schematic of a summation plot of thresholds for pulse pairs. The abscissa and ordinate indicate S_1 and S_2, sensation magnitudes of first and second pulses (intensities scaled by respective thresholds). Each point in the plot represents a pulse pair at threshold. Points on the axes represent thresholds for single pulses. The collection of all points in the plot is called the threshold locus. The locus may be thought of as separating subthreshold and suprathreshold stimulus regions. The shape of the locus depends upon the delay between pulses, as well as other variables. The inset shows the time wave form of a pulse pair. It consists of two pulses of intensities I_1 and I_2, each of duration T, separated by a delay D. This plot is a useful summary of summation between two pulses.

at a number of angles the threshold points may be connected to form a *threshold locus*.

Thresholds for pulse pairs frequently show one of the following forms of interaction: summation, partial summation, probability summation, partial cancellation, and cancellation. These outcomes lie at progressively greater distances from the origin.

Early studies of pulse-pair sensitivity were made by Granit and Davis (1931), Bouman and van den Brink (1952), and Blackwell (1963), all using two increments of equal size. They found summation at the briefest durations, partial summation at intermediate delays, and probability summation at the longest delays. Blackwell's data also showed partial cancellation at intermediate delays. Ikeda (1965) made extensive measurements with a variety of amplitude ratios, including both increments and decrements. Like Blackwell, he found intermediate delays at which like-signed pairs showed partial cancellation, and speculated that such results might be due to a biphasic internal response, with two lobes of opposite sign. Cancellation between like-signed pairs would occur when the negative phase of the second response overlapped the positive phase of the first response.

Subsequent work has confirmed this result, and has refined Ikeda's insight in the context of a linear filter followed by a nonlinear detection process (Rashbass, 1970, 1976; Roufs, 1973, 1974a; Watson & Nachmias, 1977). The effects of background intensity (Ikeda, 1965; Roufs, 1973, 1974a; Uetsuki & Ikeda, 1970) and spatial configuration of the target (Watson & Nachmias, 1977) have also been investigated. These developments have generally shown that the pulse-pair results can be understood in terms of the same model used to explain visibility of other waveforms such as sinusoids and single pulses.

7.2. Data

Figure 6.15 shows thresholds collected by Rashbass (1970). These data closely resemble those of Ikeda (1965) for a 30-min disk target on a 6° surround. The threshold plotted is the scaled contrast of the first pulse (S_1).

For like-signed pulses (filled symbols) the thresholds show progressively less summation with increasing delay, reaching a minimum of about 1 at around 60 msec. At this delay, the pair has the same threshold as either pulse alone. If the response to the two pulses did not interact, probability summation should result, and the thresholds at the longest delay are consistent with this condition ($S_1 \approx 0.84$). The minimum at 60 msec shows *less* than probability summation, and is therefore consistent with partial cancellation.

Thresholds for opposite-signed pairs (open symbols) show progressively less cancellation with increasing delay, reaching a minimum at about 60 msec, then rising again to a value consistent with probability summation. At short delays, the pairs partially cancel ($S_1 > 1$), but at intermediate delays they show partial summation ($S_1 = 0.53$). In other words, a pair of pulses of opposite sign is considerably more visible than a single pulse alone, or than a like-signed pair at the same delay. Roufs's data for like-signed (Roufs, 1973) and opposite-signed pairs (Roufs, 1974a) show a similar pattern. He used a 1° disk target and no surround. Qualitatively, this behavior agrees with Ikeda's hypothesis: at a delay of about 60 msec, like-signed pairs cancel because opposite-signed phases of the responses overlap; opposite-

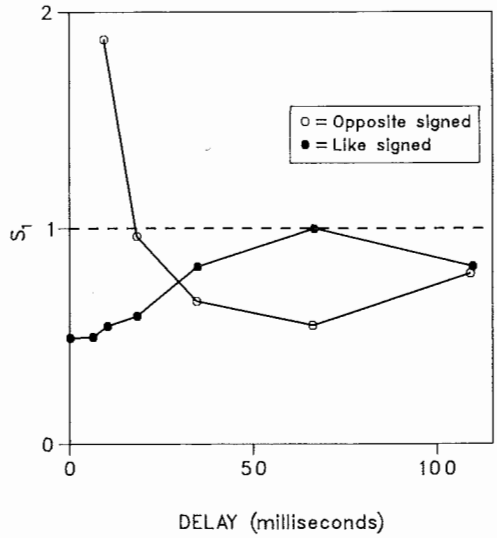

Figure 6.15. Sensitivity to pulse pairs as a function of delay between pulses. The ordinate indicates the intensity of the first pulse divided by its threshold (S_1). Both pulses were equal in intensity and 2 msec in duration. Filled symbols indicate like-signed pulse pairs (both increments or both decrements), and open symbols, opposite-signed. The target was a 17° disk; background was 700 td. Data from Rashbass (1970). Like-signed pairs summate best with 0 delay, and show a slight cancellation at about 65-msec delay. Opposite-signed pairs summate best at about 65-msec delay.

signed pulses summate because like-signed phases of the responses overlap.

The cases pictured in Figure 6.15 correspond to rays lying at 45° (like-signed pairs) and 135° (opposite-signed pairs) in the summation diagram of Figure 6.14. More complete threshold contours are shown in Figure 6.16. The curve in each figure is an ellipse centered at the origin with axes along the diagonals whose equation is

$$1 = S_1^2 + S_2^2 + 2S_1S_2L_D \qquad (60)$$

where L_D is a constant at each delay D. An ellipse leaning to the left has a positive value of L_D; a lean to the right has a negative value. Apart from its possible theoretical meaning, the reasonable fit of the ellipse recommends L_D as a summary measure of pulse-pair summation. The variation of L_D with delay from Rashbass's experiments is shown in Figure 6.17.

Several authors have examined the effect of background intensity on pulse-pair thresholds. All report a change in the time scale of the results, so that, for example, the minimum threshold for opposite-signed pulses moves to longer delays as the background is reduced. The data of Uetsuki and Ikeda (1970) also show less cancellation between like-signed pulses at lower backgrounds.

Watson and Nachmias (1977) and Breitmeyer and Ganz (1977) have used pulse pairs to examine the temporal response to gratings. Figure 6.18 shows the variation in L_D with spatial frequency at four selected delays. In each case, L_D increases with spatial frequency. At the three longer delays, values go from negative to positive, indicating that the negative lobe of the function disappears as spatial frequency increases.

7.3. Theory

Theoretical concerns relating to pulse-pair data focus on models that can account for (1) the elliptical threshold locus and (2) the form of L_D (or some comparable measure of summation versus delay). Most treatments assume an initial linear filter, but differ on the nature of the nonlinear detection stage.

Rashbass (1970) proposed that visual transients are filtered by an impulse response $h(t)$, then squared and integrated over an epoch E of about 200 msec. The stimulus was seen whenever the result was greater than one. At threshold,

$$\int_0^E [C(t) * h(t)]^2 \, dt = 1 . \qquad (61)$$

This model predicts elliptical threshold loci, and leads elegantly to the conclusion that L_D is the inverse Fourier transform of the amplitude response $|H(w)|$ (the autocorrelation function) of the filter. In support of this model, the transform of L_D does resemble qualitatively the TCSF, though no quantitative comparison of the two functions under the same conditions has been made. When transformed, the negative lobe of L_D will result in attenuation at low temporal frequencies (transience). Because transience as reflected in the TCSF is reduced when background intensity is reduced or spatial frequency raised, these manipulations should also reduce the size of the negative lobe of L_D, and they do (Broekhuijsen, Rashbass, & Veringa, 1976; Watson & Nachmias, 1977; Fig. 6.18).

An alternative is the working model developed in Section 4. A stimulus is seen whenever the noise-perturbed output of a linear filter exceeds a criterion. At threshold,

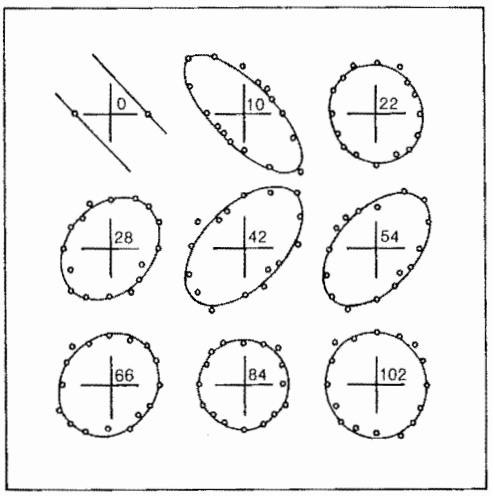

Figure 6.16. Summation between pulses at various delays. The pulses were 2-msec changes in the intensity of a 700-td, 17° disk with no surround. The abscissa and ordinate in each figure indicate S_1 and S_2, respectively, as explained in Figure 6.14. The delay between pulses in msec is indicated near the origin of each plot. The curves are ellipses of the form $1 = S_1^2 + S_2^2 + 2S_1S_2L_D$. The eccentricity of the ellipse, parameterized by L_D, varies as a function of delay. The elliptical threshold contours are predicted by the model of Rashbass. (From C. Rashbass, The visibility of transient changes of luminance, *Journal of Physiology*, 1970, *210*. Reprinted with permission.)

$$\int_a^b |C(t) * h(t)|^\beta \, dt = 1 . \qquad (62)$$

Here a and b are the time limits of the stimulus and β is a parameter determined by the slope of the psychometric function which typically has a value of between 3 and 6 (Nachmias, 1981; Watson, 1979). This model, when associated with a plausible impulse response, also predicts elliptical threshold loci (Rashbass, 1976; Roufs, 1974a; Watson & Nachmias, 1977).

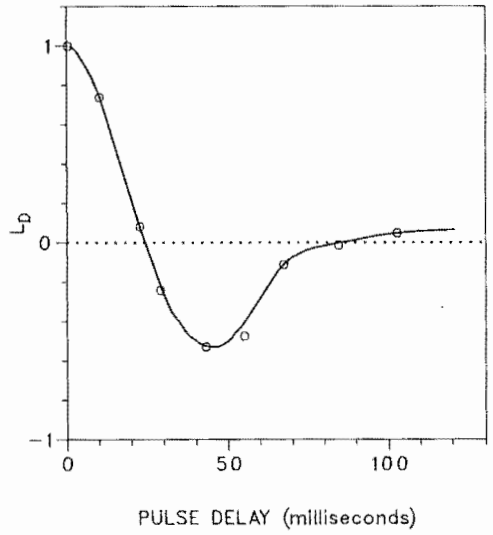

Figure 6.17. Variation in summation between pulse pairs as a function of delay. The quantity plotted is the eccentricity parameter L_D from the ellipses in Figure 6.16. When L_D is positive, like-signed pulses summate and opposite-signed pulses cancel; when it is negative, like-signed pulses cancel and opposite-signed pulses summate. According to Rashbass's model, this function is the Fourier transform of the amplitude spectrum of an underlying linear filter. (From C. Rashbass, The visibility of transient changes of luminance, *Journal of Physiology*, 1970, *210*. Reprinted with permission.)

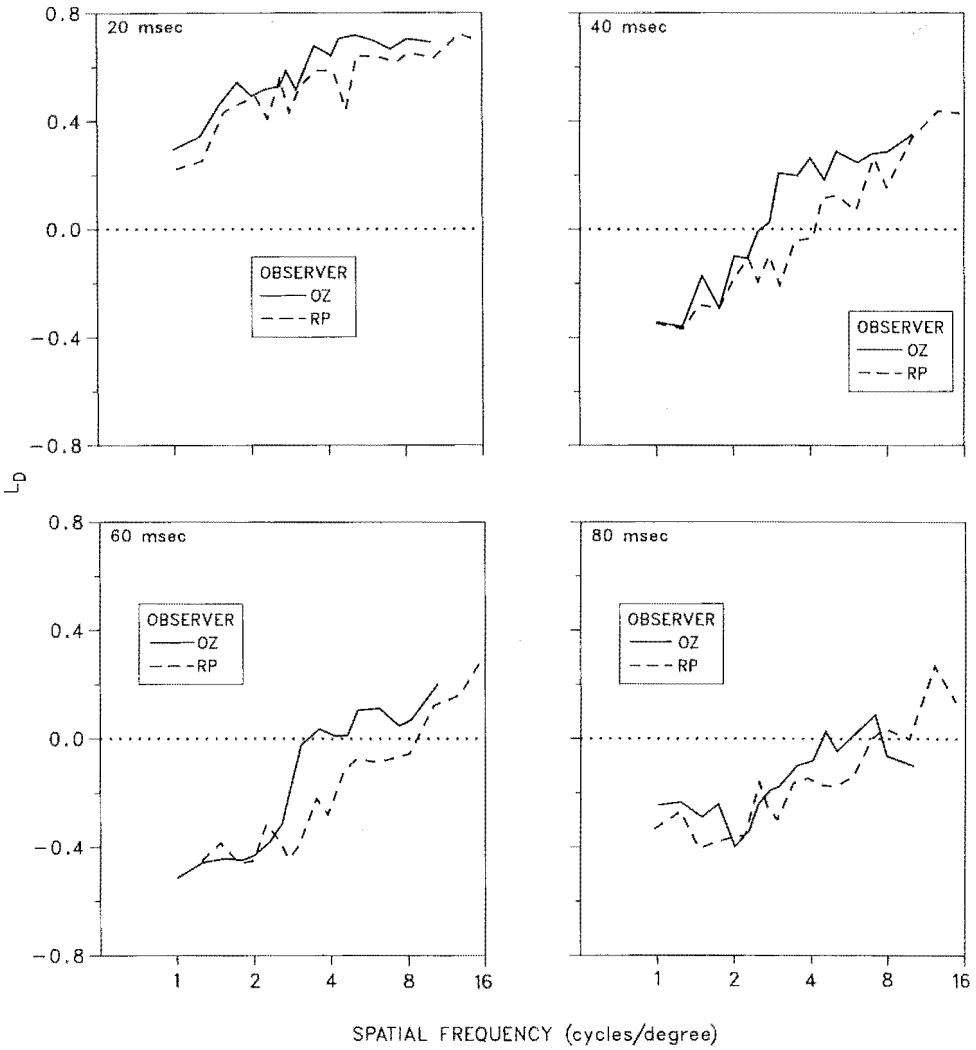

Figure 6.18. Summation between pulses as a function of the spatial frequency of the target. Delay between pulses was 20, 40, 60, or 80 msec. The value plotted is L_D, the parameter of an ellipse fitted to pulse-pair thresholds. Positive values of L_D indicate summation between like-signed pulses and cancellation between opposite-signed pulses; negative values indicate the opposite. L_D increases with spatial frequency at all four delays, so that at the highest spatial frequencies no negative values are obtained. This shows that the system becomes more sustained at higher spatial frequencies. Because the stimuli are briefly exposed, the change in L_D with spatial frequency is unlikely to be due to eye movements. Target was 2 × 1.5° with a 6° diameter surround. Background and surround luminance were about 15 cd·m^{-2}. (a) Observer OZ, (b) observer RP (from Watson, Note 1).

Unlike Rashbass's model, it can predict threshold for stimuli of long durations. For example, it correctly predicts that when the delay between pulses is very long, the contour will be a square with rounded corners, not an ellipse (Watson & Nachmias, 1977).

The defining equations of the two models are quite similar; only the exponent and limits of integration differ. Indeed a third model, a linear filter not followed by probability summation, can also be represented by Eq. (62), by setting the exponent to infinity. This allows a test among these models. Equation (62) predicts that sensitivity to a sinusoid will increase as the β^{-1} power of duration. Estimates of β obtained in this way are between 3 and 6, in agreement with the predictions of the working model (Watson, 1979).

The assumptions made about the final detection stage of the model can have considerable effect upon the interpretation of experimental results. For example, Roufs and Blommaert (1981) assume a deterministic threshold (effectively a β of ∞), and estimate the complete impulse response from pulse-pair data. However, when a more realistic model is assumed (β between 2 and 6) the interpretation of the data is quite different (Watson, 1982). As Rashbass has pointed out, when $\beta = 2$ all phase information is lost and the complete impulse response cannot be recovered (Rashbass, 1970, 1976). Conversely, when $\beta = \infty$ the complete impulse response can be recovered quite directly from pulse-pair data (Roufs & Blommaert, 1981). Because it appears that β is nearer 3 or 4, it is possible that the impulse response might be recovered from pulse-pair data, though probably not in a simple or elegant way. More likely, a brute-force fitting procedure will be required.

8. SENSITIVITY TO INCREMENTS AND DECREMENTS

8.1. Background

A decrement in light intensity can serve as a stimulus for vision, as these dark letters on this white page attest. Therefore, the

relative visibility of increments and decrements of light is a matter of practical and theoretical interest. The practical interest arises from the question of whether positive or negative contrast (e.g., bright or dark letters) provides the better visual signal. Our theoretical interest begins with the observation that a simple linear model of temporal sensitivity predicts equality of increments and decrements, because they should produce internal responses equal in magnitude but opposite in sign.

Thresholds for both increments and decrements have been measured by numerous authors. Wherever substantial or consistent differences are found, the threshold for a decrement is lower than for an increment. But the reliability of these differences, between subjects and across conditions, is less than might be desired.

8.2. Data

Using a red, 10-min increment or decrement upon a 10°, 10,400-td largely green surround, Boynton, Ikeda, and Stiles (1964) found a decrement threshold 0.17 log unit lower than an increment. Patel and Jones (1968) used disks of several sizes and durations 7° from the fovea upon a 14° surround at various backgrounds. They reported a decrement advantage of about 0.3 log units for a 15-min, 50-msec target on a 6.1 quanta·degree^{-2}·sec^{-1} background. The advantage declined for larger targets, longer durations, and higher backgrounds.

Short (1966) also showed consistently greater visibility of decrements. He used a 57-min disk, 100 msec long, positioned 15° into the nasal visual field, upon a large surround, and found a difference averaging about 0.24 log unit at low backgrounds (below about 1 td) almost vanishing at higher backgrounds. There were, however, sizable differences among the three observers.

Herrick (1956), using a 1° target, no surround, various durations, and backgrounds between about −1 and 4 td, and Rashbass (1970), using a 17° target, no surround, various durations, and a background of 700 td, found little difference in results for increments and decrements, but neither author directly compared the two thresholds under the same conditions. Using conditions very similar to those of Herrick, Roufs (1974a) found little consistent difference in increment and decrement thresholds. However, Roufs's observers used a threshold criterion ("agitation") that may measure thresholds different from those of other authors (see Sections 5.11 and 9.4.1.4). Contrary to the finding of Patel and Jones (1968), neither Herrick's nor Roufs's data show any systematic effect of duration.

Some explanation of this variability of results may be in order. First, it should be noted that no two of these reports have employed the same conditions. Second, without exception, the authors used methods such as yes/no and method of adjustment, which permit the observer to use different criteria for increments and decrements. Some of the differences reported are larger than might be expected to arise from criterion variations, but in general we cannot be certain what portion of the difference, if any, we should attribute to this source. It would be useful to compare the two thresholds with a method, such as two-alternative forced-choice, which is not subject to this objection.

The reports cited used spatial targets (disks) that are all of one sign. When a spatial target is used, such as a sinusoidal grating, that has positive and negative excursions of equal sign, then it is more appropriate to speak of a comparison between thresholds for positive and negative contrast. These can differ only if the local position of the spatial increments and decrements (e.g., the bright and dark bars) is relevant. This might be the case for very low spatial frequencies, but is unlikely in most other situations. Thus it is not surprising that Watson (1977) found equal thresholds for positive and negative contrast grating targets of 3.5 cycles·degrees^{-1}.

8.3. Theory

A difference between thresholds for positive and negative contrast can be included in the working model by introducing different thresholds for positive and negative excursions of the internal response (Kelly & Savoie, 1973). Thus we assume that detection occurs whenever a positive excursion exceeds 1, or a negative excursion is less than $-\rho$. The parameter ρ is the *asymmetry factor* of the model [see Section 4.3 and Eq. (52)]. Data are best described by the model when ρ is set equal to the ratio of increment and decrement thresholds. This asymmetry factor is also able to account for some aspects of the thresholds for combinations of different temporal frequencies (Section 5.10) and threshold as a function of duration (Section 6.5).

Explanations for the difference between increment and decrement thresholds have generally appealed to physiological mechanisms such as "on-center" and "off-center" cells. Cohn (1974) has offered an interesting alternative, based on the observation that the distributions of quanta absorbed during increments and decrements are different in form when the number absorbed from the background is small. But this hypothesis predicts differences over a much smaller range of backgrounds than found by Short (1966) and Patel and Jones (1968). It is difficult to judge any theory without knowing what proportion of the effect is due to different criteria for increments and decrements.

9. SPATIAL EFFECTS

9.1. Background

Though it is convenient to consider the temporal wave form in isolation from the other dimensions of the visual stimulus, sensitivity is unavoidably governed by all the dimensions in concert. In some cases, the effects of two dimensions are *separable*. Sensitivity is separable along two dimensions if it is given by the product of sensitivity along the individual dimensions. For example, if the function that describes sensitivity as a function of spatial frequency (u) and temporal frequency (w) were separable, it could be written

$$s(u,w) = s_u(u)s_w(w) \tag{63}$$

where $s_u(u)$ is a spatial contrast sensitivity function and $s_w(w)$ is a temporal contrast sensitivity function like that described in Section 5. In this case, a change in spatial configuration would only scale the results up or down by a constant factor, and we could reasonably exclude consideration of $s_u(u)$ from this chapter. In human vision, however, spatial and temporal sensitivity are not separable. Instead, the temporal response depends upon the spatial configuration of the stimulus. This dependence is evident in the full range of temporal phenomena: in sensitivity to various wave forms, in reaction times, and in discriminability of various stimuli.

Theoretical interest in this area has focused upon incorporating spatial effects into models of temporal sensitivity. This has been done either by allowing the spatial configuration to

control the parameters of a single temporal filter (Burbeck & Kelly, 1980; Kelly, 1972b; Robson, 1966) or by allowing the spatial configuration to determine the pathway in which the stimulus will be detected, different pathways having different temporal properties. The latter notion is generally associated with the idea of separate "sustained" and "transient" pathways for visual signals (Kulikowski & Tolhurst, 1973).

9.2. Spatial Effects upon Temporal Sensitivity

Four distinct aspects of the spatial configuration have been shown to influence temporal sensitivity: size, the surround, edges, and spatial frequency. These effects are evident in the threshold-duration function, as well as the TCSF, though we shall focus upon the latter.

9.2.1. Size. Enlarging a disk target lowers sensitivity at low temporal frequencies without much altering sensitivity at high frequencies. When changes do occur at high frequencies they take the form of a vertical shift of the high-frequency limb of the TCSF. These changes are illustrated in Figure 6.19. The open squares show sensitivity to a 2° disk on a large, 60° surround; the open circles are for a 65° disk with blurred edges.

9.2.2. Effects of the Surround. The filled symbols in Figure 6.19 show sensitivity to a 4° disk without a surround. Between the 2° disk and these data there is a profound loss in sensitivity at low temporal frequencies. It is not clear whether this loss is due to doubling the size of the target or removing the surround. Roufs (1972a) has shown that removing the surround from a 1° disk target has little effect upon high temporal frequencies,

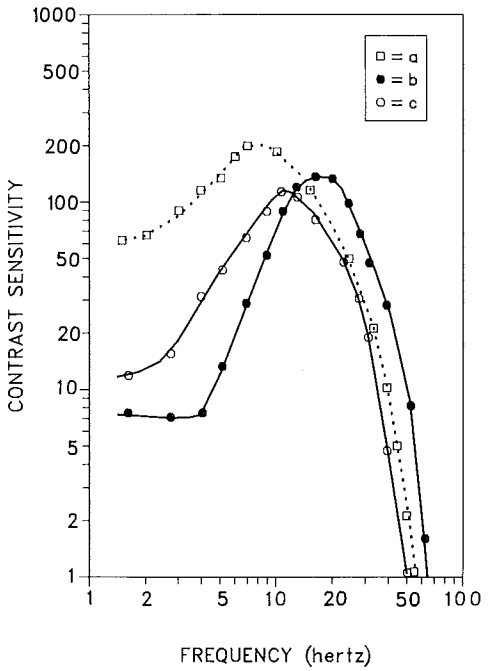

Figure 6.19. The effect of target size and surround upon temporal contrast sensitivity. Temporal wave form was sinusoidal and background intensity was 1000 td. (a) Open square: 2° disk, 60° surround, observer V (de Lange, 1958). (b) Filled circles: 4° disk, no surround (Kelly, 1959). (c) Open circles: 65° disk, blurred edges, no surround, observer P (Kelly, 1959). Enlarging the target and removing the surround reduce sensitivity at low temporal frequencies, thus making the system more transient. (From D. H. Kelly, Effects of sharp edges in a flickering field, *Journal of the Optical Society of America*, 1959, *49*. Reprinted with permission.)

but reduces sensitivity by about 0.5 log units at low frequencies. This suggests that much of the difference between the open squares and filled circles in Figure 6.19 is due to the surround. Harvey (1970), Kelly (1969b), Keesey (1970), Teller (1971), and Westheimer (1967) also provide evidence on the effect of the surround on temporal sensitivity.

Data collected without a surround are subject to other difficulties of interpretation, because the state of light adaptation in the vicinity of the border is somewhat ambiguous. For detectors whose receptive fields lie within the borders of the target, we may be fairly confident that their state of adaptation is governed by the background, regardless of the presence of the surround. But some targets may be detected by mechanisms whose receptive fields span the border of the target, and their adaptive states are much less easily determined when a surround is absent.

9.2.3. Edges. Visually effective edges in the target elevate sensitivity to low temporal frequencies. For example, Kelly (1969b) showed that blurring a 3° disk on a 16° surround reduced sensitivity by about half at low temporal frequencies but had no effect at high temporal frequencies. Very similar results were obtained by blurring the central edge of a counterphase modulated 8 × 16° bipartite field.

Enlarging a disk target moves its edges to regions of the retina of lower spatial resolution, and thus renders them less effective. Thus much of the effect of disk size may be due to this reduction in the visual effectiveness of target edges. This may also partially explain the action of the surround. Without a surround, any visual mechanism sensitive to the edge would be massively stimulated, even in the absence of the target. Presentation of the target would change its response by only a fraction. Thus removing the surround may effectively desensitize the observer to the edges at the border of the target.

9.2.4. Spatial Frequency. Robson (1966) measured the TCSF with sinusoidal gratings of four different spatial frequencies. As shown in Figure 6.20, the two highest spatial frequencies exhibit no decline in sensitivity at low temporal frequencies, whereas at the lowest spatial frequency, a very large low-frequency decline was observed. Similar results have been obtained by van Nes et al. (1967), Koenderink and van Doorn (1979), and Kelly (1972a).

Robson also noted that the shape of the TCSF at high temporal frequencies was invariant with spatial frequency, as shown by the curves superposed on the data, which are the same except for a vertical shift. A change in spatial frequency merely shifted the high-frequency limb up or down in sensitivity. Furthermore, at high spatial frequencies, the spatial contrast sensitivity function is invariant with temporal frequency, apart from a vertical shift. A summary statement of these invariances is that at high spatial and temporal frequencies, spatial and temporal contrast sensitivities are *separable* [see Section 9.1 and Eq. (63)]. This means that at these frequencies, the spatiotemporal contrast sensitivity function is simply the product of the spatial contrast sensitivity function, which describes sensitivity as a function of spatial frequency, and the TCSF. At low spatial or temporal frequencies, the two functions are clearly not separable. These interactions are easily seen in a view of the spatiotemporal contrast sensitivity function such as that provided by Koenderink and van Doorn (1979). Reproduced in Figure 6.21, their figure shows isosensitivity curves for gratings of various spatial and temporal frequencies. Separability of temporal and spatial contrast sensitivity functions is reflected by

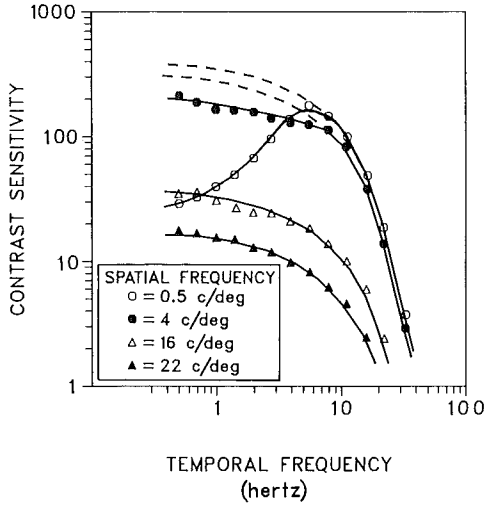

Figure 6.20. The effect of spatial frequency upon the temporal contrast sensitivity function. The target was a sinusoidal grating with a spatial frequency of 0.5, 4, 16, or 22 cycles·degree^{-1}. Background luminance was 20 cd·m^{-2}, target was 2.5 × 2.5°, surround was 10 × 10°, viewing was binocular with natural pupils from 2 m. Points are averages of four adjustment thresholds. The curves (including dashed sections) differ only in vertical position. Spatial and temporal sensitivity are separable at high temporal and spatial frequencies, but at low spatial frequencies sensitivity at low temporal frequencies is reduced. (From J. G. Robson, Spatial and temporal contrast sensitivity functions of the visual system, *Journal of the Optical Society of America*, 1966, *56*. Reprinted with permission.)

the roughly parallel contours beyond 10 Hz and 10 cycles·degree^{-1}. The valley near the origin confirms Robson's earlier observation that a decline in sensitivity at low temporal frequencies occurs only when the spatial frequency is low.

There is a qualitative agreement among the effects of disk size, edges, surrounds, and spatial frequency. It was suggested that the effects of disk size and surround upon the low temporal frequencies are mediated by the visually effective edges in the target. Edges are the repositories of high spatial frequencies. When they are removed by blurring, or made less visually effective by moving them into the periphery, the effective spatial frequency of the target is reduced and we should expect temporal sensitivity to resemble more that obtained with low spatial frequencies; that is, we should observe a more severe attenuation at low temporal frequencies. Thus enlarging a target, blurring its edges, removing its surround, or lowering its spatial frequency should all selectively lower sensitivity at low temporal frequencies, and this does occur.

9.2.5. Miscellaneous Spatial Effects upon Sensitivity. Many other experiments give a similar result through less direct means. Kulikowski and Tolhurst (1973) found that sensitivity to a grating with a square-wave temporal wave form was about twice that for a grating turned on for half a period, then off for half a period, provided the spatial frequency was low. The spectrum of the on–off wave form is equal to half the amplitude of the square-wave spectrum, plus a component at 0 Hz. If low spatial frequency detectors are purely transient they will not respond to the 0-Hz term, and the response to the square wave will be twice that to on–off, as observed. At higher spatial frequencies the system becomes more sustained and the 0-Hz term becomes more effective, reducing the difference in sensitivity between the two wave forms. Tolhurst (1975b) has shown that the detection of a brief increment upon an extended subthreshold pedestal is influenced only near the onset and offset of the pedestal when a low spatial frequency is used. For higher spatial frequencies, detection is enhanced for the duration of the subthreshold grating. Breitmeyer and Julesz (1975) demonstrated that abrupt onsets enhanced visibility relative to gradual onsets at low spatial frequencies but not at high. This is consistent with a reduced sensitivity at low temporal and spatial frequencies, because abrupt transients contain higher frequencies than do gradual transients. They also showed that of the abrupt onset and offset of a pulse, only the onset was effective in enhancing sensitivity. They provided no explanation of this effect, but in fact it is expected in a linear system that is not purely transient. The onset response transient is the step response of the system, but the offset response transient is the step response subtracted from the sustained portion of the response and thus usually has a smaller peak value. Furthermore Stromeyer, Zeevi, and Klein (1979) found that offsets and onsets enhanced visibility by about the same amount when somewhat different background intensities, and spatial and temporal wave forms were used. This discrepancy is not surprising because all of these variables will influence the degree of transience.

Legge (1978) has shown that at high spatial frequencies thresholds continue to decline as duration increases beyond the critical duration, whereas at low spatial frequencies no further improvement is found. He found in addition that brief masking pulses at the start and end of a test pulse had the same effect regardless of test duration for low spatial frequencies, but at high spatial frequencies the effects declined as duration increased. Evidently, only the start and end of the pulse are effective in the first case, whereas in the second case all parts of the signal are effective.

9.3. Spatial Effects upon Reaction Times

Reaction times to sinusoidal gratings increase with the spatial frequency of the grating (Breitmeyer, 1975; Harwerth & Levi, 1978; Lupp, Hauske, & Wolf, 1976; Vassilev & Mitov, 1976).

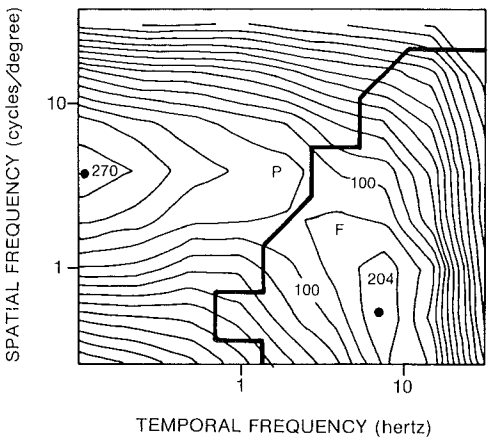

Figure 6.21. Isosensitivity curves for targets that are sinusoidal in both space and time. Each curve connects points of equal sensitivity obtained by linear interpolation from data like those in Figure 6.20. The spacing between lines is 0.1 log unit, corresponding approximately to a standard deviation. The contour at sensitivity = 100, and the peaks at 270 and 204 are marked. The heavy line separates regions the observer judged as giving sensations of "flicker" or "pattern" (see Section 9.4.1.4). Sensitivity falls when either spatial and temporal frequency are high, or when both are low. (From J. J. Koenderink & A. J. van Doorn, Spatiotemporal contrast detection threshold surface is bimodal, *Optic Letters*, 1979, *4*. Reprinted with permission.)

The differences persist when the contrast at each spatial frequency is set to equal apparent contrast (Breitmeyer, 1975) or to a fixed number of threshold units (Lupp, Hauske, & Wolf, 1976; Vassilev & Mitov, 1976). As shown in Figure 6.22, the difference between reaction times to 1 and 16 cycles·degree^{-1} is about 90 msec, and this figure is the same whether the targets are three or six times above threshold. These figures are slightly larger than those found by Breitmeyer (1975). These results have sometimes been explained in terms of the different latencies of X- and Y-type retinal ganglion cells, but as Lennie (1980a) points out, the differences in conduction times are orders of magnitude too small, and the latencies to near-threshold lights may not differ at all (Lennie, 1980b).

Tolhurst (1975a) examined the distributions of reaction times to near-threshold high and low spatial frequency gratings at various durations. The distribution was unimodal to a high spatial frequency (3.5 cycles·degree^{-1}), but bimodal to low. This outcome is consistent with the low-frequency grating being detected only at its onset or offset, as would be the case for a transient mechanism. This view is reinforced by Tolhurst's observation that the position of the second mode of the distribution is always about 250 msec after the offset of the target.

9.4. Sustained and Transient Mechanisms

To characterize the dynamic behavior of some visual cells, Cleland et al. (1971) adopted the terms *sustained*, indicating a response extending for the duration of the stimulus, and *transient*, indicating a response primarily at stimulus onset and offset. Watson and Nachmias (1977) have proposed formal definitions for these terms. Transient behavior is indicated by an impulse response whose integral is 0, for example, a biphasic response with positive and negative lobes of equal area. The transient amplitude response has severe attenuation at low temporal frequencies, reaching 0 at 0 Hz. In a sustained system the impulse response is all of one sign, and the amplitude response has a maximum at 0 Hz. A system intermediate between these extremes may be relatively sustained or transient. In the working model (Section 4) the degree of transience has been captured by a single parameter that governs the amplitude of a second, negative lobe in the impulse response. Further discussion of these terms was given in Section 3.

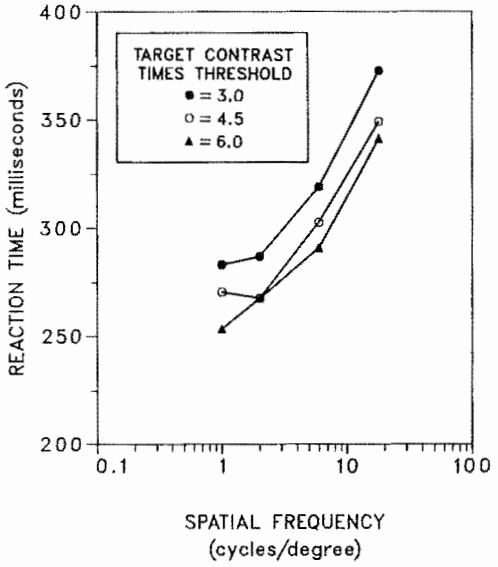

Figure 6.22. Reaction time as a function of spatial frequency. The three curves indicate target contrasts of 3, 4.5, or 6 times threshold. Thresholds were estimated as the 50% point of a yes/no frequency-of-seeing curve. Targets were 5.3 × 3.8° gratings with no surround. Background intensity was 23 cd·m^{-2}. A 2.3-mm diameter artificial pupil was used. Reaction times increase by about 90 msec between spatial frequencies of 1 and 16 cycles·degree^{-1}. (From U. Lupp, G. Hauske, & W. Wolf, Perceptual latencies to sinusoidal gratings, *Vision Research, 16*. Copyright 1976 by Pergamon Press, Ltd. Reprinted with permission.)

The evidence in Sections 9.2 and 9.3 cited above indicates that the higher the effective spatial frequency of the target, the more sustained the temporal response. These and other results led Tolhurst (1973) and Kulikowski and Tolhurst (1973) to propose the existence of two classes of visual mechanisms: transient and sustained. This hypothesis has considerable implications for models of temporal sensitivity, and has found wide acceptance, so it deserves critical examination.

Mild and strong versions of this theory can be distinguished. The mild version only asserts a relationship between spatial configuration and the temporal properties of the detecting mechanism; the strong version proposes the existence of two distinct classes of mechanisms that respond in parallel to a visual stimulus. By analogy to physiology, the mild version imagines the same cells to be capable of either sustained or transient behavior depending upon stimulus conditions, whereas the strong theory assumes separate populations of sustained and transient cells acting in parallel. Examples of the mild theory are provided by Robson (1966) and Burbeck and Kelly (1980), who attribute these effects to differing spatial and temporal properties of the center and surround of retinal units. Proponents of the strong version are Kulikowski and Tolhurst (1973) and Roufs (1974a).

All the data cited to this point are consistent with either mild or strong theories. In the absence of further evidence, the mild theory would be preferred because it is more parsimonious. The strong theory would be called for by evidence of two sorts. The first would show that both sustained and transient mechanisms exist at one spatial frequency. The second would show that mechanisms operating in the two regimes are functionally distinct.

9.4.1. Evidence for Parallel Operation

9.4.1.1. Subthreshold Summation. The most direct test for parallel operation of sustained and transient mechanisms is subthreshold summation between different temporal frequencies. Sustained mechanisms are generally thought to be more sensitive at low temporal frequencies, and transient mechanisms at high. The strong theory therefore predicts that low and high temporal frequencies will excite different mechanisms, and will show little subthreshold summation. The mild theory on the other hand predicts that summation between the two frequencies will be consistent with a single pathway. Using this technique, Watson (1977) found only modest departures from the predictions of a single linear pathway with probability summation over time. However, the data could not rule out the existence of two independent pathways, one moderately selective for high temporal frequencies, the other for low. In these experiments the separation between frequency was never larger than 8 Hz; more convincing evidence of two pathways might have been provided by a larger separation.

9.4.1.2. Adaptation. If sustained and transient mechanisms respond in parallel to the same spatial target, as the

strong theory supposes, then it might be possible to adapt selectively one of the two. For example, if transient mechanisms are more sensitive at high temporal frequencies, then adapting to a high temporal frequency might reduce their sensitivity and produce a selective reduction in sensitivity at the high frequencies. More quantitative predictions have not been made, and would require assumptions regarding the temporal sensitivity of each mechanism, the manner of adaptation, and how thresholds are determined when both mechanisms are active.

Evidence for temporal frequency selective adaptation has been sought by numerous authors (Green, 1981; Nilsson, Richmond, & Nelson, 1975; Pantle, 1971; Pantle & Sekuler, 1968; Smith, 1970, 1971). Despite the variety of techniques used, these experiments are unanimous in showing very little selective adaptation. In addition, the experiments have not generally avoided various sources of artifact, such as adapting stimuli of equal contrast rather than equal "sensation magnitude," and testing and adapting stimuli with different average intensity. We may also question whether selective adaptation is compelling evidence for parallel operation of independent pathways. A single pathway may contain elements that are frequency selective and adaptable, yet do not themselves constitute a "mechanism." This issue is discussed by Watson (1977).

Tolhurst (1973) has shown that following adaptation to a stationary grating, different patterns of threshold elevation are found depending upon whether the test pattern moves or is stationary. He proposed that the stationary test revealed the adaptation of the sustained system, the moving test that of the transient system.

9.4.1.3. Discrimination at Threshold. If sustained and transient mechanisms are "separate labeled" pathways (see Section 3.6), then a stimulus that at threshold exclusively excites the transient mechanism should be perfectly discriminated from a stimulus which exclusively excites the sustained mechanism. In agreement with this prediction, Watson and Robson (1981) found that a low and a high temporal frequency were perfectly discriminated. Some of their data are shown in Figure 6.23.

9.4.1.4. Threshold Sensations. In his 1958 report, de Lange noted a difference in the nature of the flicker perception depending on "frequency" (p. 782). This observation has been echoed by numerous authors. At detection threshold a spatial pattern that is modulated sinusoidally in time may appear as primarily a spatial or a temporal variation. These two threshold sensations, called "pattern," and "flicker," "swell," and "agitation," as well as other names, have been described by van Nes et al. (1967), Rashbass (1968), Watanabe et al. (1968), Richards (1971), Keesey (1972), Kulikowski and Tolhurst (1973), and Roufs (1974a). The threshold sensation of pattern predominates at low temporal and high spatial frequencies, whereas flicker predominates at high temporal and low spatial frequencies. Figure 6.21 shows the approximate extent of these two regimes.

Van Nes et al. (1967) noted that thresholds for both sensations could be measured for the same stimulus. At detection threshold either pattern or flicker is evident; at some higher contrast the other sensation emerges. Keesey (1972) had observers adjust the contrast of a thin bar to each threshold at a number of temporal frequencies, thus tracing out TCSFs for each of the two criteria. The two curves differed in shape, and Keesey proposed that the two thresholds were due to different mechanisms with different temporal properties. Kulikowski and Tolhurst (1973) used the same technique with spatial grating targets, with the results shown in Figure 6.24. The two curves

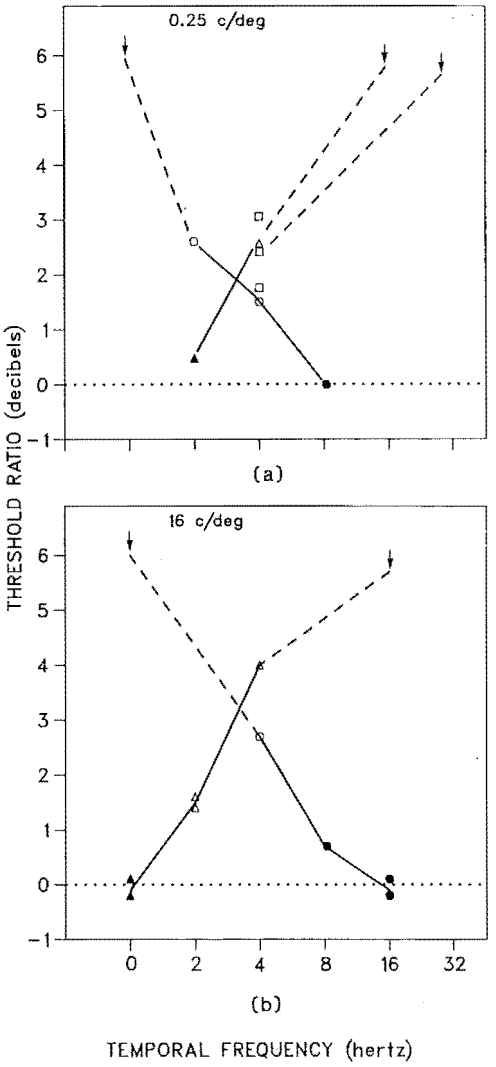

Figure 6.23. Ratio of identification and detection thresholds for different temporal frequencies. The stimuli were patches of spatial grating modulated sinusoidally in time. The spatial envelope was a Gaussian in both horizontal and vertical dimensions, with width between 1/e points of 12° (a), and 3/16° (b). Background intensity was 340 $cd \cdot m^{-2}$, viewing was binocular with natural pupils. In each experiment two temporal frequencies were used, one indicated by the arrow, the other by the horizontal position of the data point. On each trial the observer tried to detect and identify the stimulus, and separate thresholds for detection and identification were estimated from the same data. When the ratio of these two thresholds is 1 (0 dB), the two frequencies are discriminated as well as they are detected. The filled symbols show cases in which a statistical test indicated that the two stimuli were discriminated as well as they were detected. This occurs only when one temporal frequency is very high and the other very low. These results are consistent with two labeled pathways, one selective for high temporal frequencies, the other for low. Similar results are obtained at both low (a) and high (b) spatial frequencies. (From A. B. Watson & J. G. Robson, Discrimination at threshold: Labelled detectors in human vision, *Vision Research, 21*. Copyright 1981 by Pergamon Press, Ltd. Reprinted with permission.)

intersect at an intermediate temporal frequency, so that at high temporal frequencies, flicker sensitivity is greater than pattern, whereas at low temporal frequencies the reverse is true. Their interpretation was essentially that of Keesey: each criterion was attributed to a different mechanism, as though the two curves described the temporal contrast sensitivities of distinct flicker and pattern detectors. As further evidence for

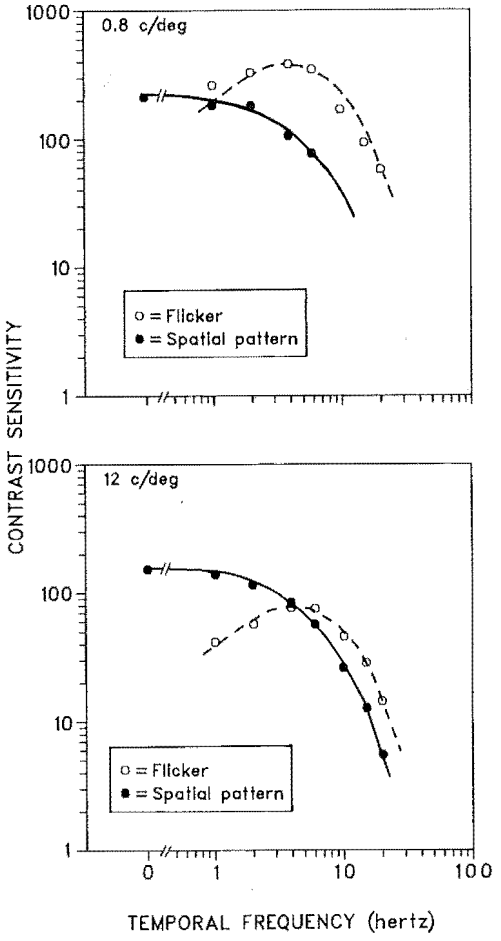

Figure 6.24. Temporal contrast sensitivity functions measured with flicker and pattern criteria. The spatial target was a sinusoidal grating of 0.8 (upper graph) or 12 cycles·degree^{-1} (lower graph). Temporal wave form was sinusoidal. Open symbols result when the observer is instructed to adjust contrast until the stimulus appears to "flicker"; filled symbols result when contrast is adjusted until "spatial pattern" is evident. The curves in the lower graph are the same as those in the upper graph but shifted vertically by different amounts. Flicker and pattern thresholds have different temporal contrast sensitivity functions which move independently with changes in spatial frequency. Flicker sensitivity is high at low spatial and high temporal frequencies; pattern sensitivity is high at high spatial and low temporal frequencies. (From J. J. Kulikowski & D. J. Tolhurst, Psychophysical evidence for sustained and transient mechanisms in human vision, *Journal of Physiology*, 1973, *232*. Reprinted with permission.)

this idea, they noted that a change in spatial frequency shifted each curve vertically, but did not change its shape. This meant that within each pathway, spatial and temporal sensitivities were separable. Furthermore, the vertical shifts were different for the two criteria, implying that the two mechanisms had different spatial sensitivities, the flicker mechanism being relatively more sensitive at low spatial frequencies and the pattern mechanism at high, in agreement with Figure 6.21.

King-Smith and Kulikowski (1975) used flicker and pattern criteria and the technique of subthreshold summation to examine the spatial selectivity of sustained and transient mechanisms. The receptive fields they inferred from their data were two to four times wider for the flicker than for the pattern criterion. This agrees with the generally higher spatial acuity of the pattern criterion (see Fig. 6.21).

Although the two sensations discussed are robust and vivid, a compelling argument that they are due to parallel independent mechanisms has not yet been provided. Furthermore, various results suggest that observers are not very good at describing their own threshold criteria, and that at threshold in the flicker regime observers retain some information about pattern, whereas in the pattern regime they retain information about temporal attributes.

Nachmias (1967) found "sustained" and "transient" threshold-duration functions at high and low spatial frequencies, respectively, even though he used forced choice between orthogonal orientations to measure threshold. If only sustained mechanisms convey pattern information, only sustained threshold duration curves should have been observed. Similarly, Derrington and Henning (1981) have shown that at both high and low rates of temporal modulation, thresholds for forced-choice discrimination between orientations of 0 and 90° are similar to thresholds for simple detection measured with a two-interval forced-choice method. When the rate of temporal modulation is high (10 Hz), the orientation thresholds show little decline in sensitivity at low spatial frequencies. If the mechanisms that detect low spatial, high temporal frequency stimuli conveyed no information about spatial pattern, they would be incapable of distinguishing between gratings at right angles, and threshold for this discrimination would be higher than for detection. As Derrington and Henning note, this result casts doubt upon the ability of the observer to describe the information present in a threshold stimulus, because their observers were unaware of spatial information in stimuli whose orientations they judged correctly.

Watson and Robson (1981) looked at discrimination at detection threshold between gratings of various spatial frequencies. Even when they were well within the transient regime (16 Hz), observers could discriminate perfectly between very different spatial frequencies. Again this suggests that if there are distinct transient mechanisms, they are not entirely without spatial selectivity.

9.4.2. Other Differences between Sustained and Transient Regimes. Although the experiments cited in Section 9.4.1.3 clearly indicate spatial selectivity in the mechanisms that operate in the transient regime, they do not imply that the spatial selectivity is the same as that in the "sustained" regime. For example, Derrington and Henning (1981) only examined discrimination between orthogonal gratings, and not between gratings at smaller angles. Sharpe and Tolhurst (1973) found that spatial adaptation had a considerably broader orientation bandwidth (22°) when the gratings drifted than when they were stationary (13°). Pantle (1973) examined summation between gratings an octave apart in spatial frequency and found more summation when the compound pattern moved than when it was stationary. Watson and Robson (1981) compared the relative discriminability of spatial frequency at threshold for gratings modulated at high and at low spatial frequencies. They found that discrimination was much poorer at high temporal frequencies; only an octave difference in spatial frequency was required for perfect discrimination at 0 Hz, but 2–3 octaves was required at 16 Hz. To summarize, the mechanisms that detect patterns at high temporal frequencies do not appear to be completely without spatial selectivity, but do seem to be less selective for spatial frequency and orientation than are the mechanisms that detect stationary or slowly moving patterns.

Another difference in the selectivities of the mechanisms that serve the "sustained" and "transient" regimes is that the

latter are selective for direction of motion, whereas the former are not. E. Levinson and Sekuler (1975) showed that the sum of two gratings drifting in opposite directions (equal to a counterphase grating of twice the contrast) was little more visible than either component alone, as though each was detected by a separate direction-selective mechanism (see Section 10). Watson, Thompson, Murphy, and Nachmias (1980) showed that this result held only when the spatial frequency was low or the temporal frequency was high, that is, when the velocity was above about $1°\cdot sec^{-1}$. This corresponds closely to the "transient" regime as reflected by "flicker" sensations (see Figure 6.21). Watson et al. (1980) also showed that the observers were able to discriminate the direction of motion at detection threshold in the "transient" regime but not in the sustained regime. This is again consistent with the idea that the transient mechanisms respond selectively to motion, and signal motion to the observer.

10. IMAGE MOTION AND TEMPORAL SENSITIVITY

Much of the temporal variation in light intensity in natural visual experience arises from motions of objects or of the eye. In this section, we consider briefly some relationships between temporal sensitivity and sensitivity to image motion. The theory of motion sensing is dealt with at greater length in Watson and Ahumada (1983a, 1983b, 1985).

10.1. Moving Images

Consider an image as defined in Section 2 with a contrast distribution $C(x, y, t)$. Let the image be moved at a rate of $r°\cdot sec^{-1}$ in direction θ. The speed in the horizontal direction is $r_x = r \cos \theta$, and in the vertical direction, $r_y = r \sin \theta$. The contrast distribution in the moving image is then

$$C_{r,\theta}(x,y,t) = C(x - r_x t, y - r_y t, t) . \quad (64)$$

The three-dimensional Fourier transform of the original image can be written $\tilde{C}(u, v, w)$, where u and v are horizontal and vertical spatial frequency in cycles·degree^{-1} and w is temporal frequency in hertz. This (complex) transform describes the spatial and temporal frequencies that make up the image. The transform of the moving image is then

$$\tilde{C}_{r,\theta}(u,v,w) = \tilde{C}(u, v, w + r_x u + r_y v) . \quad (65)$$

Thus moving an image does not introduce new spatial frequencies, but rather alters the temporal frequency associated with each spatial frequency component. For example, if the original image is constant in time ($w = 0$ Hz for all u,v), then movement imparts to each spatial frequency a temporal frequency equal to the inner product of velocity (r_x, r_y) and spatial frequency (u, v), that is, $r_x u + y_y v$. This is equivalent to the product of the spatial frequency and the component of the velocity in the direction of the spatial frequency. In the simple case of a vertical sinusoidal grating of frequency u cycles·degree^{-1} moving horizontally at speed $r°\cdot sec^{-1}$, the resulting temporal frequency is ru. This is the rate at which contrast will vary over time at any point in the image.

Equation (65) states the fundamental relationship between the velocity of an image and its temporal frequency components. It forms a general basis for understanding the relationship between sensitivity to temporal fluctuations and to moving patterns.

10.2. Direction Selectivity

A mechanism is *direction selective* if it responds primarily or exclusively to movement of a pattern in one direction but not in another. In view of the eye's evolutionary adaptation to its environment, we might expect it to be optimized for the analysis of motion, and hence to contain direction-selective mechanisms. A review of the literature on direction selectivity is given by Sekuler (1975). Evidence for direction selectivity is of three sorts: subthreshold summation, adaptation, and discrimination at threshold.

10.2.1. Subthreshold Summation. E. Levinson and Sekuler (1975) noted that a sinusoidal grating modulated sinusoidally in time is equal to the sum of two gratings with half as much contrast moving in opposite directions,

$$\cos(2\pi ux)\cos(2\pi rut) = \tfrac{1}{2}\{\cos[2\pi u(x - rt)] + \cos[2\pi u(x + rt)]\} , \quad (66)$$

where r is the speed of motion. A direction-selective mechanism would respond to only one or the other of the two moving components. Thus if the counterphase grating is detected by a direction-selective mechanism, it should have a threshold about twice that for either of the drifting components. Their data were largely consistent with this direction-selective prediction.

Using a forced-choice method, Watson et al. (1980) tested this prediction at a wider range of spatial and temporal frequencies. They found it held only when the velocity was above about $1°\cdot sec^{-1}$. At lower velocities, moving and counterphase thresholds were more nearly equal. They proposed that within this latter range the stimuli were detected by nondirection-selective mechanisms. These two regimes correspond roughly to the sustained and transient regimes discussed in Section 9.4, which supports a suggestion of E. Levinson and Sekuler (1975) that the direction-selective mechanisms are part of the transient system.

These important results further constrain any model of temporal sensitivity. It must acknowledge that temporal fluctuations with a "velocity" above 1 cycle·degree^{-1} are detected by direction-selective mechanisms. This is a further nonlinearity in the detection pathway, because in a direction-selective system, response to left and rightward moving stimuli will fail to add. This is so even though each direction-selective mechanism by itself may be linear. A model of a linear direction-selective mechanism is given in Section 10.3.

10.2.2. Discrimination at Threshold. If two stimuli are detected by different labeled mechanisms, they should be discriminated as well as they are detected (see Section 3.6). By this logic, if gratings are detected by direction-selective mechanisms, two gratings that drift in opposite directions should be identified as well as they are detected. Watson et al. (1980) tested this prediction by measuring separate thresholds for detecting and identifying the direction of a grating moving in either of two opposite directions. As shown in Figure 6.25, thresholds for detecting and for identifying the direction are about equal at 2 cycles·degree^{-1} regardless of the temporal frequency, and at 8 cycles·degree^{-1} when the temporal frequency is high. These are roughly the same conditions in which subthreshold summation shows direction-selective results. These

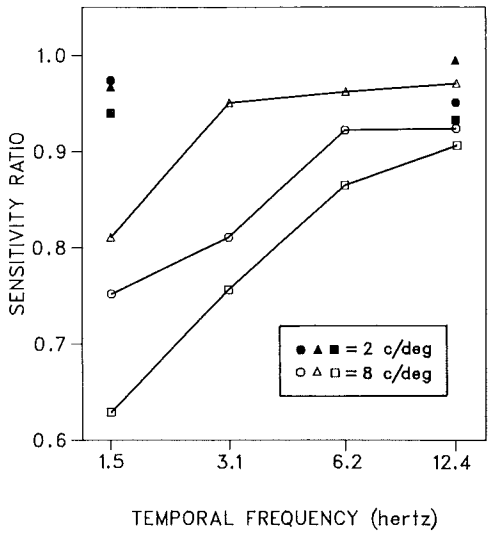

Figure 6.25. Ratio of thresholds for detecting and for identifying the direction of a moving grating. Each trial consisted of two intervals; in one a grating moved either to the left or the right. The observer reported the interval containing the grating, and the grating direction. Detection thresholds were estimated from interval judgments, identification thresholds from direction judgments. Open symbols are for 8 cycles·degree^{-1}, filled symbols are for 2 cycles·degree^{-1}. Different symbols are for three different observers. Detection and identification thresholds are about equal except when the spatial frequency is high and the temporal frequency is low, that is, at low velocities. (From A. B. Watson, P. G. Thompson, B. J. Murphy, & J. Nachmias, Summation of gratings moving in opposite directions, *Vision Research, 20*. Copyright 1980 by Pergamon Press, Ltd. Reprinted with permission.)

results are consistent with the existence of direction-selective mechanisms at medium to high velocities and nondirection-selective mechanisms at low. However, when the velocity is low, the retinal velocity of the target may be due more to eye movements than to motions of the target, thus preventing correct identification of direction. This possibility has been excluded by Mansfield and Nachmias (1981), who showed that the results of Watson et al. (1980) are essentially unaltered by image stabilization.

10.2.3. Adaptation. Following adaptation to a leftward moving grating, threshold is elevated more for a leftward-moving grating than for a rightward-moving grating (Pantle & Sekuler, 1969; Sekuler & Ganz, 1963; Tolhurst, 1973). This is consistent with the idea that the leftward-moving grating selectively excites, and adapts, a mechanism selective for leftward motion. The smaller threshold elevation in the unadapted direction is usually attributed to a nondirection-selective element in the pathway prior to the direction-selective stage (E. Levinson & Sekuler, 1975).

10.2.4. Summary. For grating stimuli, detection in one regime appears to be direction selective, and in the other regime, nondirection selective. These two regimes correspond roughly to the "transient" and "sustained" regimes, respectively. In light of the evidence that many, perhaps all, stimuli are detected by the same mechanisms that detect gratings (N. Graham, 1977), this suggests that many of the stimuli used to study temporal sensitivity are detected by direction-selective mechanisms. This view is not inconsistent with the working model used throughout this chapter, because the nonlinearity implicit in direction selectivity can be part of the threshold process. However, it does require that models of temporal sensitivity take on an explicitly spatiotemporal character when they wish to explain the visibility of targets that move. Section 10.3 shows how this may be done.

10.3. Model of a Motion Sensor

To answer the need for an explicit theory of sensitivity to moving stimuli, Watson and Ahumada (1983a, 1983b, 1985) have constructed a model of a direction-selective motion sensor. The sensor is a linear spatiotemporal filter with a temporal amplitude response equal to that of the working model described in Section 4. The spatial amplitude response is a Gaussian, centered on a frequency of u, v, with a bandwidth of 1 octave. The impulse response is approximately a patch of sinusoidal grating moving briefly in a direction orthogonal to its bars. The sensor is selective for direction, but also for spatial frequency, orientation, and location. Each sensor is a discrete entity located at a point, and the visual field is imagined to be covered by sensors at different locations, orientations, and spatial frequencies.

When stimulated by targets that are separable in space and time, this sensor behaves identically to the linear filter of the working model. The motion sensor may be regarded as a version of the working model in which selectivity for direction and for spatial frequency have been made explicit.

A second, nonlinear stage of the model uses the output of the linear sensors to estimate the two-dimensional velocity of image components localized in space and spatial frequency (Watson & Ahumada, 1985). However, the spatial and temporal sensitivities of the model are governed by the first stage, so that the second stage is beyond the scope of this chapter.

10.4. Stroboscopic Apparent Motion

Stroboscopic apparent motion is the illusion of smooth motion produced by a rapid sequence of static views of an object in motion, as in movies and television. Recently, this phenomenon has been reexamined (Morgan 1980; Watson & Ahumada, 1982; Watson, Ahumada, & Farrell, 1983). Watson and colleagues have explained the relationship between this illusion and the spatial and temporal sensitivity of the eye. They note that in a plot of the spatiotemporal frequency domain, with u running horizontally and w vertically, the spectrum of a line moving to the left with velocity r is a line impulse passing through the origin with slope $-r$. The spectrum of stroboscopic motion is the same, with the addition of parallel replicas at intervals of the strobe frequency (Crick, Marr, & Poggio, 1981, made the same observation). They reason that these replicas will be ineffective, and smooth and stroboscopic motion will appear identical, when the replicas lie outside the region of spatial and temporal frequency to which the eye is sensitive. They note that to a first approximation, this region is a rectangle with halfwidth of $\hat{w}$ Hz and halfheight of $\hat{u}$ cycles·degree^{-1} (see Fig. 6.21). This leads to the prediction that, for smooth and strobed lines to appear identical, the strobe rate must be greater than or equal to $\hat{w} + \hat{u}r$. Figure 6.26 shows the success of these predictions for two observers. For both observers, the temporal frequency limit is about 30 Hz, which is a good estimate of the CFF under their conditions. The spatial limits are 13 cycles·degree^{-1} (ABW) and 6 cycles·degree^{-1} (JEF), which are low but not unreasonable, given the brief exposure, low contrast, and other masking components. In conclusion, stroboscopic apparent motion can be qualitatively explained in terms of the known temporal and spatial filtering action of the eye. From a practical point of view, this explanation provides a formula

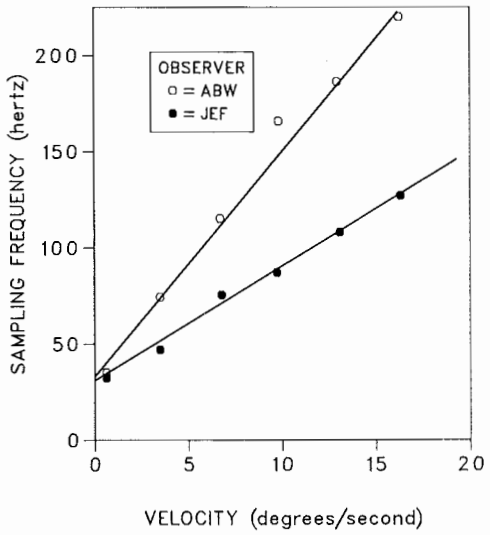

Figure 6.26. Critical temporal sampling frequency as a function of velocity for a moving line. Critical sampling frequency is the lowest rate at which the image can be time-sampled (strobed) keeping smooth and strobed motion indistinguishable. Critical sampling frequency was measured by means of a forced-choice task in which the observer selected which of two presentations he or she believed to be strobed. The stimulus was a vertical line 50 min in length and 0.65 min wide which moved horizontally at the specified velocity (r). Observers fixated a point in the center of the path of travel. The distance traveled was $\sqrt{r}$ 5/4° and the duration $5/(4\sqrt{r})$ sec. Background intensity was 50 cd·m^{-2}. The straight lines are fitted by eye, and are consistent with the hypothesis that stroboscopic apparent motion is due to spatial and temporal filtering by the visual system. The slope and intercept of the line are estimates of the spatial and temporal frequency limits of the filter. For both observers, the intercept is about 30 Hz; the slopes are 6 cycles· degree^{-1} (JEF) and 13 cycles·degree^{-1} (ABW). (From Watson, Ahumada, & Farrell, 1983.)

that can be used to specify the temporal strobe rate required to display any particular moving image.

11. LIGHT ADAPTATION AND TEMPORAL SENSITIVITY

11.1. Background

The sensitivity of the eye declines as the average level of illumination increases, and this phenomenon is referred to as *light adaptation*. A comprehensive discussion of light adaptation is provided by Barlow (1972) (also see Hood & Finkelstein, Chapter 5, and Pokorny & Smith, Chapter 8). The degree of adaptation is not the same for all stimuli, and this has made the subject a matter of continuing interest in all areas of vision research. This is certainly true in the area of temporal sensitivity, in which the amount of adaptation depends upon the temporal wave form of the stimulus. For example, light adaptation has a greater effect on low temporal frequencies than on high, and on long pulses than on short. The following sections document some of these results, and show that they may have a common interpretation in terms of a linear model whose parameters depend upon background intensity.

11.2. Intensity and Contrast Thresholds

Recall that target contrast is defined as target intensity divided by background intensity. This creates a possible source of confusion in discussing light adaptation, because contrast and intensity thresholds change at different rates as a function of background intensity. For example, if intensity thresholds rise in proportion to background, contrast thresholds remain constant, whereas if intensity thresholds remain constant, contrast thresholds decline in proportion to background intensity. In general, if the slope of the relation between log intensity threshold and log background is S, then that between log contrast threshold and log background is $S - 1$. Similar rules apply for sensitivity, defined as the inverse of threshold. For example, the slope relating log intensity sensitivity and log background would be $-S$, and that between log contrast sensitivity and log background would be $1 - S$.

11.3. Weber, de Vries-Rose, and Linear Laws

As background intensity is raised from zero, thresholds usually pass in sequence through three regimes. In the first, threshold intensity is unaltered by background intensity. This regime is called *linear*, because the principle of superposition, as applied to target and background, is upheld. The second regime, which has considerable theoretical importance but few empirical instances, is the *de Vries-Rose law*, in which the intensity threshold rises as the square root of background intensity (de Vries, 1942; Rose, 1942). This is the behavior expected of an ideal detector limited only by quantum fluctuations (though it may also be generated by quite different processes). Note that de Vries-Rose behavior may be exhibited by a detector whose responses, prior to the decision stage, are linear. Thus the "linear" designation applied to the previous regime should not be taken too literally. In the third regime, intensity thresholds rise in proportion to the background intensity. This is the well-known *Weber law*. In a plot of log threshold intensity versus log background intensity, these three laws are straight lines with slopes of 0, ½, and 1, respectively. In a plot of log contrast sensitivity, they are transformed into straight lines of slope 1, ½, and 0. These three sorts of adaptation behaviors are sketched in the insets to Figure 6.27. As with most sensory "laws," these rules should be regarded only as prototypes, which approximate the data within some regime.

11.4. Sinusoidal Wave Forms

Figure 6.27 illustrates some general properties of the effect of background intensity upon temporal sensitivity. (1) Intensity thresholds rise with increasing background intensity. (2) The rate of rise increases as background increases. This rate of rise is approximately consistent with the linear law at the lowest backgrounds, with the de Vries-Rose law at intermediate backgrounds, and with the Weber law at the highest backgrounds. (3) The rate of rise is greater at low temporal frequencies than at high. Consequently, the Weber regime begins at a lower background for lower temporal frequencies.

There is a lower limit to the background intensity that may be used to measure thresholds for sinusoidal targets, reached when background intensity and threshold intensity are equal. The linear region, when it is present, extends from this lowest usable background up no farther than 1.5 log units. The de Vries-Rose law appears only as a brief transition between linear and Weber regions.

Another perspective on the relations among contrast sensitivity, temporal frequency, and background intensity is provided in Figure 6.28. Each curve links points of equal contrast

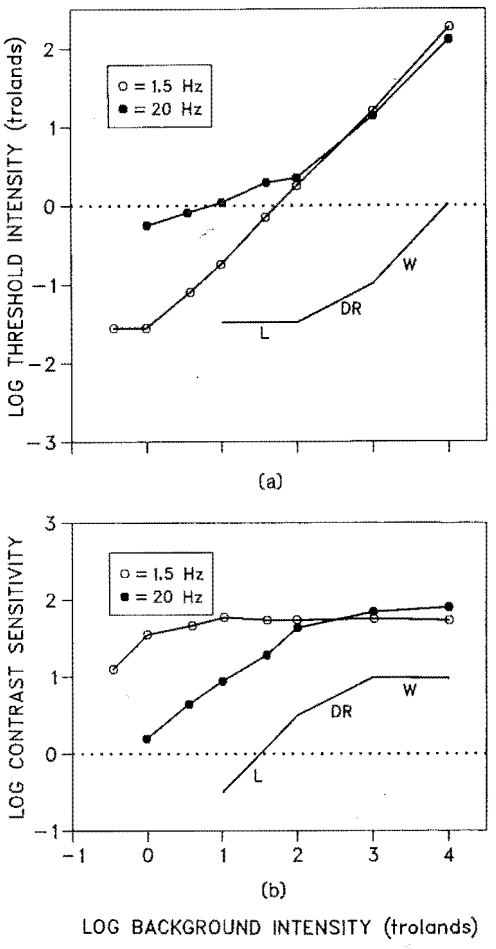

Figure 6.27. Threshold as a function of background intensity. The temporal wave form was sinusoidal at 1.5 or 20 Hz. The spatial target was a 2° disk with no surround. Thresholds were measured by adjustment. The same data are plotted both as intensity thresholds (a) and contrast sensitivities (b). The small insets show the log-log slopes corresponding to linear (L), de Vries-Rose (DR), and Weber (W) laws. The data pass in sequence through each of the laws. At the lower temporal frequency adaptation is more pronounced and the Weber law regime is entered at a lower background intensity (data from de Lange, 1958).

sensitivity. The outermost curve, for a sensitivity of 1, represents the CFF. It grows roughly in proportion to log background intensity, as prescribed by the Ferry-Porter law. This figure also illustrates the relative insensitivity of low frequencies to background intensity, and the enlarged bandwidth at higher backgrounds.

Because light adaptation affects each temporal frequency differently, the TCSF changes shape as background intensity is altered. This is evident in Figures 6.7, 6.28, and 6.29. At the lowest backgrounds, it is "low-pass" in form, showing relative attenuation only at high frequencies. As background intensity is increased, low temporal frequencies move quickly into the Weber regime and show no further improvement in contrast sensitivity. The high frequencies, on the other hand, continue to gain in sensitivity so that the relative attenuation at low frequencies becomes pronounced, and a clear peak in sensitivity emerges at a middle frequency. Furthermore, as backgrounds become more intense, higher frequencies show greater gains in contrast sensitivity. One by one the lower frequencies reach their Weber regime and cease to improve, whereas higher frequencies continue to accrue sensitivity. As a result, the peak in sensitivity increases and moves to higher and higher frequencies, the high-frequency limb moves progressively rightward, and the overall bandwidth of the TCSF is enlarged. These effects agree with the common observation that the light-adapted eye is "faster" and more "transient." In terms of the working model, these changes correspond to a decrease in the time constant (τ), an increase in the transience parameter (ζ), and an increase in sensitivity (ξ) as background is increased.

An alternative view of data like those in Figure 6.28 is given in Figure 6.29. The data in panel (a) of this figure are the same as those in Figure 6.7, but are plotted here as intensity sensitivities rather than contrast sensitivities, achieved by simply dividing each contrast sensitivity by the corresponding background intensity. In log-log coordinates, these divisions correspond to vertical shifts. Despite substantial differences in experimental conditions, and differing behavior at the low frequencies, all three experiments show that, as noted by Kelly (1961a) and J. Z. Levinson and Harmon (1961), above about 1 td all the data appear to approach a common curve. Where

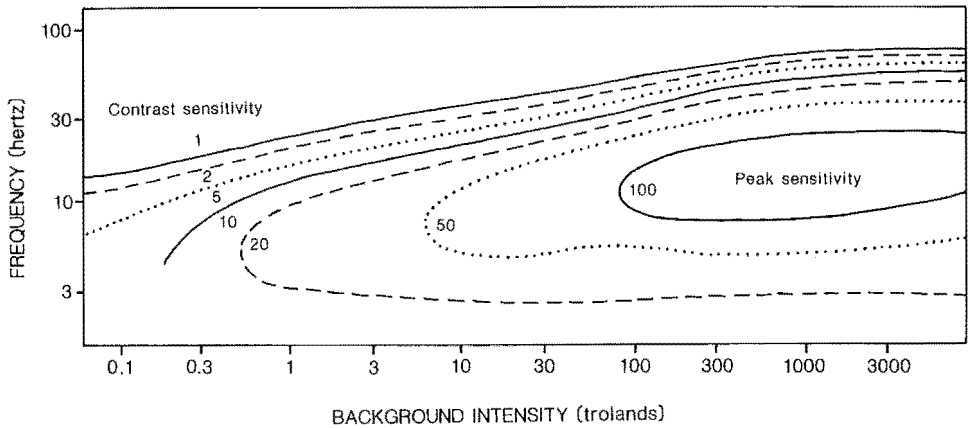

Figure 6.28. Temporal contrast sensitivity as a function of frequency and background intensity. Each line is an isosensitivity curve, obtained by interpolation from data of Figure 6.29, joining points of equal contrast sensitivity. The contrast sensitivity associated with each curve is indicated on the figure. Target was a 60° disk with no surround, modulated sinusoidally. Monocular viewing with a 1.55-mm-diameter artificial pupil. The CFF is indicated by the outermost curve labeled "1." As background intensity increases, peak sensitivity and the CFF move to higher frequencies; sensitivity at low temporal frequencies remains more or less constant. (From D. H. Kelly, Visual responses to time-dependent stimuli, *Journal of the Optical Society of America, 1961, 51.* Reprinted with permission.)

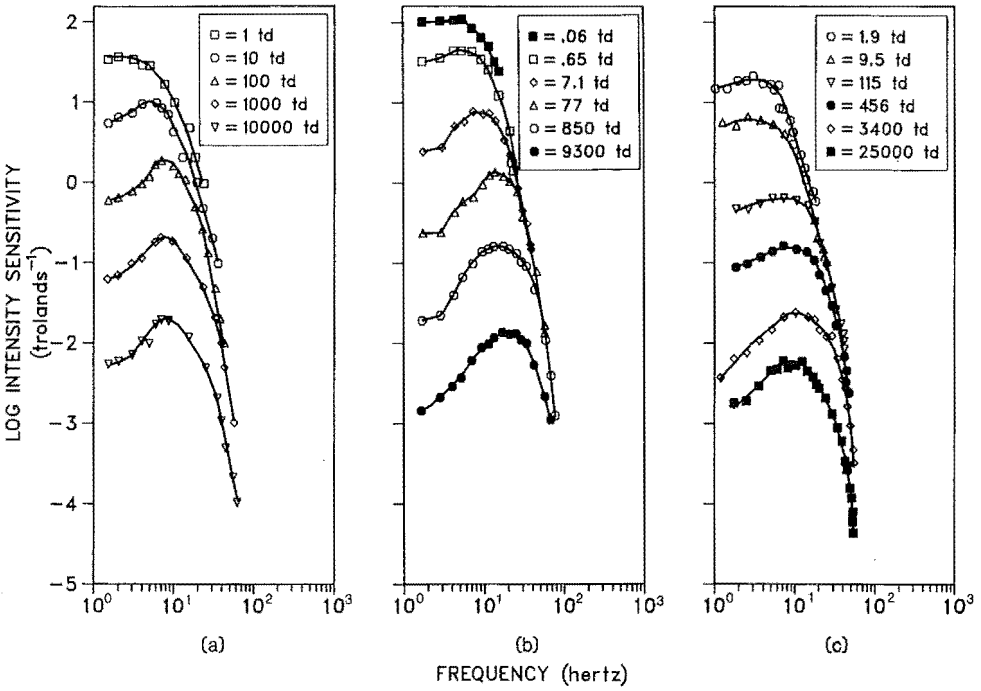

Figure 6.29. Intensity sensitivity as a function of temporal frequency at various background intensities. (a) de Lange (1958), observer V, 2° disk, no surround; (b) Kelly (1961a), 60° disk, no surround; (c) Roufs (1972a), observer HJM, 1° disk, no surround. Increasing background intensity reduces intensity sensitivity at all except the highest frequencies. At the highest temporal frequencies, the curves for different background intensities approach a common curve. This illustrates that at the very highest temporal frequencies, the system approaches linear adaptation behavior.

curves for two adaptation levels coincide, then over that region of frequency and background intensity, thresholds obey the linear rule (Kelly, 1961a). Note, however, that at any given frequency, the linear rule extends, if at all, only over a small range of backgrounds from the lowest upon which it is visible up by 1 log unit or less. Beyond that point, sensitivity moves towards the Weber law. Likewise, at any given background, only a very small range of frequencies will be included in the linear regime, extending down from the CFF. Kelly (1969a) and Kelly and Wilson (1978) have attributed this linear high-frequency asymptote to a diffusion process (see Section 5.11).

Because a large part of the effect of light adaptation takes the form of vertical and horizontal shifts of the high-frequency limb of the TCSF, we might expect that suitable scaling of frequency and sensitivity (equivalent to horizontal and vertical displacements in log-log coordinates) would approximately superimpose the TCSFs measured at different background intensities. Roufs has attempted this exercise, with the results shown in Figure 6.30. The curves agree only to within a factor of about 5, the largest discrepancies being at the lower temporal frequencies. Furthermore, Roufs used a small target and no surround. Use of a surround and/or a larger target (as in the data of de Lange and Kelly in Fig. 6.29), would produce still larger discrepancies at low frequencies. The scaling does not work well at low temporal frequencies because, as we have seen, the TCSF becomes more transient at high backgrounds, and this change is not included in the scaling operations performed in Figure 6.30. Nevertheless this scaling procedure provides a useful condensation of at least the high-frequency data, and Roufs has shown how it provides a qualitative explanation of the luminance dependence of pulse thresholds (see Section 6.5.3).

11.5. Pulse Wave Forms

As shown in Section 6, the function relating threshold to duration for a rectangular pulse (the threshold-duration curve) has an initial segment that falls with a slope of −1, and a second segment that falls at a more gradual rate. The transition between these two segments occurs at the critical duration T_c with intensity threshold I_c (the critical intensity). A rough summary of the effect of light adaptation upon pulse thresholds can therefore be obtained from plots of T_c and I_c as functions of background intensity. These are seen in Figure 6.31, which shows that critical duration declines as background intensity is raised, going from about 100 msec at 0 log td to about 25 msec at 4 log td. The figure also shows the differences that may be expected between observers in the same or different laboratories, and the degree of precision with which statements may be made about critical duration. Because both are measures of the time scale of the temporal response, we might expect a simple relation between the critical duration and the corner frequency of the TCSF. In particular, Section 6.5.3 gives theoretical reasons why these two quantities should be inversely related. Roufs (1972a) has shown that they are, and this may be appreciated by comparison of Figures 6.30 and 6.31.

Just as the adaptational changes in the TCSF cannot be captured completely by scaling of sensitivity and corner frequency, so too changes in the threshold-duration curve are not completely characterized by changes in critical duration and critical intensity. In both cases, the missing parameter is the transience, which also increases with background intensity. As noted in Section 6.5.2, a transient system shows little or no improvement in sensitivity beyond the critical duration, whereas

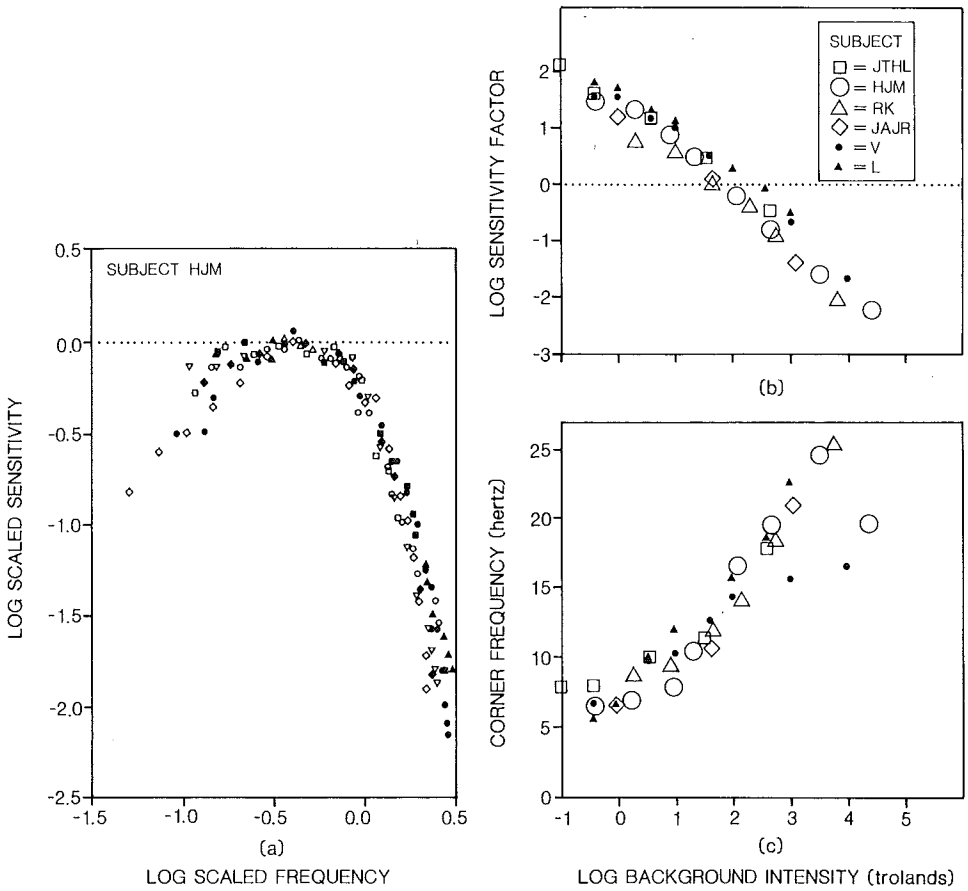

Figure 6.30. Temporal contrast sensitivity functions at different background intensities shifted so as to approximately superpose. (a) Log-scaled sensitivity as a function of log-scaled temporal frequency. Scaled sensitivity is intensity sensitivity divided by a sensitivity factor; scaled temporal frequency is frequency divided by a corner frequency. The sensitivity factor is determined by shifting the curve for each background intensity vertically until it has a peak sensitivity of 1; corner frequency was determined by then shifting each curve horizontally until it had a sensitivity of 0.5 at a frequency of 1. Different symbols are for different background intensities. The curves superimpose reasonably well at high temporal frequencies, but poorly at low. Data from observer HJM. (b) Sensitivity factor as a function of background intensity. (c) Corner frequency as a function of background intensity. (b) and (c) include data of four observers from Roufs (1972a) and two from de Lange (1958). Circles are derived from (a). This figure illustrates that much of the change in the TCSF with background intensity may be expressed as a change in overall sensitivity (a vertical shift) and a change in the corner frequency (an horizontal shift). Sensitivity declines and the corner frequency increases as background increases. (From J. A. J. Roufs, Dynamic properties of vision—I. Experimental relationships between flicker and flash thresholds, *Vision Research, 12*. Copyright 1972 by Pergamon Press, Ltd. Reprinted with permission.)

a sustained system continues to improve at a rate of about 0.25 in log-log coordinates. Thus we expect the second limb of the threshold-duration curve to be somewhat flatter at higher background intensities than at low. This trend is evident in Barlow's data shown in Figure 6.11.

11.6. Other Wave Forms

At very low background intensities (below 1 td) some authors have found that the threshold for a decrement may be as much as 0.3 log unit less than for an increment. This difference tends to disappear at more intense backgrounds.

Pulse-pair thresholds (see Section 7) show the effect of light adaptation in two ways. First, as background intensity increases, the time scale of the results is compressed so that, for example, the delay, at which threshold for an opposite-signed pair is least, moves from about 50 msec at 328 td to about 70 msec at 61.2 td (Ikeda, 1965; Uetsuki & Ikeda, 1970). Second, on less intense backgrounds, the second, negative lobe of the L_D function is reduced or absent. This effect is evident in data of Uetsuki and Ikeda (1970). Because this second lobe is associated with the transience of the linear model, this result is consistent with an increasing degree of transience as background level is raised. This result agrees with observations made with sinusoids and pulses. Roufs (1974a) has also studied the effects of light adaptation upon pulse-pair thresholds.

11.7. Spatial Effects

As noted in Section 9, temporal contrast sensitivity is not separable from the spatial configuration of target and surround. Likewise, the effects of adaptation upon temporal sensitivity

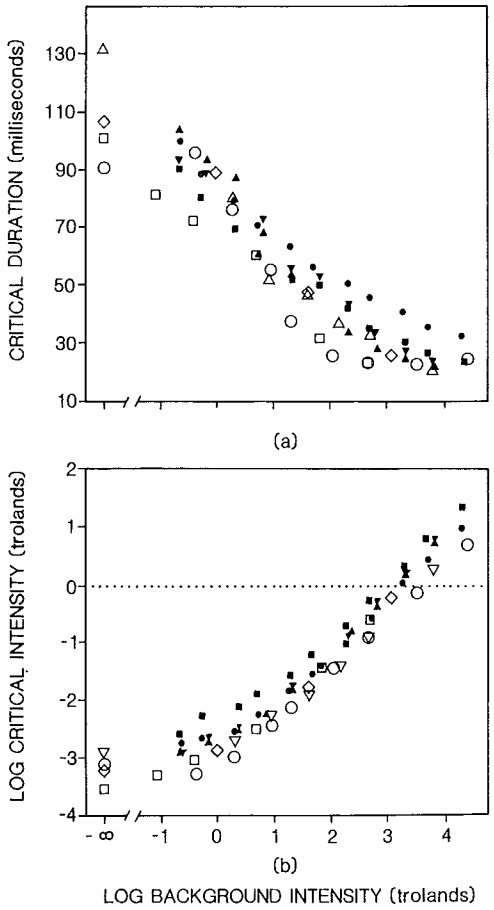

Figure 6.31. Critical duration T_c (a) and critical intensity I_c (b) as functions of background intensity. Critical duration is the longest duration of a rectangular pulse for which reciprocity holds between intensity and duration (Bloch's law). The critical intensity is the threshold intensity at the critical duration. Filled circles are averages of eight subjects of C. H. Graham and Kemp (1938), filled square are average of two subjects of Keller (1941), filled triangles are two subjects of Herrick (1956), open symbols are subjects from Roufs (1972a). Target was a 1° hemidisk (C. H. Graham & Kemp, 1938; Keller, 1941) or a 1° disk (Herrick, 1956; Roufs, 1972a). Critical duration declines from about 100 msec at 0 log td to about 25 msec at 4 log td. Critical intensity increases with background intensity, entering a Weber regime at the more intense backgrounds. (From J. A. J. Roufs, Dynamic properties of vision—I. Experimental relationships between flicker and flash thresholds, *Vision Research, 12*. Copyright 1972 by Pergamon Press, Ltd. Reprinted with permission.)

depend upon spatial configuration. I have suggested that many of the complex spatial effects may be understood by considering the visually effective spatial frequency of the target. To this point, only disk targets have been considered. For a disk target, this frequency is generally low, and may be lowered by enlarging the disk or removing the surround. Consequently, we might expect that data for low spatial frequency grating targets would resemble thresholds for disks.

The first experiments to consider the different effects of background intensity on the TCSF at low and high spatial frequencies were conducted by van Nes et al. (1967). Their measurements were made with drifting, rather than sinusoidally modulated gratings, but as noted in Section 10, thresholds for these two stimuli agree to within a factor of 2. As expected, at a low spatial frequency (0.64 cycles·degree^{-1}) their data show a progressively stronger attenuation at low temporal frequencies as background level is raised. At 11 cycles·degree^{-1}, however, this feature is absent. Above about 1 td, background intensity merely shifts the curve vertically and horizontally with little change in shape. Data from Kelly (1972a), some of which are shown in Figure 6.32, confirm these observations. One way of describing the interaction between spatial configuration and light adaptation is that if the effective spatial frequency is low, the transience increases with background intensity; if the effective spatial frequency is high, the system is sustained at all background intensities.

Kelly's data also show that at low spatial frequencies, as with disk targets, the adaptive response proceeds from a Weber law at low temporal frequencies to a linear rule near to the CFF, passing through an intermediate regime at middle frequencies. Kelly's data suggest that at higher spatial frequencies the intermediate de Vries-Rose regime is enlarged, so that the linear regime may be absent altogether and the Weber regime present only at the highest backgrounds.

11.8. Summary

The following is a summary of the effects of background intensity on temporal contrast sensitivity. The "strength" of adaptation can be characterized by the slope of the relation between log threshold intensity and log background. This is equivalent to the exponent of a power law relating these two quantities. As we have seen, this slope is bounded by values of 0 (linear regime) and 1 (Weber regime). We note the following trends in the strength of adaptation:

1. As background intensity increases, strength increases.
2. As temporal frequency increases, strength decreases.
3. As spatial frequency increases, strength decreases.

Regarding the form of the TCSF, as background intensity is increased, the following occur:

1. Contrast sensitivity increases.
2. Corner frequency increases.
3. Transience increases.

12. SUMMARY

This chapter reviews a small part of the very large literature on human visual temporal sensitivity. An effort has been made to show that the visibility of many different wave forms, both periodic and aperiodic, can be understood in the context of a rather simple model of temporal sensitivity. Some of the effects of spatial configuration and background intensity upon temporal sensitivity have also been examined.

Much of experimental and theoretical effort in this area has been spent finding ever better mathematical representations of the relation between the stimulus temporal wave form $I(t)$ and threshold, and of including ever more refined parametric effects of spatial wave form and background intensity. This endeavor now seems largely complete. A model like the one proposed in Section 4 seems likely to provide a fairly complete quantitative account of the visibility of arbitrary temporal wave forms.

However, a major task for the future will be the integration of models of temporal sensitivity with models of spatial and chromatic sensitivity. We may expect future theoretical developments also to include physiological explanations of temporal

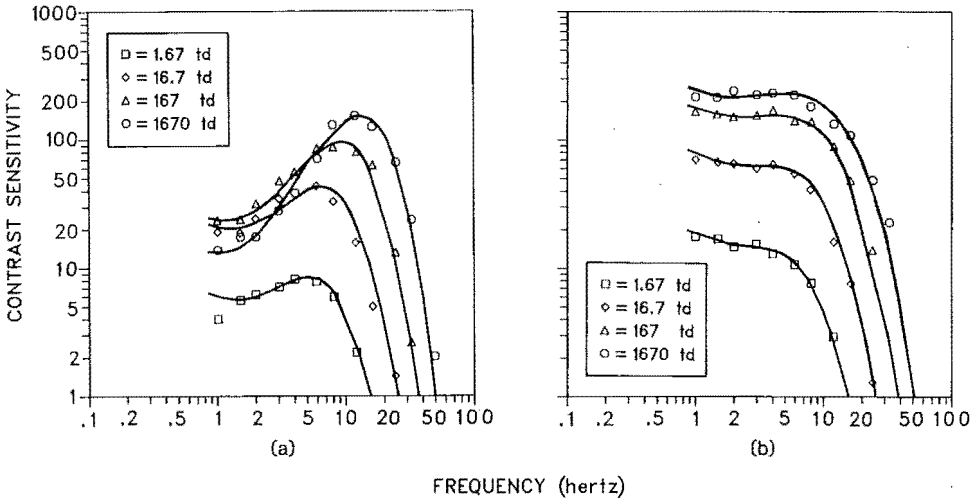

Figure 6.32. The temporal contrast sensitivity function for a uniform field (a) and a 3 cycles·degree^{-1} grating (b) at various background intensities. Data for the uniform field show increasing attenuation at low temporal frequencies as background intensity increases, but data for 3 cycles·degree^{-1} do not. This illustrates that the changes in shape of the TCSF due to adaptation occur primarily at low spatial frequencies. At a low temporal frequency, the adaptation effect is stronger for low spatial frequencies than for high. Background intensities were 1.67 (squares), 16.7 (diamonds), 167 (triangles), and 1670 td (circles). Monocular viewing, 7° circular target, 2.3-mm artificial pupil. Solid lines are from a model proposed by Kelly (1971b). (From D. H. Kelly, Adaptation effects on spatio-temporal sine-wave thresholds, *Vision Research, 12.* Copyright 1972 by Pergamon Press, Ltd. Reprinted with permission.)

sensitivity (which cells do what, and why?). We may hope for a better understanding of sustained and transient channels in human vision. Do they exist, what are their roles, and how are they involved in the processing of temporal, spatial, motion, and chromatic information? An area largely untouched in this chapter that seems likely to receive more attention in the future is the relation between wavelength and temporal sensitivity. This includes the wavelength distribution when it is constant (separable from the temporal wave form) and when it changes as a function of time. Another challenge is the effect of temporal wave form upon color discrimination.

Finally, we are likely to see less emphasis upon sensitivity per se and more upon visual information processing of suprathreshold temporal and spatiotemporal stimuli. A prime example is the study of how we deduce the speed and direction of motion of objects from the spatiotemporal intensity distribution I (x, y, t) (Fahle & Poggio, 1981; Watson & Ahumada, 1983a, 1983b, 1985).

REFERENCE NOTE

1. Watson, A. B. Unpublished observations on summation between pulse pairs as a function of delay and spatial frequency.

REFERENCES

Arend, L. E. Response of the human eye to spatially sinusoidal gratings at various exposure durations. *Vision Research*, 1976, *16*, 1311–1317.

Barlow, H. B. Temporal and spatial summation in human vision at different background intensities. *Journal of Physiology*, 1958, *141*, 337–350.

Barlow, H. B. Dark and light adaptation: Psychophysics. In L. Hurvich & D. Jameson (Eds.), *Handbook of sensory physiology*. New York: Springer-Verlag, 1972.

Baumgardt, E., & Hillman, B. Duration and size as determinants of peripheral retinal response. *Journal of the Optical Society of America*, 1961, *51*, 340–344.

Blackwell, H. R. Neural theories of simple visual discrimination. *Journal of the Optical Society of America*, 1963, *53*, 129–160.

Bloch, A. M. Experience sur la vision. *Comptes Rendus de la Société de Biologie (Paris)*, 1885, *37*, 493–495.

Bouman, M. A. Peripheral contrast thresholds of the human eye. *Journal of the Optical Society of America*, 1950, *40*, 825–832.

Bouman, M. A., & van den Brink, G. On the integrative capacity in time and space of the human peripheral retina. *Journal of the Optical Society of America*, 1952, *42*, 617–620.

Boynton, R. M., Ikeda, M., & Stiles, W. S. Interactions among chromatic mechanisms as inferred from positive and negative increment thresholds. *Vision Research*, 1964, *4*, 87–117.

Bracewell, R. *The Fourier transform and its applications*. New York: McGraw-Hill, 1978.

Breitmeyer, B. G. Simple reaction time as a measure of the temporal response properties of transient and sustained channels. *Vision Research*, 1975, *15*, 1411–1412.

Breitmeyer, B. G., & Ganz, L. Temporal studies with flashed gratings: Inference about human transient and sustained channels. *Vision Research*, 1977, *17*, 861–865.

Breitmeyer, B. G., & Julesz, B. The role of on and off transients in determining the psychophysical spatial frequency response. *Vision Research*, 1975, *15*, 411–415.

Brindley, G. S. The Bunsen-Roscoe law for the human eye for very short durations. *Journal of Physiology*, 1952, *118*, 135–139.

Broekhuijsen, M., Rashbass, C., & Veringa, F. The threshold of visual transients. *Vision Research*, 1976, *16*, 1285–1289.

Burbeck, C., & Kelly, D. H. Spatiotemporal characteristics of visual mechanisms: Excitatory-inhibitory model. *Journal of the Optical Society of America*, 1980, *70*, 1121–1126.

Burbeck, C., & Kelly, D. H. A mechanism in the distal retina that accounts for the fading of stabilized images. *Supplement to Investigative Ophthalmology & Visual Science*, 1982, *22*, 50.

Cleland, B. G., Dubin, M. W., & Levick, W. R. Sustained and transient neurones in the cat's retina and lateral geniculate nucleus. *Journal of Physiology*, 1971, *217*, 473–496.

Cohn, T. E. A new hypothesis to explain why the increment threshold exceeds the decrement threshold. *Vision Research*, 1974, *14*, 1277–1279.

Crick, F. H. C., Marr, D. C., & Poggio, T. An information processing approach to understanding the visual cortex. In F. O. Schmitt, F. G. Worden, G. Adelman, & S. G. Dennis (Eds.), *The organization of the cerebral cortex*. Cambridge: MIT Press, 1981.

de Lange, H. Experiments on flicker and some calculations on an electrical analogue of the foveal systems. *Physica*, 1952, *18*, 935–950.

de Lange, H. Relationship between critical flicker frequency and a set of low frequency characteristics of the eye. *Journal of the Optical Society of America*, 1954, *44*, 380–389.

de Lange, H. Research into the dynamic nature of the human fovea-cortex systems with intermittent and modulated light. I. Attenuation characteristics with white and colored light. *Journal of the Optical Society of America*, 1958, *48*, 777–784.

Derrington, A. M., & Henning, G. B. Pattern discrimination with flickering stimuli. *Vision Research*, 1981, *21*, 597–602.

de Vries, H. The quantum character of light and its bearing upon the threshold of vision, the differential sensitivity and visual acuity of the eye. *Physica*, 1942, *10*, 553.

Fahle, M., & Poggio, T. Visual hyperacuity: Spatiotemporal interpolation in human vision. *Proceedings of the Royal Society of London*, 1981, *B213*, 451–477.

Ferry, E. S. Persistence of vision. *American Journal of Science*, 1892, *44*, 192–207.

Fourtes, M. G. F., & Hodgkin, A. L. Changes in the time scale and sensitivity in the omatidia of Limulus. *Journal of Physiology*, 1964, *172*, 239–263.

Graham, C. H., & Kemp, E. H. Brightness discrimination as a function for the duration of the increment intensity. *Journal of General Physiology*, 1938, *21*, 635–650.

Graham, C. H., & Margaria, R. Area and intensity-time relation in the peripheral retina. *Journal of Physiology*, 1935, *113*, 299–305.

Graham, N. Visual detection of aperiodic spatial stimuli by probability summation among narrowband detectors. *Vision Research*, 1977, *17*, 37–652.

Granit, R., & Davis, W. A. Comparative studies of the peripheral and central retina. *Journal of Physiology*, 1931, *98*, 644–653.

Green, M. Psychophysical relationships among mechanisms sensitive to pattern, motion, and flicker. *Vision Research*, 1981, *21*, 971–983.

Harvey, L. O. Flicker sensitivity and apparent brightness as a function of surround luminance. *Journal of the Optical Society of America*, 1970, *60*, 860–864.

Harwerth, R. S., & Levi, D. M. Reaction time as a measure of suprathreshold grating detection. *Vision Research*, 1978, *18*, 1579–1586.

Henkes, H. E., & van der Tweel, L. H. (Eds.). *Flicker*. The Hague: W. Junk, 1964.

Herrick, R. M. Foveal luminance discrimination as a function of the duration of the decrement or increment in luminance. *Journal of Comparative Physiology and Psychology*, 1956, *49*, 437–443.

Ikeda, M. Temporal summation of positive and negative flashes in the visual system. *Journal of the Optical Society of America*, 1965, *55*, 527–534.

Ives, H. E. A theory of intermittent vision. *Journal of the Optical Society of America*, 1922, *6*, 343–361.

Keesey, U. T. Variables determining flicker sensitivity in small fields. *Journal of the Optical Society of America*, 1970, *60*, 390–398.

Keesey, U. T. Flicker and pattern detection: A comparison of thresholds. *Journal of the Optical Society of America*, 1972, *62*, 446–448.

Keller, M. The relation between the critical duration and intensity in brightness discrimination. *Journal of Experimental Psychology*, 1941, *28*, 407–418.

Kelly, D. H. Effects of sharp edges in a flickering field. *Journal of the Optical Society of America*, 1959, *49*, 730–732.

Kelly, D. H. Visual responses to time-dependent stimuli. I. Amplitude sensitivity measurements. *Journal of the Optical Society of America*, 1961, *51*, 422–429. (a)

Kelly, D. H. Visual responses to time-dependent stimuli. II. Single-channel model of the photopic visual system. *Journal of the Optical Society of America*, 1961, *51*, 747–754. (b)

Kelly, D. H. Sine waves and flicker fusion. *Documenta Ophthalmologica*, 1964, *18*, 16–35.

Kelly, D. H. Diffusion model of linear flicker responses. *Journal of the Optical Society of America*, 1969, *59*, 1665–1670. (a)

Kelly, D. H. Flickering patterns and lateral inhibition. *Journal of the Optical Society of America*, 1969, *59*, 1361–1370. (b)

Kelly, D. H. Theory of flicker and transient responses, I. Uniform fields. *Journal of the Optical Society of America*, 1971, *61*, 537–546. (a)

Kelly, D. H. Theory of flicker and transient responses, II. Counterphase gratings. *Journal of the Optical Society of America*, 1971, *61*, 632–640. (b)

Kelly, D. H. Adaptation effects on spatio-temporal sine-wave thresholds. *Vision Research*, 1972, *12*, 89–101. (a)

Kelly, D. H. Flicker. In L. Hurvich & D. Jameson (Eds.), *Handbook of sensory physiology*. New York: Springer-Verlag, 1972. (b)

Kelly, D. H. Visual contrast sensitivity. *Optica Acta*, 1977, *24*, 107–129.

Kelly, D. H. Motion and vision. I. Stabilized images of stationary gratings. *Journal of the Optical Society of America*, 1979, *69*, 1266–1274.

Kelly, D. H. Motion and vision. IV. Isotropic and anisotropic spatial responses. *Journal of the Optical Society of America*, 1982, *72*, 432–439.

Kelly, D. H., & Savoie, R. E. A study of sine-wave contrast sensitivity by two psychophysical methods. *Perception & Psychophysics*, 1973, *14*, 313–318.

Kelly, D. H., & Wilson, H. R. Human flicker sensitivity: Two stages of retinal diffusion. *Science*, 1978, *202*, 896–899.

King-Smith, P. E., & Kulikowski, J. J. Pattern and flicker detection analysed by subthreshold summation. *Journal of Physiology*, 1975, *249*, 519–548.

Koenderink, J. J., Bouman, M. A., Bueno de Mesquita, A. E., & Slappendel, S. Perimetry of contrast detection thresholds of moving spatial sine wave patterns. I. The near peripheral visual field (eccentricity 0°–8°). *Journal of the Optical Society of America*, 1978, *68*, 845–849.

Koenderink, J. J., & van Doorn, A. J. Spatiotemporal contrast detection threshold surface is bimodal. *Optics Letters*, 1979, *4*, 32–34.

Krauskopf, J., & Mollon, J. D. The independence of the temporal integration properties of the individual chromatic mechanisms in the human eye. *Journal of Physiology*, 1971, *219*, 611–623.

Kulikowski, J. J., & Tolhurst, D. J. Psychophysical evidence for sustained and transient mechanisms in human vision. *Journal of Physiology*, 1973, *232*, 149–163.

Landis, C. *An annotated bibliography of flicker fusion phenomena*. Armed Forces National Research Council Vision Committee Secretariat. Ann Arbor, Mich., 1953.

Legge, G. E. Sustained and transient mechanisms in human vision: Temporal and spatial properties. *Vision Research*, 1978, *18*, 69–81.

Lennie, P. Parallel visual pathways: A review. *Vision Research*, 1980, *20*, 561–594. (a)

Lennie, P. Perceptual signs of parallel pathways. *Philosophical Transactions of the Royal Society*, 1980, *B290*, 23–37. (b)

Levinson, E., & Sekuler, R. The independence of channels in human vision selective for direction of movement. *Journal of Physiology*, 1975, *250*, 347–366.

Levinson, J. Z. Fusion of complex flicker II. *Science*, 1960, *131*, 1438–1440.

Levinson, J. Z. One stage model for visual temporal integration. *Journal of the Optical Society of America*, 1966, *56*, 95–97.

Levinson, J. Z., & Harmon, L. D. Studies with artificial neurons—III. Mechanisms of flicker fusion. *Kybernetic*, 1961, *1*, 19–29.

Lupp, U., Hauske, G., & Wolf, W. Perceptual latencies to sinusoidal gratings. *Vision Research*, 1976, *16*, 969–972.

Mansfield, R. J. W., & Nachmias, J. Perceived direction of motion under retinal image stabilization. *Vision Research*, 1981, *21*, 1423–1425.

Matin, L. Critical duration, the differential luminance threshold, critical flicker frequency and visual adaptation, a theoretical treatment. *Journal of the Optical Society of America*, 1968, *58*, 404–415.

Morgan, M. J. Spatiotemporal filtering and the interpolation effect in apparent motion. *Perception*, 1980, *9*, 161–174.

Nachmias, J. Effect of exposure duration on visual contrast sensitivity with square-wave gratings. *Journal of the Optical Society of America*, 1967, *57*, 421–427.

Nachmias, J. On the psychometric function for contrast detection. *Vision Research*, 1981, *21*, 215–223.

Nilsson, T. H., Richmond, C. F., & Nelson, T. M. Flicker adaptation shows evidence of many visual channels selectively sensitive to temporal frequency. *Vision Research*, 1975, *15*, 621–624.

Norman, M. F., & Gallistel, C. R. What can one learn from a strength-duration experiment? *Journal of Mathematical Psychology*, 1978, *18*, 1–24.

Owen, W. G. Spatiotemporal integration in the human peripheral retina. *Vision Research*, 1972, *12*, 1011–1026.

Pantle, A. Adaptation to pattern spatial frequency: Effects on visual movement sensitivity in humans. *Journal of the Optical Society of America*, 1970, *60*, 1120–1124.

Pantle, A. Flicker adaptation—I. Effect on visual sensitivity to temporal fluctuations of light intensity. *Vision Research*, 1971, *11*, 943–952.

Pantle, A. Visual effects of sinusoidal components of complex gratings: Independent or additive? *Vision Research*, 1973, *13*, 2195–2204.

Pantle, A., & Sekuler, R. W. Velocity sensitive elements in human vision: Initial psychophysical evidence. *Vision Research*, 1968, *8*, 445–450.

Pantle, A., & Sekuler, R. W. Contrast response of human visual mechanisms sensitive to orientation and direction of motion. *Vision Research*, 1969, *9*, 397–406.

Patel, A. S., & Jones, R. W. Incremental and decremental visual thresholds. *Journal of the Optical Society of America*, 1968, *58*, 696–699.

Porter, T. C. Contributions to the study of flicker: II. *Proceedings of the Royal Society of London*, 1902, *70A*, 313–329.

Rashbass, C. Spatio-temporal interaction in visual resolution. *Journal of Physiology*, 1968, *196*, 102–103.

Rashbass, C. The visibility of transient changes of luminance. *Journal of Physiology*, 1970, *210*, 165–186.

Rashbass, C. Unification of two contrasting models of the visual increment threshold. *Vision Research*, 1976, *16*, 1281–1283.

Richards, W. Motion perception in man and other animals. *Brain, Behavior, and Evolution*, 1971, *4*, 162–181.

Riggs, L. A., Armington, J. C., & Ratliff, F. Motions of the retinal image during fixation. *Journal of the Optical Society of America*, 1954, *44*, 315–321.

Robson, J. G. Spatial and temporal contrast sensitivity functions of the visual system. *Journal of the Optical Society of America*, 1966, *56*, 1141–1142.

Rose, A. The relative sensitivities of television pick-up tubes, photographic film, and the human eye. *Proceedings of the Institute of Radio Engineers*, 1942, *30*, 295–300.

Roufs, J. A. J. Dynamic properties of vision—I. Experimental relationships between flicker and flash thresholds. *Vision Research*, 1972, *12*, 261–278. (a)

Roufs, J. A. J. Dynamic properties of vision—II. Theoretical relationships between flicker and flash thresholds. *Vision Research*, 1972, *12*, 279–292. (b)

Roufs, J. A. J. Dynamic properties of vision—III. Twin flashes, single flashes and flicker fusion. *Vision Research*, 1973, *13*, 309–323.

Roufs, J. A. J. Dynamic properties of vision—IV. Thresholds of decremental flashes, incremental flashes and doublets in relation to flicker fusion. *Vision Research*, 1974, *14*, 831–851. (a)

Roufs, J. A. J. Dynamic properties of vision—VI. Stochastic threshold fluctuations and their effect on flash-to-flicker sensitivity ratio. *Vision Research*, 1974, *14*, 871–888. (b)

Roufs, J. A. J., & Blommaert, F. J. J. Temporal impulse and step responses of the human eye obtained psychophysically by means of a drift-correcting perturbation technique. *Vision Research*, 1981, *21*, 1203–1221.

Schober, H. A. W., & Hilz, R. Contrast sensitivity of the human eye for square-wave gratings. *Journal of the Optical Society of America*, 1965, *55*, 1086–1091.

Sekuler, R. Visual motion perception. In E. C. Carterette & M. P. Friedman (Eds.), *Handbook of perception V: Seeing*. New York: Academic Press, 1975.

Sekuler, R., & Ganz, L. Aftereffect of seen motion with a stabilized retinal image. *Science*, 1963, *139*, 419–420.

Sharpe, C. R. The contrast sensitivity of the peripheral visual field to drifting sinusoidal gratings. *Vision Research*, 1974, *14*, 905–906.

Sharpe, C. R., & Tolhurst, D. J. The effects of temporal modulation on the orientation channels of the human visual system. *Perception*, 1973, *2*, 23–29.

Short, A. D. Decremental and incremental visual thresholds. *Journal of Physiology*, 1966, *185*, 646–654.

Smith, R. A. Adaptation of visual contrast sensitivity to specific temporal frequencies. *Vision Research*, 1970, *10*, 275–279.

Smith, R. A. Studies of temporal frequency adaptation in visual contrast sensitivity. *Journal of Physiology*, 1971, *216*, 531–552.

Sperling, G. Critical duration, supersummation, and the narrow domain of strength-duration experiments. *The Behavioral and Brain Sciences*, 1979, *2*, 279–282.

Sperling, G., & Sondhi, M. M. Model for visual luminance discrimination and flicker detection. *Journal of the Optical Society of America*, 1968, *58*, 1133–1145.

Stromeyer, C. F., III, Zeevi, Y. Y., & Klein, S. Response of visual mechanisms to stimulus onsets and offsets. *Journal of the Optical Society of America*, 1979, *69*, 1350–1354.

Teller, D. Y. Sensitization by annular surrounds: Temporal (masking) properties. *Vision Research*, 1971, *11*, 1325–1335.

Tolhurst, D. J. Separate channels for the analysis of the shape and the movement of a moving visual stimulus. *Journal of Physiology*, 1973, *231*, 385–402.

Tolhurst, D. J. Reaction times in the detection of gratings by human observers: A probabilistic mechanism. *Vision Research*, 1975, *15*, 1143–1149. (a)

Tolhurst, D. J. Sustained and transient channels in human vision. *Vision Research*, 1975, *15*, 1151–1155. (b)

Tulunay-Keesey, U. Contrast thresholds with stabilized and unstabilized targets. *Journal of the Optical Society of America*, 1982, *72*, 1284–1286.

Tulunay-Keesey, U., & Jones, R. M. The effect of micromovements of the eye and exposure duration on contrast sensitivity. *Vision Research*, 1976, *16*, 481–488.

Tulunay-Keesey, U., & Jones, R. M. Contrast sensitivity measures and accuracy of image stabilization systems. *Journal of the Optical Society of America*, 1980, *70*, 1306–1310.

Uetsuki, T., & Ikeda, M. Study of the temporal response by the summation index. *Journal of the Optical Society of America*, 1970, *60*, 377–381.

van Nes, F. L., Koenderink, J. J., Nas, H., & Bouman, M. A. Spatiotemporal modulation transfer in the human eye. *Journal of the Optical Society of America*, 1967, *57*, 1082–1088.

Vassilev, A., & Mitov, D. Perception time and spatial frequency. *Vision Research*, 1976, *16*, 89–92.

Virsu, V., Rovamo, J., Laurinen, P., & Nasanen, R. Temporal contrast sensitivity and cortical magnification. *Vision Research*, 1982, *22*, 1211–1217.

Watanabe, A., Mori, T., Nagata, S., & Hiwatashi, K. Spatial sine wave responses of the human visual system. *Vision Research*, 1968, *8*, 1245–1263.

Watson, A. B. The visibility of temporal modulations of a spatial pattern.

Doctoral dissertation, University of Pennsylvania. 1977.

Watson, A. B. Probability summation over time. *Vision Research*, 1979, *19*, 515–522.

Watson, A. B. A single-channel model does not predict visibility of asynchronous gratings. *Vision Research*, 1981, *21*, 1799–1800.

Watson, A. B. Derivation of the impulse response: Comments on the method of Roufs and Blommaert. *Vision Research*, 1982, *22*, 1335–1337.

Watson, A. B., & Ahumada, A. J., Jr. A theory of apparently real motion. *Investigative Ophthalmology and Visual Science*, 1982, *22*(Suppl.), 143.

Watson, A. B., & Ahumada, A. J., Jr. *A look at motion in the frequency domain* (NASA Technical Memorandum 84352). Washington, D.C.: U.S. Government Printing Office, 1983. (a)

Watson, A. B., & Ahumada, A. J., Jr. A model of the human motion sensor. *Journal of the Optical Society of America*, 1983, *73*, 1862. (b)

Watson, A. B., & Ahumada, A. J., Jr. A model of human visual motion sensing. *Journal of the Optical Society of America*, 1985, *2*, 322–342.

Watson, A. B., Ahumada, A. J., Jr., & Farrell, J. *The window of visibility: A psychophysical theory of fidelity in time-sampled visual motion displays* (NASA Technical Paper 2211). Washington, D.C.: U.S. Government Printing Office, 1983.

Watson, A. B., & Nachmias, J. Patterns of temporal interaction in the detection of gratings. *Vision Research*, 1977, *17*, 893–902.

Watson, A. B., & Robson, J. G. Discrimination at threshold: Labelled detectors in human vision. *Vision Research*, 1981, *21*, 1115–1122.

Watson, A. B., Thompson, P. G., Murphy, B. J., & Nachmias, J. Summation and discrimination of gratings moving in opposite directions. *Vision Research*, 1980, *20*, 341–347.

Westheimer, G. Spatial interaction in human cone vision. *Journal of Physiology*, 1967, *190*, 139–154.

Wyszecki, G., & Stiles, W. S. *Color science*. New York: Wiley, 1967.